

https://dspace.org/

Improving the gold leaching process of refractory ores and tailings using the Jetleach reactor

Mbayo, Jean Jacques Kalombo

2020
https://hdl.handle.net/10539/31306

Downloaded from a DSpace repository. https://dspace.org/



IMPROVING THE GOLD LEACHING PROCESS OF REFRACTORY ORES AND TAILINGS USING THE JETLEACH REACTOR

Jean Jacques Kalombo Mbayo

A dissertation submitted to the faculty of Engineering and the Built Environment, University of Witwatersrand, Johannesburg, in fulfillment of the requirements for the degree of Master of Science in Engineering

Johannesburg 2020

DECLARATION

I declare that this dissertation is my own unaided work. It is being submitted for the degree of Master of Science in Engineering to the University of the Witwatersrand, Johannesburg. It has not been submitted before for any other degree or examination in any other University.

Jean Jacques Kalombo Mbayo



27th Day of March 2020

ABSTRACT

The cyanidation process of refractory gold ores has been the subject of numerous investigations aimed at improving the gold recovery and the leaching kinetics. Many pretreatments methods have been developed in this regard and numerous new leaching configurations have been introduced in the process. However, even after many improvements, the leaching of refractory gold ore remains a process of some duration (24 hours or more to reach acceptable gold recoveries). From recent literature investigations, hydrodynamic cavitation has been found to be a promising new approach which may advantageously enhance the cyanidation process. This approach results in the enhancement of mass transfer kinetics of multiphase streams due to impacting two pulp streams against one another in a vessel called the "Jetleach reactor (Jetleach)''.

In this work the Jetleach reactor was applied to three different refractory gold ores. Two rougher flotation concentrates from West Africa (DIO and MVO) and one flotation concentrate from the Ergo plant in South Africa. Results from a comparative cyanidation test between the Jetleach process and conventional methods, here represented by the normal leaching in agitated vessel and bottle rolling methods, have shown impressive results. On the DIO sample, the Jetleach reactor has shown an improvement of almost 8% and 19% gold recovery compared to the normal leaching and bottle rolling method, respectively, while on the MVO sample, the improvement was about 10% compared to the normal leaching method and 17% compared to the bottle rolling tests. On the Ergo sample, the improvement of gold recovery was over 12% compared to both two conventional methods.

Cyanidation using one factor at a time (OFAT) experiment revealed that the pump pressure, the feed pulp solid percentage and the oxygen flowrate are the parameters significantly influencing the gold recovery. However, cyanidation, using design of experiments (DOE) and response surface methodology strategy, has shown that, in addition to these three significant parameters, three other interactions between parameters also have a significant effect on the gold recovery.

The analysis done on the Jetleach residues, using the Scanning Electron Microscope (SEM), have revealed the presence of cavities and cracks on the surface on some particles which could explain one reason for the faster leaching kinetics and higher gold recoveries. The particle size analysis, undertaken on the feed and the residue of the Jetleach reactor, revealed

a size reduction of particles after passing through the reactor. This size reduction can also be one of the elements contributing to faster leaching kinetics.

In pursuing the understanding of the generation of cavitation in the Jetleach reactor, a visualization test using a high-speed camera was conducted on a transparent tube reactor, operating with water to simulate the process in the Jetleach. Images collected from the high-speed camera have shown the presence of cavities generated in the water and the collapsing process of same. These images also revealed that cavitation was directly connected to the pump pressure. The higher the pressure of the pump, the larger the resulting cavitation zone.

This work has shown that the Jetleach reactor is able to improve the leaching kinetics and the gold recovery of all three refractory gold ores involved in this project. The reactor was also able to reduce the cyanide and oxygen consumption on the Ergo sample. Therefore, an integration of this reactor in the cyanidation process, will result in benefits in terms of both metal recovery improvement and reagent consumption reduction.

PUBLICATIONS

This work has produced some publications.

- ***Journal Publications***

1. Jean Jacques Kalombo Mbayo, Henry Simonsen and Sehliselo Ndlovu, 2019. Improving the gold leaching of refractory ores using the Jetleach reactor. Elsevier; Minerals Engineering 134, pp. 300-308.

- ***Conference Proceedings***

1. Jean Jacques Kalombo Mbayo, Henry Simonsen and Sehliselo Ndlovu. Use of cavitation to enhance the leaching kinetics of refractory gold ores (Jetleach). International Mineral Processing Congress, Cape Town, South Africa, 18th July – 22nd October 2020.

2. Jean Jacques Kalombo Mbayo, Henry Simonsen and Sehliselo Ndlovu. Improving the gold leaching of refractory ores using the Jetleach reactor. Minerals Engineering International Conference - Sustainable Mineral 18. Windhoek, Namibia 13th – 15th June 2018.

DEDICATION

Dedicated to

my parents, Sylvain Mbayo and Godelieve Mutombo and my nine siblings, Mano, Dyna, Isabel, Jerry, Carine, Chancelle, Yannick, Melissa and Alison for their understanding and support

my cousin, Mimi Nkulu and her husband Franly Nkulu for their support and guidance

AKNOWLEDGEMENT

I wish to express my special gratitude to my supervisors Profs. S. Ndlovu and H. Simonsen for the many inspirational discussions, helpful suggestions, insight and technical guidance throughout this work.

DRD Gold/Ergo plant, is gratefully acknowledged for the samples and reagents used in this study as well as for the gold fire assays.

The National Research Foundation of South Africa and John Davidson Foundation are gratefully acknowledged for their financial contribution to the research.

The workshop team of the School of Chemical and Metallurgical Engineering is gratefully acknowledged for their technical support and help to build all the reactors involved in this study.

While many other persons have contributed either directly or indirectly to this work, I would like to mention some of them by name: Prof M. Dworzanowski, Dr. M. Bwalya, Rodney Gurney, Hopewell Gumede, Bruce Mothibedi and Janet Smith, many thanks for their continued interest and support.

Finally, special thanks to the Metals Extraction and Recovery Research Group (MERG) for the teamwork.

TABLE OF CONTENTS

DECLARATION ..... **I**

ABSTRACT ..... **II**

PUBLICATIONS ..... **IV**

DEDICATION ..... **V**

AKNOWLEDGEMENT ..... **VI**

TABLE OF CONTENTS ..... **VII**

LIST OF FIGURES ..... **XIV**

LIST OF TABLES ..... **XVII**

CHAPTER 1 INTRODUCTION **1**

1.1 Background **2**

1.2 Problem statement **3**

1.3 Research questions **3**

1.4 Research objectives **3**

1.5 Research hypothesis **4**

1.6 Research methodology **4**

1.7 Dissertation Layout **4**

1.8 Summary **5**

CHAPTER 2 LITERATURE REVIEW **6**

2.1 Introduction **6**

2.2 Causes of refractoriness and pre-treatment methods.....6
2.2.1 Causes of refractoriness.....7
2.2.1.1 Physically locked gold.....7
2.2.1.2 Chemically locked gold;.....8
2.2.1.3 Reactive gangue minerals.....8
2.2.1.4 Adsorption of gold.....9
2.2.1.1 Passivation of gold.....9
2.2.2 Pre-treatment methods of refractory gold ores.....9
2.2.2.1 Flotation of some refractory ores.....9
2.2.2.2 Pre-aeration.....10
2.2.2.3 Roasting or high temperature oxidation.....11
2.2.2.4 Pressure oxidation.....12
2.2.2.5 Biological oxidation.....15
2.2.2.6 Ultra-fine grinding.....18
2.2.2.7 Mechano-chemical activation.....20
2.2.2.8 Discussion.....21

2.3 CHEMISTRY OF GOLD CYANIDATION.....23
2.3.1 Chemistry of cyanide solutions.....23
2.3.2 Mechanism of gold dissolution in cyanide solutions.....24
2.3.2.1 Mechanism of cyanidation.....24
2.3.2.2 Thermodynamic considerations.....25
 Anodic reaction of gold oxidation.....25
1. Adsorption of cyanide on gold surface (peak at a potential of -0.4V).....25
2. The electrochemical extraction of an electron.....25
3. Combination of the adsorbed intermediate with another cyanide ion (peak at 0.3V) 25
1. Oxygen reduction into hydrogen peroxide.....27

2.4 CONSIDERATION OF REACTION KINETICS.....32
2.4.1 Kinetic Models.....34
2.4.2 Mass transfer.....35
2.4.2.1 Mass transfer through the boundary layer.....35
2.4.2.2 Mass transfer in bulk solution.....37

2.4.3 Absorption of gases in liquids....37
2.4.4 Particulate factors of the slurry....39
2.4.4.1 Particle size....39
2.4.4.2 Shape and texture....39
2.4.4.3 Mineralogical factors....40
2.4.4.4 Porosity....40
2.4.4.5 Effect of competing species....40
2.4.5 Practical parameters affecting the cyanidation process....40
2.4.5.1 Concentration of Oxygen....40
2.4.5.2 Cyanide Concentration....41
2.4.5.3 pH....42
2.4.5.4 Particle Size....42
2.4.5.5 Temperature....43
2.4.5.6 Pressure....43
2.4.5.7 Slurry Density....43
2.4.5.8 Mixing....43
2.4.5.9 Presence of interfering minerals and ions in solution....44

2.5 IMPROVEMENT IN THE GOLD CYANIDATION PROCESSES....45
2.5.1 Merrill-Crowe Process....45
2.5.2 Carbon Adsorption process....45
2.5.2.1 Carbon-in-pulp (CIP) process....46
2.5.2.2 Leaching Section....46
2.5.2.3 Adsorption Section....47
2.5.2.4 Carbon-in-leach (CIL) process....48
2.5.3 High pressure and/or elevated temperature cyanidation....49
2.5.3.1 The Leachox Process (Aachen reactor)....49
2.5.3.2 Jet reactor technology....50
2.5.4 Intensive cyanidation....51
2.5.4.1 ACACIA Reactor....52
2.5.4.2 The Inline Leach Reactor (ILR)....53

2.6 CAVITATION....55
2.6.1 Types of cavitation....55

2.6.2 Hydrodynamic cavitation....55
2.6.3 Mechanism of hydrocavitation....56
2.6.4 Application of hydrodynamic cavitation....58
2.6.5 Jetleach reactor....59
2.6.5.1 Characteristics....60
2.6.5.2 Setup description....63

2.7 Summary....63

CHAPTER 3 MATERIALS AND METHODS....64

3.1 Introduction....64

3.2 Experimental....64
3.2.1 Materials characterization....64
3.2.1.1 Sample from Ergo tailing plant....64
3.2.1.2 Samples from West Africa....65
3.2.2 Reagents....65

3.3 Chemical analysis....66

3.4 Methods....66
3.4.1 Comparison between conventional leaching methods and jetleaching method on refractory gold ores....67
3.4.1.1 Preliminary tests (pre-aeration)....67
3.4.1.2 Comparison of different leaching methods....68
3.4.1.3 Evaluation of the potential benefits of using the Jetleach process....71
3.4.2 Effect of physical and chemical parameters on the Jetleach process....72
3.4.2.1 One factor at a time....72
3.4.2.2 Interaction between parameters....73
3.4.3 Effect of cavitation on solid particles....74
3.4.4 Mechanism of cavitation....75
3.4.5 Experimental Design....77

3.5 Data Analysis....78

3.6 Summary....78

CHAPTER 4 CHARACTERIZATION OF REFRACTORY GOLD ORES 79

4.1 Introduction.....79

4.2 Results and discussions.....79

4.2.1 Ergo sample 79

4.2.1.1 XRD analysis 79

4.2.1.2 Gold speciation 80

4.2.1.1 Gold grain size distribution.....81

4.2.1.2 Gold liberation 81

4.2.1.3 Gold grain mineral association 82

4.2.2 Samples from West Africa.....83

4.2.2.1 XRD analysis 84

4.2.2.2 Automated Mineralogy | MLA Modal Analysis 85

4.2.2.3 Automated Mineralogy | MLA Gold Deportment 86

4.2.2.4 Gold grain size distribution.....87

4.2.2.5 Gold liberation 88

4.2.2.6 Gold grain mineral association 88

4.3 Summary and Conclusion 89

CHAPTER 5 COMPARISON BETWEEN CONVENTIONAL LEACHING METHODS AND JETLEACHING METHOD ON REFRACTORY GOLD ORES 90

5.1 Introduction.....90

5.2 Results and discussions.....91

5.2.1 Pre-aeration 91

5.2.2 Leaching.....95

5.2.2.1 Samples from West Africa.....95

5.2.2.2 Ergo sample 97

5.2.3 Potential benefits of using the Jetleach process 100

5.2.3.1 High gold production per unit of ore processed.....100

5.2.3.2 High throughput 101

5.2.3.3 Low reagents consumption 101

5.2.3.4 Smaller leaching tanks required.....102

5.2.3.5 Energy savings 104

5.3 Summary and conclusion 105

CHAPTER 6 INVESTIGATING THE EFFECT OF PHYSICAL AND CHEMICAL PARAMETERS ON THE JETLEACH 107

6.1 Introduction 107

6.2 Results and discussions 108

6.2.1 One-factor-at-a-time (OFAT) experiments 108

6.2.1.1 Effects of solids percentage 108

6.2.1.1 Effects of cyanide concentration 109

6.2.1.2 Effects of space between nozzles 110

6.2.1.3 Effects of oxygen flowrate 111

6.2.1.4 Effects of pump pressure 112

6.2.2 Interaction between parameters (DOE) 114

6.3 Summary and conclusions 125

CHAPTER 7 IMPACT OF MICRO-CAVITATION ON THE SOLID PARTICLES AND INVESTIGATION OF THE CAVITATION MECHANISM 127

7.1 Introduction 127

7.2 Results and discussions 129

7.2.1 Particle Size Distribution (PSD) 129

7.2.2 Scanning Electron Microscopy (SEM) analysis 132

7.2.3 Mechanism of cavitation generation 134

7.3 Summary and conclusion 137

CHAPTER 8 GENERAL CONCLUSION AND RECOMMENDATIONS 138

8.1 Introduction 138

8.2 Comparison between conventional methods and Jetleaching method 138

8.2.1 Pre-aeration tests 138

8.2.2 Comparison between conventional methods and Jetleaching method.....139
8.2.3 Potential benefits of using the Jetleach reactor.....140

8.3 Investigation of the effect of physical and chemical parameters.....140

8.4 Impact of Micro-cavitation on the Solid particles and investigation of the cavitation mechanism.....141
8.4.1 Particle size distribution.....141
8.4.2 Scanning Electron Microscopy (SEM).....141
8.4.3 Investigation of the mechanism of cavitation.....142

8.5 Recommendations.....142
8.5.1 Optimization.....142
8.5.2 Cost evaluation.....142
8.5.3 Deeper study and understanding of the cavitation phenomenon.....143

REFERENCES.....144

APENDIX A.....152

APENDIX B.....155

LIST OF FIGURES

Figure 2.1. : The crystal structure of Au$\mathbf{Te2}$ (Streltsov, et al., 2018). 8
Figure 2.2. : Alkaline pressure oxidation basic flow chart (Marsden & House, 2009) 14
Figure 2.3. : Acidic pressure oxidation basic flow chart (Marsden & House, 2009) 14
Figure 2.4. : Basic flow chart of a cyanidation process using biological oxidation (Miller & Brown, 2005). 16
Figure 2.5. : Gold particles locked in pyrite, all within an ore 18
Figure 2.6. : Cyanide stability based on pH.....24
Figure 2.7. : Current versus potential curves for the oxidation of gold in alkaline cyanide solutions (Nicol, et al., 1979; Nicol, 1980).....26
Figure 2.8. : Anodic cyanidation model for gold (Senanayake, G., 2008). 27
Figure 2.9. : The simplified schematic diagram of mixed potential model for the dissolution of gold in cyanide solutions (Marsden & House, 2006). 28
Figure 2.10. : Indicative Eh-pH ranges employed In Industrial gold extraction processes (Marsden & House, 2009).....29
Figure 2.11. : Pourbaix diagram illustrating features of $\boldsymbol{Au-CN-H2O}$ systems at $\mathbf{25}$℃. $\boldsymbol{CN-total=10-3mol\,l-1, AuCN2-=10-4mol\,l-1,\ Zn2+total=10-3mol\,l-1}$. 30
Figure 2.12. : Eh-pH diagram for the Fe-S-CN-H2O system at 25℃ (Marsden & House, 2009). 31
Figure 2.13. : Schematic representation of the local corrosion cell at a gold surface in contact with an oxygen-containing cyanide solution. $\boldsymbol{ia}$ is the anodic current; $\boldsymbol{ic}$ is the cathodic current (Marsden & House, 2009). 33
Figure 2.14. : (a) Effect of temperature and gas composition on oxygen solubility in water (b) Effect of temperature and pressure on pure oxygen solubility in water (Hollow, et al., 2005) 38
Figure 2.15. : Flow sheet of a modern CIP plant (Fleming, 2004). 46
Figure 2.16. : Leaching stage in 4 columns connected to the Aachen reactor (Maelgwyn Mineral Services Ltd, 2009). 49
Figure 2.17. : Aachen Reactor –Principle of Operation (Maelgwyn Mineral Services, 2009). 50
Figure 2.18. : Schematic diagram of the Jet reactor experimental set-up. 51
Figure 2.19. : Basic flow sheet of the ACACIA Reactor (Watson & Steward, 2002) 52

Figure 2.20. : InLine Leach Reactor flowsheet (Longley, et al., 2003).....54
Figure 2.21. : Phase diagram of water near the triple point explaining the liquid-vapor transition during cavitation (from French Wikipedia). 56
Figure 2.22. : the Jetleach reactor connected to a Pachuca (GRMS report, 1997). 59
Figure 2.23. : External View of the Impactor 60
Figure 2.24. : Internal View of the Impactor 60

Figure 3.1 : Operations stages necessary to achieve the objectives assigned 67
Figure 3.2 : Set-Up for the bottle rolling experiments.....69
Figure 3.3 : Set-Up for the normal leaching experiments.....70
Figure 3.4 : Set-Up for Jetleach Experiments.....71
Figure 3.5 : Setup to study the mechanism of micro-cavitation 76

Figure 4.1 : Gold liberation by grade.....82
Figure 4.2 : X-ray diffractograms of the feed and concentrate samples. 85
Figure 4.3 : SEM photomicrographs, MLA particle maps and EDS spectra of selected gold grains. 87
Figure 4.4 Grain size distribution data of gold (discrete and cumulative).....87
Figure 4.5 : Modes of gold occurrence. 88

Figure 5.1 : Variation of the Eh during pre-aeration on the Ergo sample 93
Figure 5.2 ariation of pH during pre-aeration.....93
Figure 5.3 : Variation of the oxygen concentration during pre-aeration 94
Figure 5.4 : Comparative Trends in Gold Recovery for the DIO sample.....96
Figure 5.5 : Comparative Trends in Gold Recovery for the MVO Sample.....97
Figure 5.6 : Comparative Trends in Gold Recovery without addition of activated carbon.....98
Figure 5.7 : Holding filter for activated carbon 99
Figure 5.8 : Comparative Trends in Gold Recovery with addition of activated carbon.....100
Figure 5.9 : First example of a leaching circuit with four reactors (A) 103
Figure 5.10 : Second example of a leaching circuit with four reactors (B).....103

Figure 6.1 : Effect of solid percentage on gold recovery (Ergo sample).....108
Figure 6.2 : Effect of cyanide concentration on gold recovery (Ergo sample).....109

Figure 6.3 : Effect of the spacing between nozzles on gold recovery (Ergo sample).....110
Figure 6.4 : Effect of oxygen flowrate on gold recovery (Ergo sample).....112
Figure 6.5 : Effect of pump pressure on gold recovery (Ergo sample).....113
Figure 6.6 : Pareto chart showing significants factors (Design Expert 11).....117
Figure 6.7 : Cubic representation of the interaction between pump pressure-oxygen flowrate and solid percentage.....118
Figure 6.8 : Effect of pump pressure, space between nozzles, solid percentage, oxygen flowrate and cyanide concentration on the gold recovery.....119
Figure 6.9 : 2D and 3D representation of the interaction effect between oxygen flowrate and pump pressure on gold recovery.....121
Figure 6.10 : 2D representation of the interaction effect between oxygen flowrate and solid percentage on gold recovery.....122
Figure 6.11 : 2D representation of the interaction effect between cyanide concentration and oxygen flowrate on gold recovery.....123
Figure 6.12 : Residuals vs Runs.....124

Figure 7.1 : Schematic representation of the cavitation mechanism in the Jetleach.....128
Figure 7.2 : Particle size analysis distribution of Ergo sample A before Jetleaching.....130
Figure 7.3 : Particle size analysis distribution of Ergo sample A after Jetleaching.....130
Figure 7.4 : Particle size analysis distribution of Ergo sample B before Jetleaching.....131
Figure 7.5 : Particle size analysis distribution of Ergo sample B after Jetleaching.....131
Figure 7.6 : Silicate and pyrite particles before Jetleaching (no presence of cracks or/and cavities on the surface).....132
Figure 7.7 : Presence of cavities on the surface of a silicate particle after Jetleaching.....133
Figure 7.8 : Presence of cracks and cavities on the surface of a silicate particle after Jetleaching.....133
Figure 7.9 : Generation of macro cavitation.....135

LIST OF TABLES

Table 2.1 : Classification of refractory gold ores based on the host mineral (Yannopoulos, 1991) 7
Table 2.2 : Classification of refractory gold ores based on the gold recovery. (Asamoah, et al., 2014) 7
Table 2.3 : different cyanide complexes anions with stability constant (Kumar, et al., 2016) 31

Table 3.1 : Parameters range for experiment 72
Table 3.2 : Levels of factors involved in the two-levels DOE 73
Table 3.3 : Experimental design 77

Table 4.1 : X-ray diffraction results (Relative Abundance) 79
Table 4.2 : Detailed X-ray diffraction results 80
Table 4.3 : Gold speciation results 80
Table 4.4 : Particle size distribution of flotation concentrate 81
Table 4.5 : Assay by size fraction 81
Table 4.6 : Ergo Conc Sinks-Liberation by Grade (Discrete) 81
Table 4.7 : Gold association (details and synthesis) 83
Table 4.8 : XRD of Diorites and Meta-volcanic gold sample 84
Table 4.9 : Results of the Modal Analysis 86
Table 4.10 : Gold mineral associations (%) 89

Table 5.1 : Pre-aeration process of slurry before cyanidation 92
Table 5.2 : Effect of pre-aeration on gold recovery and cyanide consumption 95
Table 5.3 : Overall reagents consumption 102

Table 6.1 : design of experiment to evaluate the significants parameters 115
Table 6.2 : ANOVA for selected factorial model (Response : Gold recovery) 116

CHAPTER 1 INTRODUCTION

The gold metallurgical industries of South Africa are facing one of the biggest challenges ever: “how to keep the gold exploitation economical viable”. The depletion of free-milling ores and the ever increasingly strict environmental regulations can rapidly change a prosperous company into a non-viable operation. Therefore, the cost of gold processing is the determining factor for keeping many gold companies running. It is thus, crucial for many companies in South Africa and worldwide, to find a way to improve gold recovery and reduce operational costs associated with gold processing in order to remain globally viable and competitive.

With the depletion of high grade and easy to process ores, companies are being forced to consider treating refractory ores instead. These are associated with relatively poor recoveries and an increase in operational costs. There is thus, a need to identify ways to improve recoveries and reduce operational costs in the treatment of refractory gold ores. It has been shown by Metzner in 1993 that the South African mineral's industry loses approximately R8 500 million per year due to valuable in gold minerals reporting to tailings streams. Refractory gold ores are generally defined as ores that, because of the mineral matrix, do not give economic recoveries in normal cyanide circuits even when ores particles are finely ground to around 53 to 75 microns (Flatman , et al., 2008). South Africa has abundant resources of refractory gold ores (mining reserves and tailings); therefore, an effective treatment of these ores can bring considerable economic benefits (Zhu, et al., 2012).

For refractory gold ores to be economically processed, methods such as the chlorination of carbonaceous ores, roasting of sulphidic ores, pressure oxidation of sulphidic, pyritic and arsenopyritic ores, and bacterial oxidation of sulphidic ores have been developed in order to improve the leaching kinetics and recoveries (Loftus, et al., 1997). In addition, in order to reduce the production cost and the environment impacts, the use of other reagents (thiosulphate, thiourea, thiocyanate, chloride and bromide) has been investigated. However, cyanidation still appears to give the best practical results. Moreover, in the cyanidation process, other physical and chemical methods such as cyanidation at high pressure, intensive cyanidation, even by increasing temperature, pressure, cyanide or oxygen concentration; have also been investigated (Flatman , et al., 2008).

Despite its dominance over all the other alternative processes, the cyanidation process remains a process of somewhat long duration (24h or more of cyanidation time, depending on the type of ores). Since operational costs associated with the treatment of refractory ores continue to increase, it would be advantageous to find ways to reduce the leaching time. From recent literature investigations, hydrodynamic cavitation has been found to be a promising new approach which should influence the cyanidation process. This approach results in the enhancement of mass transfer kinetics of multiphase fluid streams brought about by, inter alia, impacting two pulps streams against one another in a device called a ‘‘Jetleach Reactor’’.

The ‘‘Jetleach Reactor’’ is a device designed to create and propagate micro-cavitation and amplify the erosion action of particles by impacting two pulp streams against one another at a high velocity. The cavitation process produces bubbles which, once collapsing, propagate stress at the inter-phase of bubbles-particles, with an increase of the local pressure and temperature (Tsaih , et al., 2004). Many changes such as cracks propagation, internal stress or mechanical activation may happen under emission of such extreme energy, and thus result in an increase in the leaching kinetics.

1.1 Background

An initial concept leading to the development of the Jetleach system arose from the need to treat chromite particles with a chrome-to-iron ratio that was below market specifications (GMRS report, 1997). The investigators were then alerted to an experiment that had been attempted to liberate diamonds by ‘‘firing’’ slurry streams of kimberlite against one another. The process, when applied to the chrome sands, resulted in a satisfactory degree of surface polishing. Later, this approach was then embodied into the Jetleach system in which comminuted ore is mixed with a liquid (water) to form a pulp. Two streams of the pulp are then projected against one another through a pair of coaxially aligned nozzles in a chamber filled with oxygen. The impact leads to some comminution of the solid particle in the pulp and to the erosion or exposure of the ore minerals, thus permitting an enhanced attack on the ore by the lixiviants in the pulp and under pressurized atmosphere.

When applied to free milling and non-refractory gold ores, the Jetleach has shown impressive results by improving the gold recovery by 2% while decreasing dramatically the leaching time by 90% compared to the normal CIL circuit (GMRS report, 1997). After such results, observed on free milling and non-refractory ores, this project has been initiated to investigate

and verify if the Jetleach reactor can also improve the gold recovery and the leaching kinetics of refractory ores and tailings. The research further seeks to determine the parameters that affect this process and to understand the mechanism by which the Jetleach reactor can reduce the leaching time. The expected gains of using the Jetleach reactor, in a leaching process, are energy savings by reducing dramatically the time of leaching, reducing the number or the size of tanks required for leaching, a high throughput and an increase in gold production per unit of ore (Loftus, et al., 1997).

1.2 Problem statement

Due to the depletion of free-milling ores, gold industries in South Africa and worldwide, are inclined to treat refractory ores. South Africa has abundant resources of refractory gold ores (mining reserves and tailings). However, refractory ores are difficult to leach with a normal cyanidation process. These ores require pretreatment methods and a very long leaching time to have an acceptable gold recovery. Consequently, this results in an increase in energy and reagent consumption.

The increase in the operational costs due to mining at depth with the additional cost related to refractory ore treatment have induced many gold companies to explore alternative ways to remain globally viable and competitive. One of the solutions has been to consider the retreatment of tailings, since these have been shown to be a way of recovering gold at a lower production cost (tailings are already ground and there is no cost related to mining). However, the big challenge related to refractory ores and the tailings processing remains on how to reduce the leaching time. As South Africa has abundant resources of refractory gold ores (tailings included), an effective treatment of these ores can bring economic benefits.

1.3 Research questions

There are three big questions around this project:

- Can the Jetleach reactor improve the leaching kinetics of refractory gold ores?
- Can this reactor give a higher gold recovery compared to the conventional leaching methods?
- Is cavitation and comminution happening in the Jetleach reactor?

1.4 Research objectives

This work has practically four objectives:

- To investigate if the hydrodynamic cavitation of micro bubbles can improve the leaching kinetics of refractory gold ores (and tailings) compared to the bottle roll and normal leaching.
- To study the impact of chemical and physical parameters such as pH, pressure, temperature, nozzle diameter, oxygen and cyanide concentration on the gold processing and recovery in a Jetleach reactor;
- To understand and explain the mechanism of leaching (crack propagation, mechanical activation or just a simple grinding technique) in the Jetleach impactor;
- To determine the expected benefits of using the Jetleach reactor in a cyanidation process

1.5 Research hypothesis

The Jetleach reactor, developed in this research, has the potential to improving the leaching kinetics as well as the gold recovery of refractory gold ores using micro-cavitation by impacting two slurries against one another at high velocity.

1.6 Research methodology

The research methodology adopted in this investigation involved the following major tasks: Literature review, materials and methods, laboratory test work and data analysis, drawing conclusions from results, recommendations and documentation.

1.7 Dissertation Layout

This section provides a summary of the all chapters and sections that are covered in this dissertation. The dissertation presented here comprises in total eight chapters. Each chapter begins with a short introduction that gives an overview of the areas that will be covered in various sections of the chapter. At the end of each chapter, a summary and conclusion are provided to summarize what has been covered and guide the reader to subsequent chapters.

- **Chapter 1 Introduction**: This chapter provides the motivation for the research, the problem statement, and the overall objectives of the study.
- **Chapter 2 Literature Review**: This chapter sets out a review related to the processing of refractory gold ores. The chapter includes: the causes of refractoriness and the pre-treatments methods available; a general knowledge of how gold dissolution is achieved in cyanide solution by emphasising on the thermodynamic and

the kinetics aspect of the process, including the parameters influencing the leaching process; the current metallurgical improvements and the use of cavitation to enhance the leaching kinetics of refractory ores.

- **Chapter 3 Materials and methods**: This chapter describes the types of materials, the experimental and data collection methods used in the study.
- **Chapters 4-7 (Results and discussions)**: These chapters cover the results obtained during laboratory tests and offers a discussion of the findings.
- **Chapter 8 Conclusions and recommendations**: This chapter gives a general conclusion of the dissertation with a summary of the findings and recommendations.
- At the end of this study, a referencing section which gives the details of all articles used in the study and an appendix section providing relevant laboratory test results and other important data are included.

1.8 Summary

This introductory chapter has discussed (in its first part) the background, problem statement and study objectives. This was then followed by a short description of the research methodology and dissertation layout. The next chapter discusses literature review.

CHAPTER 2 LITERATURE REVIEW

2.1 Introduction

Gold constitutes only 0.003 ppm of the earth's crust and is therefore considered a rare mineral (Holmes & Minnitt, 2018). This metal is generally produced from two major types of deposits mined as free milling ores and refractory ores. Free milling ores are constituted by placer mechanisms and most of the oxide ores (and some sulphide). These ores are relatively easy to process through cyanidation and generally give very high gold recovery, >90% (Ellis & Senanayake, 2004). Refractory ores on the other hand are constituted by the majority of sulphidic ores. These ores, because of the mineralogical association, are difficult to leach in cyanide solution and usually result in poor gold recovery.

With the depletion of free milling ores, many companies are now forced to process refractory gold ores. However, most of the challenges faced during the cyanidation process of refractory gold ores are usually connected to the way gold particles are associated with other minerals in the ore. The process of refractory gold ores generally includes a preliminary stage where the ore is physically or chemically pre-treated before cyanidation. It is important to understand the leaching mechanism and the parameters that can help to improve the leaching kinetics associated with cyanidation.

Therefore, this chapter provides a general overview related to the cyanidation process of refractory gold ores starting from the causes of refractoriness until the actual improvement in the cyanidation process.

2.2 Causes of refractoriness and pre-treatment methods

Refractory gold ores are defined as ores which give low gold recovery. They can also be defined as unoxidized, or partially oxidized, ores in association with different sulphidic host material as presented in **Table 2.1** below:

Table 2.1 ***: Classification of refractory gold ores based on the host mineral (Yannopoulos, 1991)***

Most common host	Pyrite
Relatively common	Arsenopyrite, Sulphides (chalcocite, covelite, pyrrhotite and galena), Nickel sulphides (arsenides and sulfo-arsenides), Iron oxides, Silicates and carbonate
Common host	Carbonaceous material and Uranium minerals (common in South Africa)
Not very common	Chalcopyrite

The refractoriness of gold ores can be classified according to the amount of gold that can be recovered by normal cyanidation as presented in **Table 2.2.2 b**elow:

Table 2.2 ***: Classification of refractory gold ores based on the gold recovery. (Asamoah, et al., 2014)***

Classification	Gold recovery
Free milling	More than 95%
Mildly refractory	80-95%
Moderately refractory	50-80%
Highly refractory	Less than 50%

Depending on the different mineral association, there are several reasons to explain the refractoriness of gold ores.

2.2.1 Causes of refractoriness

2.2.1.1 *Physically locked gold*

Gold particles are occluded and/or disseminated, within a gangue mineral insoluble to cyanide solution (e.g. silicates, sulphides and oxides). These types of ores can be effectively leached in cyanide solution after passing gold ores through ultrafine grinding (<11 µm). In 2003, Ellis showed that it is sometimes more economical to use ultrafine grinding for some oxidation process, even though this operation is very expensive (Frondel, 1938; Saunders,

1990; Bowell, 1999). However, not all physically locked refractory gold ores give the same result (higher gold recovery) after ultrafine grinding.

2.2.1.2 *Chemically locked gold;*

In this case gold is not located as discrete metals inclusion but is chemically combined with tellurides and sulfides. In 2014, Chen et al, when doing an electronic and structural investigation, revealed that gold as Au^{+1} (and silver) can be found in pyrite, incorporated into the interstitial lattice sites and/or as substituting the S atoms as shown in **Figure 2.1**.

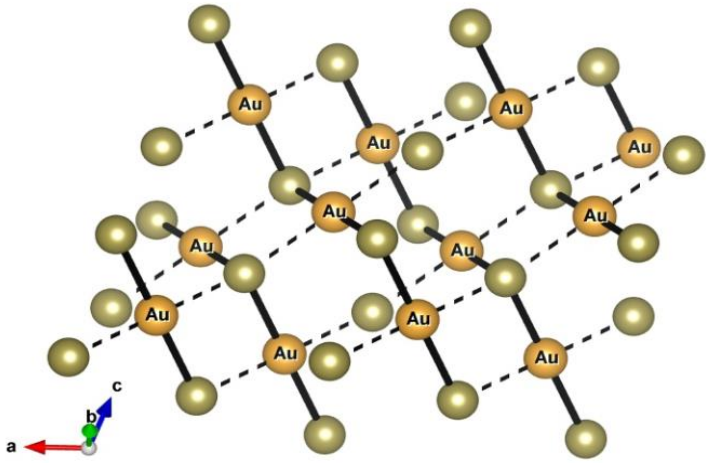


Figure 2.1. : The crystal structure of $AuTe_2$ (Streltsov, et al., 2018).

Many researchers have explained this phenomenon occurring as a result of hydrothermal alteration of granites, diorites and effusive rocks at a temperature range between 70-280℃.

2.2.1.3 *Reactive gangue minerals*

Gold particles are often accompanied by other minerals such as copper, silver, antimony and arsenic that can react with cyanide and oxygen, increasing the reagent consumption. These unwanted reactions deplete oxygen and cyanide required for gold extraction by producing different cyano-complexes. Reactive gangue minerals such as S, Cu, Zn, Fe, Ni, etc. are also named ‘‘cyanicides’’ or leach robbing minerals (Hausen, 2000; Liipo, 2003; Amankwah, et al., 2005; Adams, 2013).

2.2.1.4 *Adsorption of gold*

Some gangue, especially carbonaceous gangues and other surface-active gangue minerals (e.g., clay, silicates, etc.) can, during the leaching process, react as activated carbon. They adsorb dissolved gold from the leach liquor reducing the gold recovery. The term given to this process is called preg-robbing (Dunne, et al., 2012). Depending on the capacity to adsorb gold, carbonaceous ores can be classified in between two extremes. Mild preg-robbing ores, which have capacity to adsorb less than 1 g Au/t ore, and extreme preg-robbing ores have a capacity to adsorb more than 500 g Au/t ore (Dunne, et al., 2012). It is important to avoid a confusion between ‘‘preg-robbing’’ which is the adsorption of dissolved gold by carbonaceous matter, and ‘‘gold encapsulation’’ which usually occur during pretreatment process such as roasting and pressure oxidation.

2.2.1.1 *Passivation of gold*

Marsden and House determined in 2006 that, during leaching, some ionic species of sulphidic material may oxidize and form oxide and intermediate adsorbing layers on the surface of gold mineral that retard gold dissolution (e.g. minerals such as chalcocite, pyrrhotite, gold-telluride, chalcopyrite, pyrite and stibnite) (Bas, et al., 2017).

2.2.2 Pre-treatment methods of refractory gold ores

To overcome these numerous challenges related to refractory gold ores, many different pretreatment methods have been developed. Methods such as roasting, pressure oxidation, biological oxidation, ultra-fine grinding and mechano-chemical activation have been effectively introduced in the cyanidation process. However, when dealing with lower grade ores, it is preferable for some sulphidic ores to undergo flotation prior to the other pre-treatment methods.

2.2.2.1 *Flotation of some refractory ores*

Flotation of sulphides has become a very important process especially when dealing with low grade sulphides ores or tailings. These types of ore are mostly constituted by pyrite and arsenopyrite. Gold particles in these minerals are so intimately associated with pyrite that cyanidation for a prolonged period of time, even under ideal conditions, cannot dissolve the gold. Therefore, flotation is required to increase the grade of gold and reduce the amount of

gangue sent to cyanidation. The flotation process of gold ores is generally practiced at a pH between 6.5 and 7.5, with the use of sodium isopropyl xanthate as primary collector, Aerofroth 76 as frother and Aerofloat 208 as the secondary collector.

When dealing with tailings, or some cyanide residue, it is necessary to destroy the lime alkalinity present before floating the materials. Therefore, a conditioning step using SO_2 gas is used to reduce the pH value of residue or tailings from 10.5-11.5 to 6.5-7.5. After flotation, concentrates are thickened and filtered to remove an amount of water before the oxidation step.

A conditioning stage is also required when dealing with sulphide ores which are partially oxidized to increase the pH to the required value for flotation. However, lime acts as a depressor of free gold (as a result of texture) and consequently inhibits flotation of pyrite. Therefore, soda ash (Na_2CO_3) is used to regulate the alkalinity of the slurry. Sodium sulphide (Na_2S) can be used for the flotation of mixed ores (partially oxidized). However, since sodium sulphide can depress free gold, it should be used with caution. Elements like copper sulphate (which act as activator) can contribute to improving the flotation of pyrite and arsenopyrite.

It is very important to do extensive laboratory and pilot testing along with an economic analysis before taking the decision of using flotation at industrial scale.

2.2.2.2 *Pre-aeration*

To dissolve gold successfully in cyanide solution, oxygen is necessary for the process. However, if sulphide minerals are present in the ore, they tend to consume the oxygen thereby oxidizing to form acids. This transformation not only increases oxygen consumption, it also increases the amount of lime required to maintain the pH. The presence of iron (II) also contributes to an increase in the processing cost by increasing cyanide consumption (Jara & Bustos, 1992). Therefore, when dealing with refractory gold bearing ores and tailings containing pyrite, arsenopyrite and other sulphidic mineral, aeration of the pulp prior to cyanidation can be used to render elements such as iron and sulphur less reactive to cyanide.
Pre-aerating the ore before cyanidation can inhibit this occurrence by passivating the iron in solution resulting in Fe (II) oxidizing to Fe (III). This insoluble layer formed (hematite) on the surface then inhibits the sulphides in the ore from further decomposition (Jara & Bustos, 1992). The oxidation of iron from iron (II) to iron (III) and subsequent precipitation as iron

hydroxide minimizes loss of cyanide from the formation of ferrous cyanide complexes. The oxidation of sulphur compounds to sulphate ions avoids the consumption of cyanide to thiocyanate (SCN^-) byproduct.

2.2.2.3 *Roasting or high temperature oxidation*

Roasting is one of the first pre-treatment methods that has been applied to treat refractory gold ores. This method is most applicable to pyrite, arsenopyrite and carbonaceous ores as they are the major gold- bearing refractory minerals (LI, 2009). During roasting, oxygen converts sulfide into oxide and sulfur is released as sulfur dioxide, a gas.

Usually, roasting breaks up almost all the cyanicides minerals in the raw ore to allow an enhanced attack by cyanide solution. However, the calcines remain in association with gold. In this case, a washing step with water or acid is required.

There have been instances, where the whole raw ore is roasted before cyanidation, but this practice has become unattractive because of high overall costs involved especially when dealing with large plants or low-grade ores (Archibald, 1949). With improvements in flotation methods, the generally accepted procedure is to start with flotation then roast only the concentrate bulk.

a. Environmental issues

One of the biggest problems associated with the use of roasting is pollution of the atmosphere. Roasting of gold ores and concentrates produces very toxic gases and heavy metals such as mercury which are released into the atmosphere. Therefore, it is necessary to install gas-treatment systems to make sure that the quality of the gas released into the atmosphere meets the environmental regulations. Because these systems, which are further associated with high energy requirements, can be quite expensive, roasting of gold ore and concentrate is further associated with high capital and operating costs.

b. Processing issues

- ***Fusion of Calcines***

As discussed in the previous section, reactions taking place during roasting of pyritic and arsenopyritic ores are extremely exothermic mainly due to oxidation reactions within the ore. It is known that some particles within the ore contain higher concentrations of sulphides

and/or arsenides. These sulphides and arsenides in the particles undergo localised combustion which leads to higher and extreme local temperatures causing fusion of eutectic mixtures of iron oxides and iron sulphides. The fused mixture may sometimes occlude gold particles by creating an external protective layer that does not allow cyanide solution to reach the gold during leaching. To overcome this, a calcine-washing installation prior to cyanidation is required. However, this installation significantly increases the operating cost of the overall process.

- ***Gold lockup in recrystallized hematite***

During roasting, it is important to have a close control of the temperature and an adequate excess of air to produce porous hematite without gold lockup in its crystalline structure. However, pores formed in the hematite may be closed by recrystallization of hematite and solid solution of gold in hematite resulting in gold lockup (Yannopoulos, 1991).

- ***Calcine content***

Elements like arsenites, sulphites and soluble sulphides can be found in significant amounts in the calcine products after roasting. These elements contribute to increased cyanide and lime consumption during cyanidation. Therefore, to overcome this, it is important to do a calcine washing step prior to cyanidation.

- ***Calcite content in the ore***

The presence of calcium carbonate in the ore fed to the roaster has many negative effects. Not only does it increase the energy requirements due to the exothermic decomposition reaction and changes the gas composition by the evolution of carbon dioxide, calcium carbonate may also form calcium sulphide and/or sulphate. Calcium sulphide is deleterious to the cyanidation process as it acts as a cyanide consumer and a reducing agent. Depending on the concentration, calcium sulphate may contribute to the sealing of the calcines pores and it may also form gypsum which is deposited in pumps and conduits of the mill (Yannopoulos, 1991).

2.2.2.4 *Pressure oxidation*

The use of pressure oxidation is becoming a popular method for the pre-treatment of refractory gold ores compared to roasting. During pressure oxidation, the sulfides are

oxidized by oxygen at an elevated temperature of 190 to 250°C and at an oxygen overpressure of 350 to 700 kPa in aqueous slurry. Under these elevated temperatures and pressure, the sulfides are broken down to a solution phase consisting of metal sulphate compounds and sulphuric acid (Rusanen, et al., 2013). Pressure oxidation has been applied to different types of ores such as pyrite, arsenopyrite, stibnite, and carbonaceous material. This process has been shown to improve the gold recoveries from the range of 18-86% to the rage of 92-99.5% after using pressure oxidation at a temperature range of 225-245℃.

There are two kinds of pressure oxidation, one is done under acidic conditions while the other is done under alkaline conditions. The alkaline oxidation does not have much commercial application while the acidic process is the one that has found ready application worldwide (Haque, 2007; Flatman, et al., 2010). The difference between these two processes is that the acidic oxidation required a neutralization stage before cyanidation, while there is no neutralization stage in the alkaline process. **Figure 2.2** and **2.3** present a flow diagram of the alkaline and acidic oxidation process, respectively.

The challenge with the alkaline process is that gold recovery is generally around 10% lower compared to the acidic process due to encapsulation of unoxidized sulfides and gold entrapment in the products of alkaline oxidation. Gold is trapped in the ore because of hematite which mostly forms at the oxidized surface of the ore and consequently reduces the gold recovery.

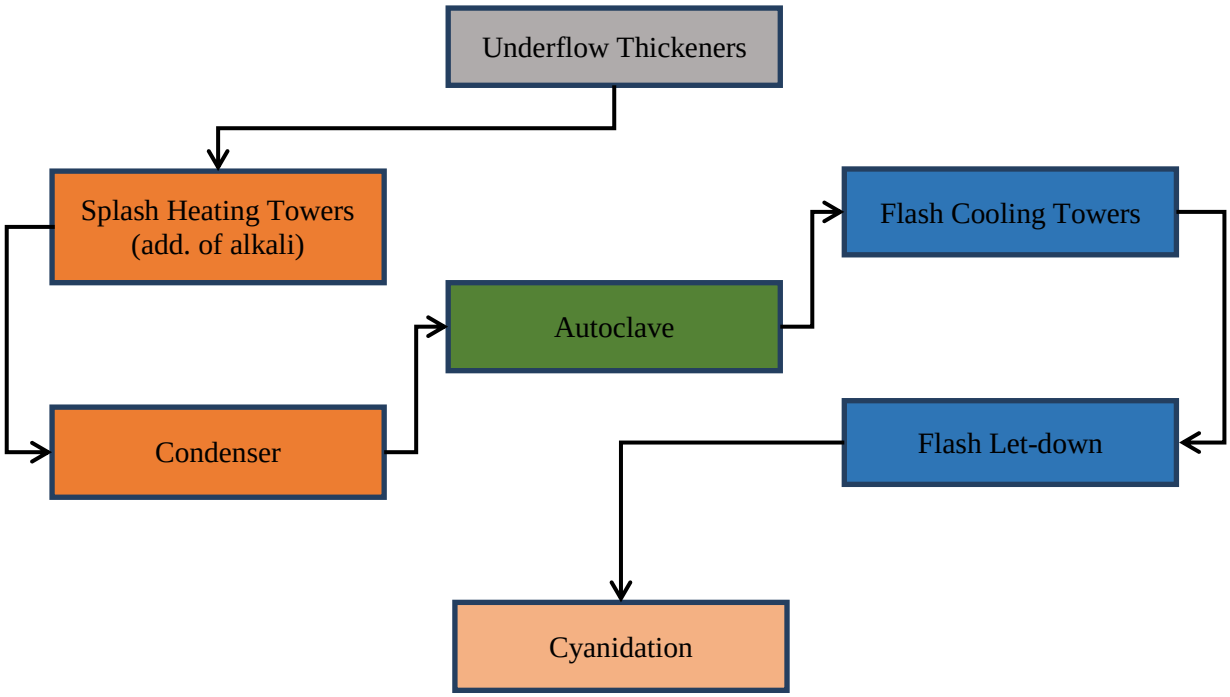


Figure 2.2. : Alkaline pressure oxidation basic flow chart (Marsden & House, 2009)

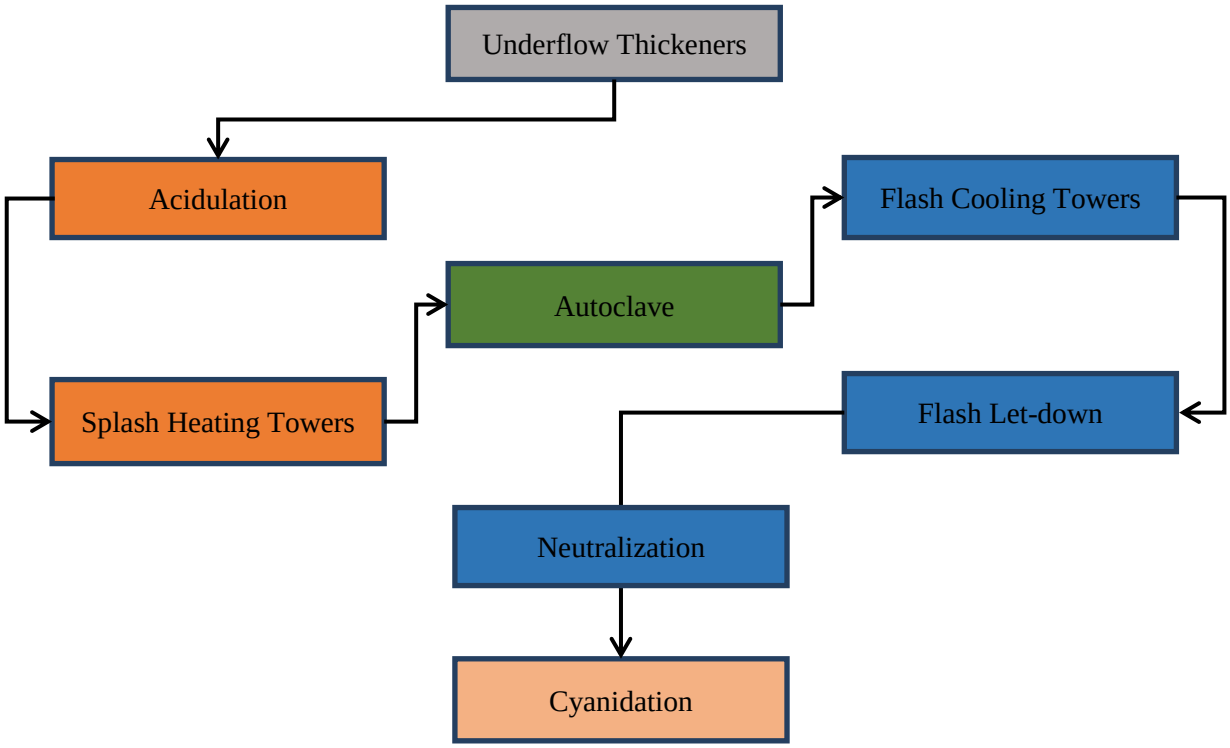


Figure 2.3. : Acidic pressure oxidation basic flow chart (Marsden & House, 2009)

The use of pressure oxidation has shown an improvement in gold recovery due to the complete destruction of the sulphide matrix which often occludes finely disseminated gold particles. The challenge in acidic pressure oxidation is the requirement of a neutralization step before the cyanidation process (LI, 2009; Liddell & Adams, 2012). This therefore, has a significant increase on the production cost. The process also requires considerable technical expertise and the installation of large capital equipment such as an oxygen plant, making the overall capital and operating costs high (Abbruzzese, et al., 1994). However, the ultrafine grinding of sulfide flotation concentrates followed by a pressure oxidation at low intensity has shown great improvement in the treatment of refractory ores. This combination is marketed as the Activox process.

Alkaline pressure oxidation presents the advantage of reducing the production cost by avoiding the neutralization stage before cyanidation. But this process generates products with entrapped gold particles (hematite on the surface of the ore) and consumes cyanide during leaching (unoxidized sulphur). Acidic pressure oxidation on the other hand generates products such as ferrous sulfate which is soluble in acid solution and therefore, will be washed away from the surface of the reacting pyrite either by hydrolysis or through precipitation as hematite. The acidic process further presents the advantage of having gold recoveries almost 10% higher compared to the alkaline process.

2.2.2.5 *Biological oxidation*

Biological oxidation of refractory ores has become a more preferable pre-treatment method of sulphides and carbonaceous gold ores compared to roasting and pressure oxidation, which are costly and environmental unfriendly. The biological process appears to have originated from bacterial investigations at the Pasteur Institute, in Paris, in the mid-1960s. This process involves the use of strains of bacteria to catalyze the decomposition of sulfide minerals. These bacteria are used to liberate the encapsulated gold grains within the sulphide matrix, by degrading iron-sulphide mineral, permitting the subsequent dissolution of gold by cyanide leaching (Ubaldini, et al., 2000).

Biological oxidation is commonly used to treat gold concentrates after either flotation or gravity concentration. A simple flowsheet can be presented as follow (**Figure 2.4**):

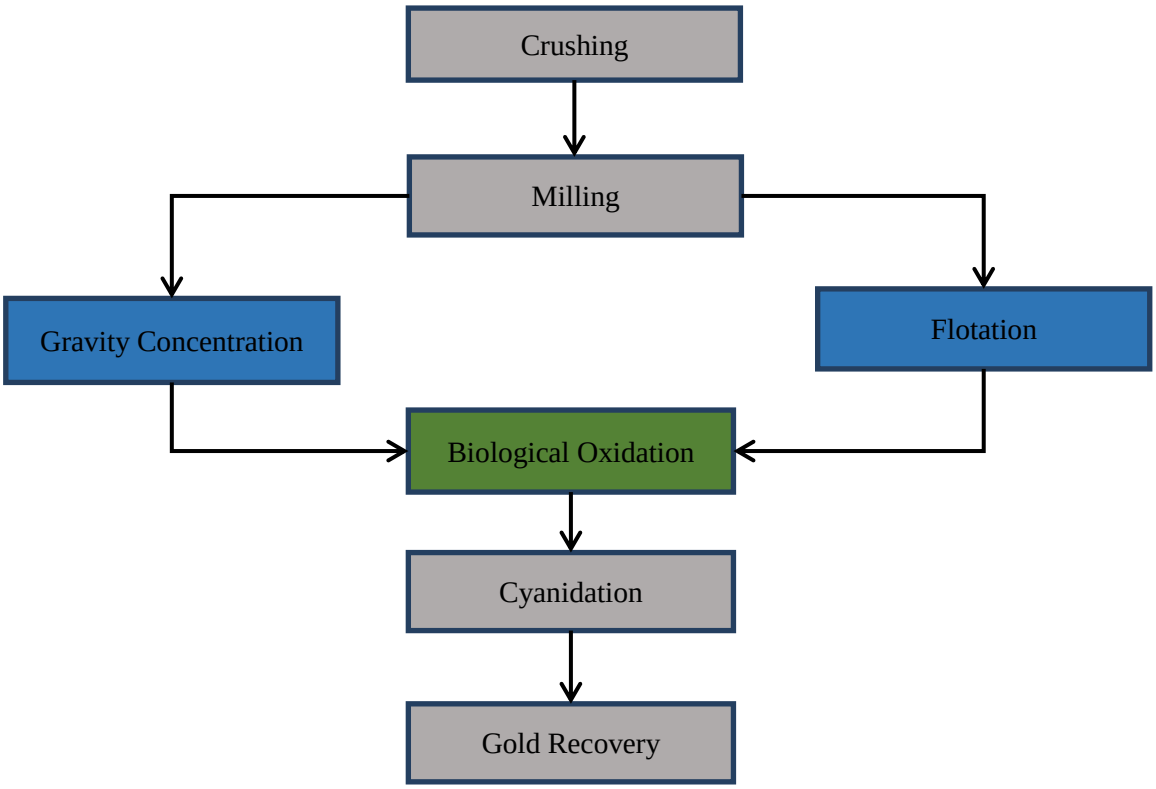


Figure 2.4. : Basic flow chart of a cyanidation process using biological oxidation (Miller & Brown, 2005).

The biological oxidation process requires a dilute slurry with a solid percentage between 15 and 20%. Therefore, addition of water to the concentrate feed for bacterial oxidation is necessary prior to cyanidation. To achieve a continuous treatment of the slurry, a sequence of agitated and aerated reactors is designed in a way that the residence time allows the growth and division of bacterial population needed for the oxidation process. It is important, depending on the type of bacteria used, to keep the working temperature between 25 - 40°C to allow growth and multiplication of bacteria. Since bio-oxidation reactions are exothermic, reactors are cooled down, to the required temperature, using water. For most refractory ores, 5 to 6 days are required to achieve a high level of oxidation. However, when only a partial oxidation is needed, 3.5 days can be enough to achieve the requirement.

It is crucial for a biological oxidation process to optimize the following parameters:

a. Particle size

There is no standard size required to process all ores and concentrates using bio-oxidation. The optimum must be established experimentally. However, a number industrial application seems to favor grinding to less than 35μm (Yannopoulos, 1991).

b. The solids concentration of the pulp

The solids concentration has been reported to be a very crucial parameter that needs to be optimized. Its influence on the process is even more than that of the particle size distribution. In 1987, Pooley reported in his work on sulfide ores that the maximum bacterial leaching rate occurs with 15 to 20% solids concentrations. A concentration more than 20% may result in a reduction in the growth of bacteria, therefore reducing the leaching rate. Sometime this can even result in the complete stopping of the oxidation process.

c. The nutrient addition

The amount of nutrient required for a biological oxidation is established by testing. However, it has been reported that to maintain bacterial activity and growth, a small amount of potassium, phosphorus, and nitrogen are required. The amount of each of the nutriment is determined by testing.

d. Aeration

It is important to determine the aeration flow rate to use during biological oxidation in order to maintain the oxidation rate and bacterial growth. It has been reported that an adequate oxidation rate and bacterial growth is maintained when operating at a relatively low aeration rate between 0.5 to 1 l/min, per liter of slurry.

e. Temperature

As said earlier, during a biological process, the temperature must be maintained around 25-40℃ to achieve an optimum bacterial activity and bacterial growth. However, the biological oxidation is an exothermic process. Therefore, to maintain the operating temperature, the reactors must be equipped with a cooling system.

The biological oxidation process presents the advantages of being low cost, simple, easy to operate and environmentally friendly (Afenya, 1991; Ofori-Sarpong, et al., 2017). With the increasingly strict environmental regulations, biological oxidation is called a “green metallurgical process” and constitutes therefore, a new hope for the future. The maintenance of the bacterial growth conditions (temp: 25°C to 40°C; pH: 1-3; O_2 and CO_2 from air) constitutes the most important factor in the biological oxidation.

However, biological oxidation has some shortcomings. It is a difficult process to control; it has long residence times, slow kinetics and the requirements of temperature tolerant bacteria (Nancharaiah, et al., 2016). One of the reasons for slow kinetics is that bacteria digestion of sulphide ores is an exothermic reaction which results in an increase in temperature. By

exceeding the working temperature of the bacteria, all reactions die down. Therefore, ores with high sulfide content require careful control of process conditions for effective treatment. There are also some side effects caused by bioleaching that may have a negative impact on the environment. For example, the process results in the production of sulphuric acid and extended use can cause the acidification of water to pH of 1 which can affect the nearby groundwater (Wang, et al., 2016).

2.2.2.6 *Ultra-fine grinding*

One of the most frequent causes of refractoriness of gold ores is the presence of gold particles finely disseminated and encapsulated within sulphide ores such as pyrite and arsenopyrite (La Brooy, et al., 1994; Gupta & Mukherjee, 2000). The mode of occurrence of gold particles within the matrix determines the pretreatment method to use prior to cyanidation (Marsden & House, 2006). The conventional milling techniques are only able to effectively liberate the pyrite from the gangue before flotation, allowing the flotation process to generate a lower mass pull of pyritic concentrate. However, gold particles remain encapsulated within the pyrite. **Figure 2.5** shows how gold particles are physically locked within pyrite minerals.

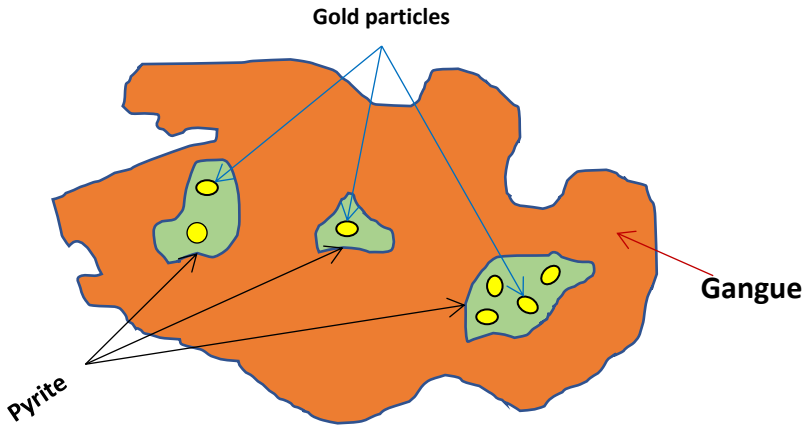


Figure 2.5. : Gold particles locked in pyrite, all within an ore

Pretreatments methods such as roasting, pressure oxidation and biological oxidation all use different level of temperature, pressure and catalysis to facilitate the reaction between the sulphidic materials (pyrite or arsenopyrite) and oxygen. These methods are able to liberate finely disseminated gold and gold in solid solution and achieve high gold recoveries. However, the environmental aspects of treating the by-products generated can alter the

economics of the process and therefore, make an alternative process route more economically attractive.

Ultra-fine grinding (UFG) is an alternative method applied to physically liberate disseminated gold from the host minerals. This method consists of reducing the particle size of the host mineral thereby exposing a part of the surface of the encapsulated gold to cyanide solution. The advantage of using this method is that the process does not involve any oxidative chemical reaction in order to alter the host mineral. Therefore, there is no need of treatment of the by-products generated. This technique uses stirred media mills to grind the ore to sizes below a few microns (Adams, 2005).

The aim of the UFG method is to reduce the particle size of the host minerals so as to increase the chances of the contact between the gold particles and the oxidizing solution (Baláž, 2005).

- ***Advantages and challenges***

The UFG is an alternative method of processing refractory gold ores in a more friendly way to the environment compared to roasting and pressure oxidation. This technique has been shown to improve the gold recovery especially when the gold particles locked in the ore are fine 1.2 to ~20 μm (Corrans & Angove, 1991; Deschênes, et al., 2003; Celep, et al., 2014). The ultrafine grinding process has the advantage of not destroying the host mineral with an oxidative chemical reaction so there are no problems of treatment of the reaction products (Ellis, 2003).

The major challenge that is yet faced in ultra-fine grinding is to attain the required product size at low energy costs and higher mill throughput because the technique is characterized by high energy requirements (Fosu, et al., 2015). Another disadvantage of fine grinding is that despite liberating the desired mineral, there is also an increase in the surface area of other host minerals such as pyrite and arsenopyrite. This can affect the oxidative and cyanide downstream processes by increasing the reagent consumption (Flatman, et al., 2010). Several studies have been done on the ultrafine-grinding using stirred media mill as a pre-treatment method to improve the gold recovery of refractory ores and concentrates in subsequent cyanide leaching (Gonzalez-Anaya, et al., 2011; Harbort, et al., 2014).

2.2.2.7 *Mechano-chemical activation*

Ultra-Fine Grinding (UFG) followed by the leaching process has been applied on many sulphidic ores and concentrates to improve the leaching kinetics of refractory gold ores. The UFG process is able to generate a distortion of the crystalline lattice of the mineral. These effects, known as mechanical activation, contribute to the transfer of electrons from the mineral to an oxidant thereby increasing the leaching rate (Hourn & Halbe, 1999). The electronic instabilities generated are not stable and have different relaxation times (short and long lived). The long-lived electronic instabilities have slow relaxation times while the short-lived ones, highly excited, have fast relaxation times.

Therefore, a separation of ultra-fine grinding and leaching in two different steps will only take advantages of the long lived instabilities, while all the short lived will no longer be present for subsequent chemical leaching (Ellis, 2003). The combination of ultra-fine grinding with the chemical leaching process, in one single step, known as mechano-chemical treatment, is a viable alternative treatment of refractory gold ores which takes advantage of both electronic instabilities. In addition, to improving the grinding efficiency, the leaching reagent functions as the grinding additive. Thus, the approach can contribute to the operational and economic benefits of the overall process (Baláž & Achimovičová, 2006; Mohammadabad, et al., 2016).

Mechano-chemical activation avoids heat loss, mineral deactivation and surface passivation while providing new surfaces and activated sites for selective leaching. Through application of the mechano-chemical approach, the reactivity of primary minerals increases through particle size reduction and surface area increase, which enables leaching to be done at lower temperatures and under atmospheric pressure conditions (Young et al., 2008).

The process has a positive influence on the hydrometallurgical operations; it results in the breakage of bonds in the lattice structure of the mineral decreasing the activation energy and in turn increasing the rate of leaching. It also results in improved leaching selectivity by increasing the dissolution and the formation of water-soluble compounds. Because of increasing the dissolution and formation of water-soluble compounds, further processing can be done in shorter reaction times (Baláž, 2005).

The application of combined mechanical activation and chemical leaching (mechano-chemical leaching) in comparison with the separate mechanical activation and subsequent chemical leaching of complex copper sulfides such tetrahedrite and enargite has been studied

by Baláž & Achimovičová, (2006). The comparison has indicated that the combined mechano-chemical leaching is 25 times more effective than the application of mechanical activation followed by a chemical leaching step (Baláž & Achimovičová, 2006).

An experiment done by Achimovičová and Balaz in 2006 has proven that the use of mechano-chemical activation of gold waste has a positive influence on gold leaching compared to normal leaching (Baláž & Achimovičová, 2006). An optimum gold recovery of 99 % was achieved from the mechano-chemically treated samples after only 90 minutes of thiourea leaching while only 78 % Au dissolution was achieved, for the same leaching time when using the normal leaching process (cyanidation).

2.2.2.8 *Discussion*

The implications of the current work can be summed up as following:
The pre-aeration method can be used to reduce the processing cost of treating sulphidic gold ores by reducing cyanide and oxygen consumption. However, the pre-aeration is not effective when the gold is locked or finely divided in pyrite, arsenopyrite or other sulphide.

Roasting and pressure oxidation are effective in liberating the gold particles from the sulfide matrix and giving high gold recoveries. However, both processes require aggressive leaching conditions such as high temperature and high pressure to achieve acceptable leaching rates and high gold recoveries. Pressure oxidation systems are very expensive to build, and reactions are carried out in autoclaves to withstand highly aggressive conditions of reactions. These autoclaves are costly to install and maintain. On the other hand, the roasting process has inherent issues, such as environment impacts and high production cost. It emits a significant amount of toxic and harmful gases and it is associated with high capital and operating costs due to high energy requirements and the need to comply with stricter environmental standards.
Bio-oxidation is one of the alternative processes to roasting and pressure oxidation which have been shown to reduce the aggressive conditions leading to lower capital and operating costs of leaching plants. It is a simple process operated under atmospheric conditions. It is environmentally friendly, flexible and easy to adapt. Unfortunately, this process suffers from very slow leaching kinetics.
Another alternative is ultra-fine grinding, which is a physical pre-treatment technique that liberates the precious metal from the sulfide matrix. This process has the advantage of not

destroying the host mineral with any oxidative chemical reaction while increasing the gold liberation. The initial fine grind of the mineral results in acceptable leaching rates obtained with less aggressive conditions. However, a disadvantage of fine grinding is the energy costs required to obtain a suitable particle size and the subsequent difficulties associated with the solid-liquid separation process. In addition, not all the refractory gold ores can be treated with ultra-fine grinding under atmospheric conditions. Furthermore, from a solid-state point of view, the application of fine grinding, prior to oxidative leaching, is not entirely effective. It deals only with long-lived excited states while the highly excited short-lived states are not available for subsequent leaching.

Therefore, the combination of fine grinding and oxidative leaching, known as mechano-chemical leaching, is a more attractive process to treat refractory gold ores compared to all the previous pretreatments methods. This process presents the advantage of increasing the leaching kinetics by using the full range of instabilities generated by the distortion of the lattice structure of the mineral.

2.3 CHEMISTRY OF GOLD CYANIDATION

The cyanidation process of gold is a hydrometallurgical technique discovered in the 19th century to extract gold from low grade ore. As in all hydrometallurgical processes, cyanidation has two important considerations that need to be understood. The possibility and extent to which the reaction can proceed (the thermodynamic properties of the reaction) and the rate at which the reaction can take place (the kinetic properties).

2.3.1 Chemistry of cyanide solutions

Gold is naturally very stable, it does not get corroded when exposed to air and does not react in most aqueous solutions, some strong acids included. Gold only dissolve in solutions containing complexing ligands (e.g. cyanide) and under oxidizing conditions. There are three types of salts widely used as cyanide sources for gold cyanidation, sodium cyanide ($NaCN$), potassium cyanide (KCN) and calcium cyanide [$Ca(CN)_2$]. When in contact with water, all three salts decompose and ionize to their respective metal cations and free cyanide anions (CN^-) as presented in the reactions below:

$$NaCN \rightarrow Na^+ + CN^- \quad (2.1)$$

$$KCN \rightarrow K^+ + CN^- \quad (2.2)$$

$$Ca(CN)_2 \rightarrow Ca^{2+} + 2CN^- \quad (2.3)$$

As presented in **Figure 2.6** below, in acidic solutions, free cyanide anions are extremely unstable and hydrolyze to form a very toxic gas, (HCN). At pH values below 9.5 almost 50% of cyanide exists as free cyanide and 50% as hydrogen cyanide. Free cyanide ions only become more stable at higher pH values.

Sometimes, during leaching, hydrogen cyanide and free cyanide can also react with oxygen forming cyanate (CNO^-) which does not contribute to the leaching of gold. These unwanted reactions, presented below, contribute also to reducing free cyanide available to dissolve gold (Marsden & House, 2009).

$$CN^- + H_2O \rightarrow HCN + OH^- \quad (2.4)$$

$$4HCN + 3O_2 \rightarrow 4CNO^- + 2H_2O \quad (2.5)$$

$$3CN^- + 2O_2 + H_2O \rightarrow 3CNO^- + 2OH^- \quad (2.6)$$

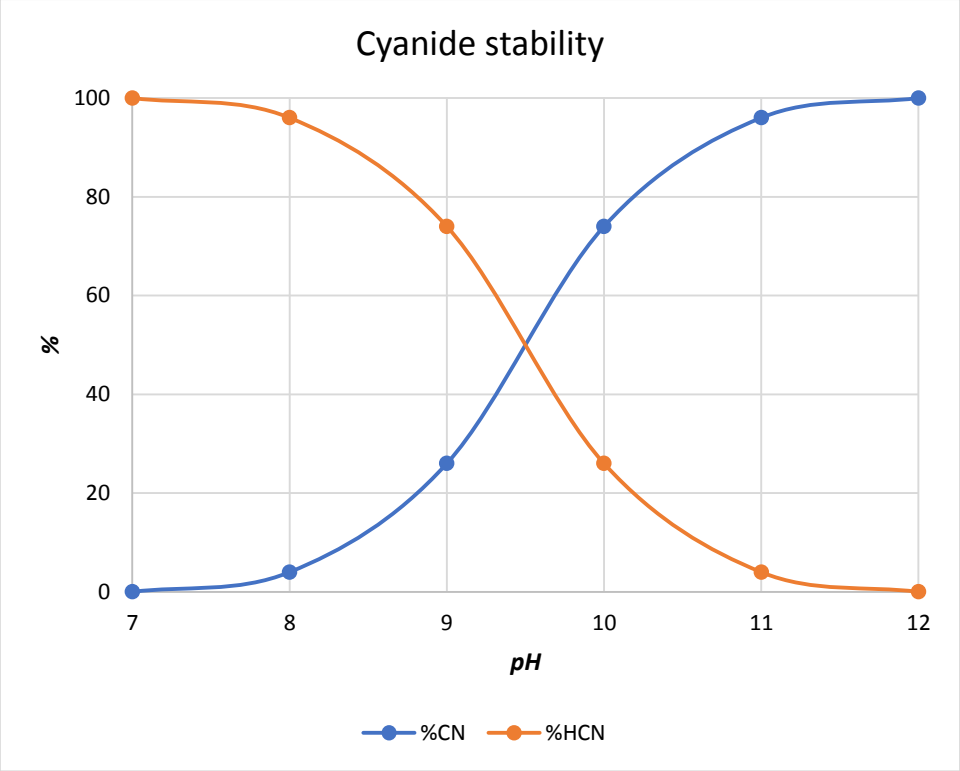


Figure 2.6. : Cyanide stability based on pH

2.3.2 Mechanism of gold dissolution in cyanide solutions

2.3.2.1 *Mechanism of cyanidation*

Gold easily dissolves in cyanide solution and under oxidizing conditions to form a stable complex ion $[Au(CN)_2^-]$. Oxygen reduction is done in two steps, the first step is the formation of hydrogen peroxide as an intermediate product. The second step is characterised by hydrogen peroxide acting also as an oxidizing agent as presented in the reactions below.

$$2Au + 4CN^- + O_2 + 2H_2O \rightarrow 2Au(CN)_2^- + H_2O_2 + 2OH^- \quad (2.7)$$

$$2Au + 4CN^- + H_2O_2 \rightarrow 2Au(CN)_2^- + 2OH^- \quad (2.8)$$

The summation of the two partial reactions give the equation (2.9), known as Elsner equation:

$$4Au + 8CN^- + O_2 + 2H_2O \rightarrow 4Au(CN)_2^- + 4OH^- \quad (2.9)$$

The Elsner's equation is stoichiometrically correct but it does not describe the electrochemical phenomenon associated with the gold dissolution (Marsden & House, 2009).

2.3.2.2 *Thermodynamic considerations*

The thermodynamic stabilities of metals and other species in aqueous solutions can be explained using the redox potential-pH diagram (Pourbaix diagram). However, it is important to talk about the electrochemical mechanism of gold dissolution in order to understand the Pourbaix diagram.

The mechanism of gold dissolution is characterised by the anodic oxidation of gold and the cathodic reduction of oxygen. The complete mechanism of diffusion of gold ion through the interfaces can be summarized into important steps presented below (Wadsworth, et al., 2000).

- ***Anodic reaction of gold oxidation***

The oxidation of gold in cyanide solution can be describe in three steps as presented below:

1. ***Adsorption of cyanide on gold surface (peak at a potential of -0.4V)***

$$Au + {CN^-}_{(Aq)} \rightarrow {AuCN_{(s)}}^- \quad (2.10)$$

2. ***The electrochemical extraction of an electron***

$${AuCN_{(s)}}^- \rightarrow AuCN_{(s)} + e^- \quad (2.11)$$

3. ***Combination of the adsorbed intermediate with another cyanide ion (peak at 0.3V)***

$$AuCN_{(s)} + CN^- \rightarrow {Au(CN)_2}^-{}_{(Aq)} \quad (2.12)$$

The overall oxidation reaction of gold can therefore be summarised as follow:

$${Au(CN)_2}^- + e^- \rightarrow Au + 2CN^- \quad (2.13)$$

The Nernst equation of gold oxidation is presented below:

$$E_h = -0.60 + 0.118pCN + 0.059\log\left(C_{{Au(CN)_2}^-}\right)V \quad (2.14)$$

It has been shown by Kirk et al (1979) that Au(I) is formed throughout a potential range of -0.65 to 0.55V. At higher potentials, it is possible to also form Au(III). This was later on confirmed by Nicol (1980), in a study where current versus potential curves were plotted. Nicol demonstrated that the anodic reaction of gold in cyanide solution is characterised by three peaks occurring respectively at potentials of about -0.4V, 0.3V and 0.6V as presented in **Figure 2.7**.

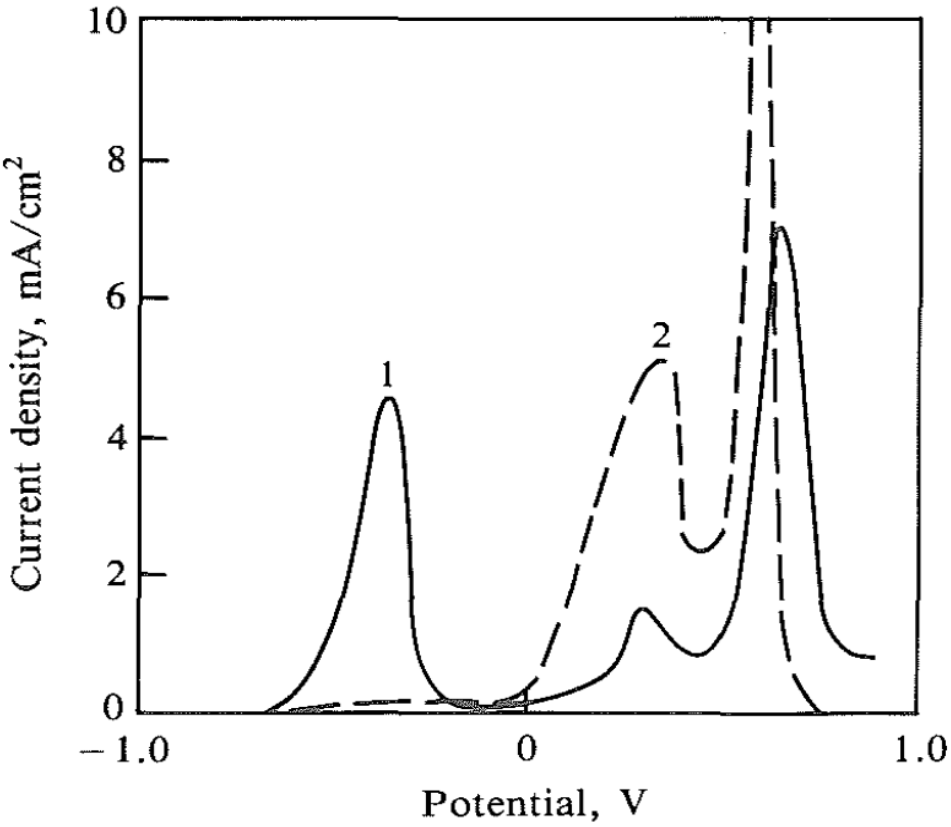


Figure 2.7. : Current versus potential curves for the oxidation of gold in alkaline cyanide solutions (Nicol, et al., 1979; Nicol, 1980).

This study also revealed that the three peaks are associated with the generation of three passivating films. The first peak, at -0.4V, is associated with the formation of a cyanide film on the gold surface during adsorption of cyanide. The second peak, usually observed at 0.3V, is associated with the complexation reaction between the adsorbed intermediate AuCN and free cyanide. The passivation of gold can be avoided by using heavy metals such as lead, mercury, bismuth and thallium, which disrupt the formation of the passivating film (Marsden & House, 2009). Since the potential during gold cyanidation does not overreach 0.5V, the last peak occurring at 0.6 to 0.7V is not likely to occur due to the highly positive potential required. This peak is however, believed to be caused by the formation of an oxide layer of Au (III) which passivates the surface of gold (Marsden & House, 2009).

The anodic mechanism of gold oxidation has been studied in detail by Senanayake (2008) to explain the complete solid-liquid interaction taking place in the cyanidation process (**see Figure 2.8**).

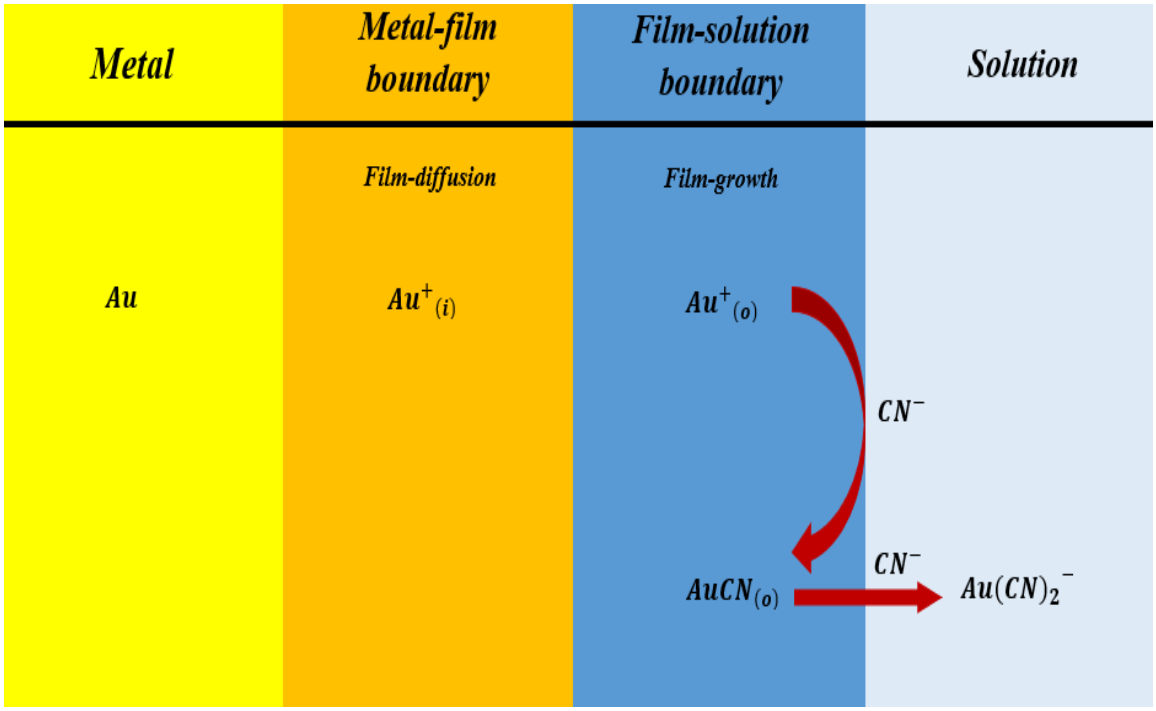


Figure 2.8. : Anodic cyanidation model for gold (Senanayake, G., 2008).

- **Cathodic reduction of oxygen**

1. ***Oxygen reduction into hydrogen peroxide***

$$O_2 + 2H_2O + 2e^- \rightarrow H_2O_2 + 2OH^- \quad E_h = 0.69 - 0.059pH - 0.0295pO_2 \tag{2.15}$$

2. Hydrogen peroxide decomposition

$$2H_2O_2 \rightarrow O_2 + 2H_2O \tag{2.16}$$

3. Oxygen reduction to hydroxide ions

$$O_2 + 2H_2O + 4e^- \rightarrow 4OH^- \qquad E^0 = 0.401\,V \tag{2.17}$$

Sometimes, hydrogen peroxide can also be reduced into hydroxide ions as follow:

$$H_2O_2 + 2e^- \rightarrow 2OH^- \qquad E^0 = 0.88\,V \tag{2.18}$$

However, it has been shown by Marsden (1992) that the above reaction (2.18) is difficult to take place and the dissolution rate of gold using only hydrogen peroxide (in absence of free oxygen) is very slow.

Schematically, the electrochemical reaction and the corrosion reaction of gold leaching in cyanide solution can be described as presented in **Figure 2.9** below:

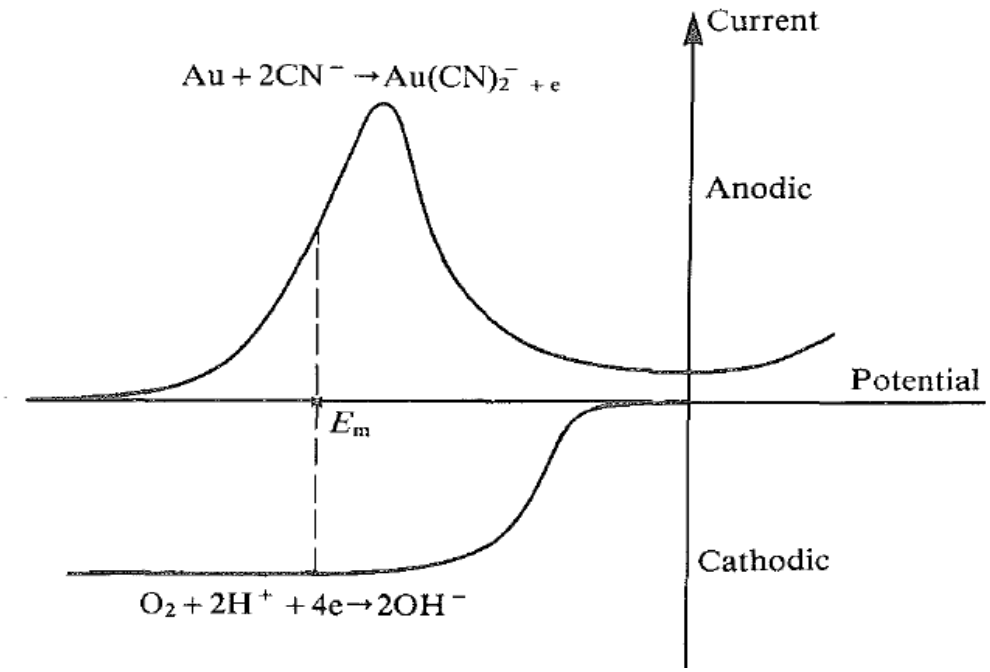


Figure 2.9. : The simplified schematic diagram of mixed potential model for the dissolution of gold in cyanide solutions (Marsden & House, 2006).

This figure simply shows how the oxidation of gold at the anode is coupled to the reduction of oxygen at the cathode. During cyanidation, the gold surface immersed in an aerated alkaline cyanide solution will experience dissolution. The rate of the overall reaction is governed by the fact that the rate of the oxidation process is equal to the rate of the reduction process. This potential is known as the mixed potential, or potential at which the two rates are equal.

- **Pourbaix diagram**

The thermodynamic stabilities of metals and other species in aqueous solutions can be explained using the redox potential-pH diagram or Pourbaix diagram. The Pourbaix diagram is characterized by many lines subdividing the diagram into different areas. Each area represents a zone of stability of a specific species or phase while each line represents the conditions where the activities of reactants and products of the considered reaction are in equilibrium.

The redox potential diagram of gold presented in **Figures 2.10** and **2.11** indicate that in a cyanide solution, the reaction of gold to produce the Au(I) complex takes place more readily than that of the formation of the Au(III) aqua cation. This is because the Eh value of the Au(I) complex reaction is more negative than the one for Au(III) ion. It has been shown by

Wadsworth et al. (2000) that gold dissolution in alkaline cyanide solution as $Au(CN)_2^-$ occurs at the redox potential range of -0.4 and -0.7 V. The Pourbaix diagram can also be used to explain the role of other minerals competing with gold during cyanidation (such as iron and copper). Iron is one of the most competitive metal that disturbs the cyanidation process. It can be seen from **Figure 2.12** and from **Table 2.3** that Fe(II) is more reactive than even Au(I) complex ion because the reaction producing Fe(II) complex, in cyanide solution, has a more negative value compared to the reaction generating the Au(I) complex. Therefore, most of the cyanide will first react with Fe(II) before reacting with Au(I) (Kumar, et al., 2016). This phenomenon is also observed when dealing with copper and zinc.

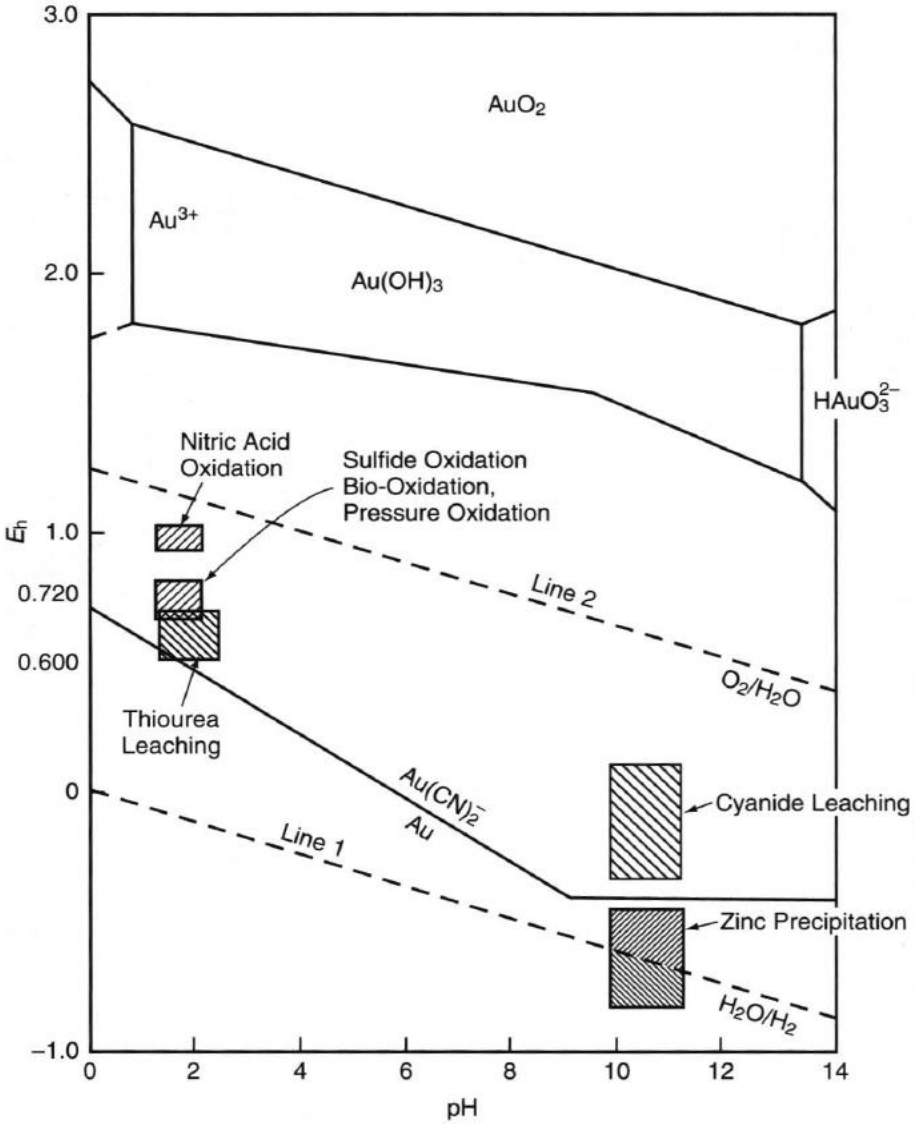


Figure 2.10. : Indicative Eh-pH ranges employed In Industrial gold extraction processes (Marsden & House, 2009).

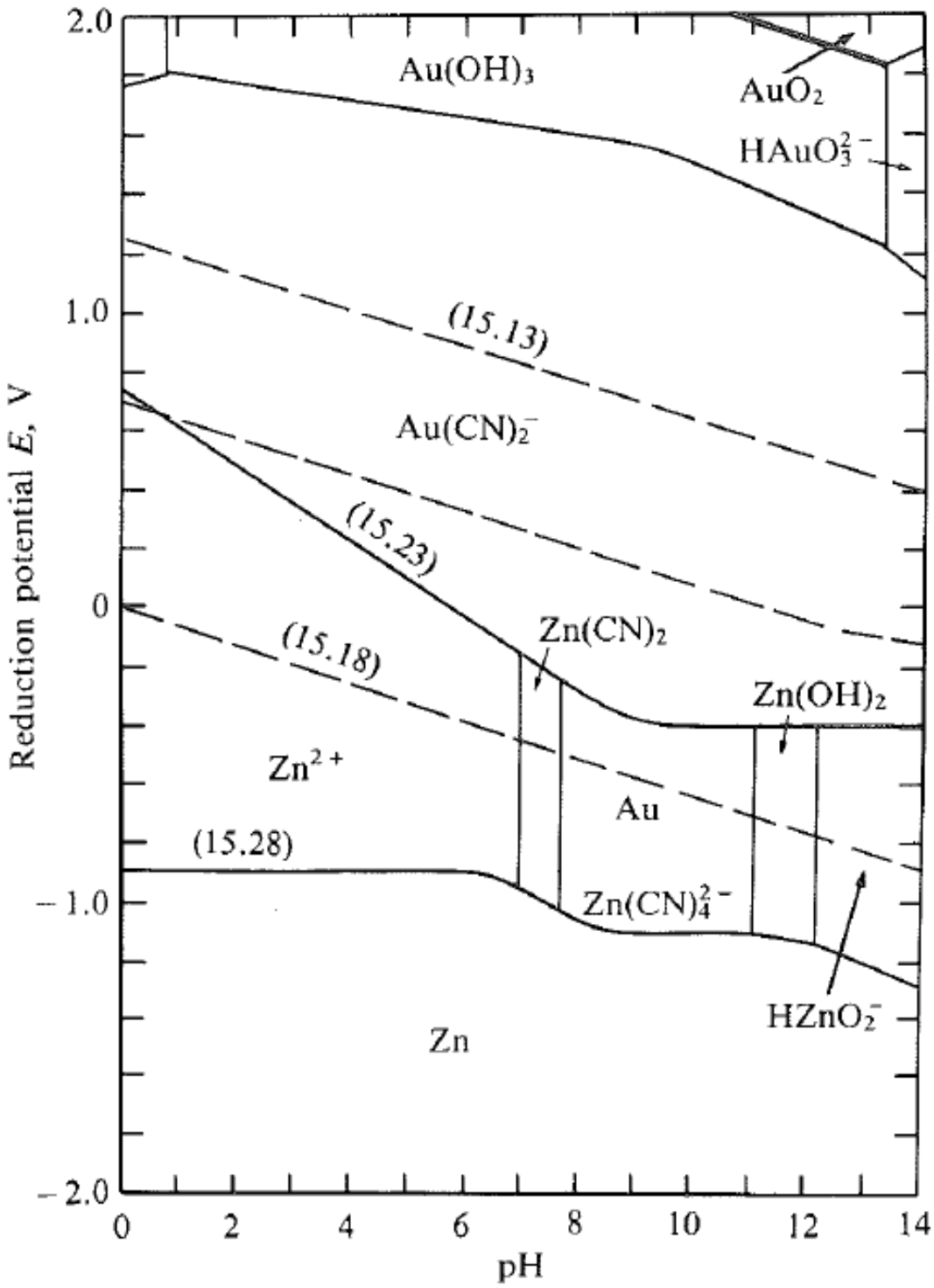


Figure 2.11. : Pourbaix diagram illustrating features of $Au - CN - H_2O$ systems at 25℃. $[CN^-]_{total} = 10^{-3} mol\ l^{-1}$, $[Au(CN)_2{}^-] = 10^{-4} mol\ l^{-1}$, $[Zn^{2+}]_{total} = 10^{-3} mol\ l^{-1}$.

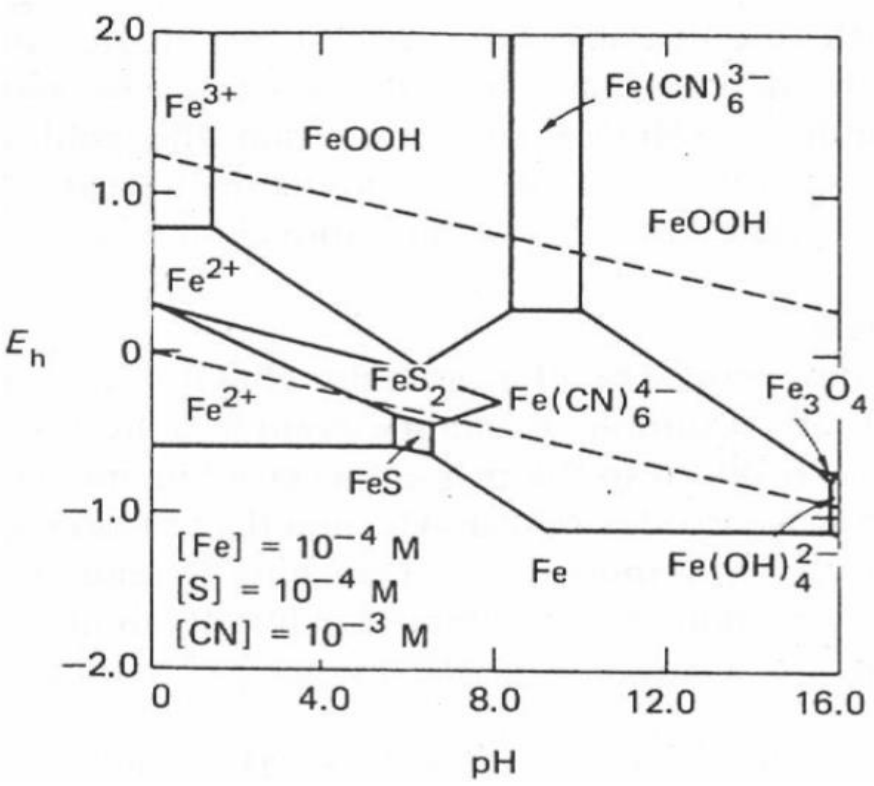


Figure 2.12. : Eh-pH diagram for the Fe-S-CN-H_2O system at 25℃ (Marsden & House, 2009).

Table 2.3 ***: different cyanide complexes anions with stability constant (Kumar, et al., 2016)***

Anions of cyanide	Name	Type of complex	Stability Constant (log K at 25℃)
[Co(CN)6]3−	hexacyanocobaltate (III)	Strong	64
[Fe(CN)6]3−	hexacyanoferrate (III)	Strong	43.6
[Pd(CN)4]2−	tetracyanopalladat(II)	Strong	42.4
[Pt(CN)4]2−	tetracyanoplatinate (II)	Strong	40
[Hg(CN)4]2−	tetracyanomercurate (II)	Strong	39
[Au(CN)2]2−	dicyanoaurate (I)	Strong	37
[Fe(CN)6]4−	hexacyanoferrate (II)	Strong	35.4
[Ni[CN)4]2−	tetracyanonickelate (II)	Weak	30.2
[Cu(CN)4]3−	tetracyanocuperate (I)	Weak	23.1
[Ag(CN)2]−	dicyanoargentate (I)	Weak	20.5
[Zn(CN)4]2−	tetracyanozincate (II)	Weak	19.6
[Cd(CN)4]2−	tetracyanocadmium (II)	Weak	17.9

("A **stability constant** (formation constant, binding constant) is an equilibrium constant for the formation of a **complex** in solution. It is a measure of the strength of the interaction between the reagents that come together to form the complex. There are two main kinds of complex: compounds formed by the interaction of a metal ion with a ligand and supramolecular complexes, such as host–guest complexes and complexes of anions. The stability constant(s) provide the information required to calculate the concentration(s) of the complex(s) in solution. https://en.wikipedia.org/wiki/Stability_constants_of_complexes")

2.4 CONSIDERATION OF REACTION KINETICS

The thermodynamic considerations can only predict if a reaction is able to happen. However, for design and economics considerations, it is important to also determine how fast a reaction is expected to happen (reaction rate).

The chemical reaction kinetics and the mass transport of each reacting species are the two principal components controlling all heterogeneous reactions. For the cyanidation process, the reaction mechanism can be summarised in four stages as follow (see **Figure 2.13**):

a. Mass transport of oxygen gas into the solution phase and subsequent dissolution;
b. Mass transport of cyanide and dissolved oxygen ($CN^-, O_{2(dis)}$) through the solution-solid boundary layer, to the solid surface;
c. Electrochemical reaction at the solid surface, including adsorption and desorption at the solid surface and across the electrical double layer;
d. Mass transport of reacted species ($Au(CN)_2{}^-$, H_2O_2 and OH^-) through the boundary layer into bulk solution.

When stage c is the controlling rate factor, the reaction is chemically controlled. However, the reaction is mass transport controlled when the major controlling factor is a, b or d. A reaction is under mixed control when it is controlled at the same time by the mass transport and the electrochemical reaction. It is also important to note that a reaction that is mass transport controlled can change to chemical or electrochemical reaction control when the rate limiting reactant concentration is increased.

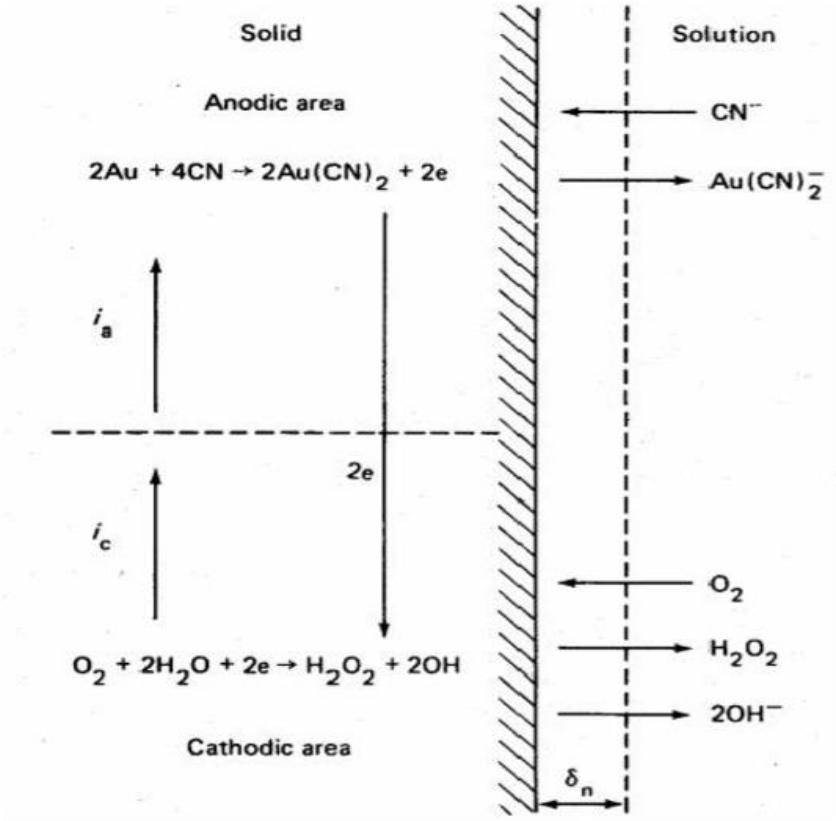


Figure 2.13. : Schematic representation of the local corrosion cell at a gold surface in contact with an oxygen-containing cyanide solution. i_a is the anodic current; i_c is the cathodic current (Marsden & House, 2009).

In most industrial cyanidation processes, the chemical or electrochemical reaction step is rarely the rate limiting step unless when operating at high cyanide and oxygen concentration (intensive cyanidation). It has been proven that in the cyanidation process, cyanide and oxygen diffusion are two most important parameters which determine the rate limiting conditions. Therefore, the rate limiting factor will be provided by the slower diffusion rate between the two species (Marsden & House, 2009).

- At low cyanide concentration the rate of dissolution increases when the cyanide concentration increases while the mixed potential decreases.
- At higher cyanide concentration, the rate of gold dissolution is no longer dependent on the cyanide concentration and the mixed potential keeps on decreasing. An increase in the oxygen concentration will result in an increase in the rate of dissolution. This is due to the fact that the reduction curve of oxygen will be shifted in a positive direction. It is therefore important, for a given oxygen concentration, to

determine the cyanide concentration at which the rate of both anodic and cathodic reactions occur.

2.4.1 Kinetic Models

The rate equation for a reaction involving two substances A and B can be written as follow:

$$Rate = k[A]^a[B]^b \tag{2.19}$$

Where:

- Rate = rate of reaction in $mol\ dm^{-3}s^{-1}$
- k = rate constant
- $[A]$ and $[B]$ = concentrations in $mol\ dm^{-3}$
- a and b = orders of reaction with respect to A and B

The rate constant for a reaction can therefore, be expressed using the Arrhenius equation, as shown below,

$$k = A\ e^{-E_a/RT} \tag{2.20}$$

Where:

- A = the Arrhenius constant related to collision frequency of solution species
- E_a= the activation energy for the reaction
- R = the gas constant
- T = temperature in Kelvins

The derivation of equation (2.20) leads to the value of the activation energy as presented in equation (2.21). E_a is graphically represented by plotting log k versus $1/T$ and calculating the slope of the line (E_a/R).

$$E_a = RT^2 \frac{d\ lnk}{d\ T} \tag{2.21}$$

When the value of E_a is greater than 40 kJ/mol., the reaction is chemically controlled, while the reaction is mass transport controlled when it is between 5 and 20kJ/mol. However, the reaction is mixed when the activation energy is between 20 and 40 kJ/mol. The activation energy of most cyanidation processes of gold have their activation energies within the range showing mass transfer as the limiting rate (Marsden & House, 2009).

The kinetics of a reaction can also be represented by the general expression below:

$$dC/dt = -k_m C^n \tag{2.22}$$

Where

- C: the concentration of reacting species
- t: time
- k_m: a rate constant
- n: the reaction order

The integration of equation (2.22) produces another equation that shows how the concentration evolves with time for a given rate constant and reaction order. For a first order reaction (n=1), the concentration after a given time t can be express as follows:

$$C_t = C_0\, e^{-kt} \qquad (2.23)$$

With C_0 the initial concentration of reactant.

It is important to note that most cyanidation process can be approximated to the first order reaction, except for the intensive cyanidation which has higher order reactions.

2.4.2 Mass transfer

There are two major considerations related to the mass transfer in heterogeneous systems. Mass transfer through the boundary layer close to the solid particle and the mass transfer in the bulk solution.

2.4.2.1 *Mass transfer through the boundary layer*

There is always a boundary layer which is established between the solid surface and the bulk solution. This theory comes by assuming that the velocity of the solution at the solid surface must be equal to zero. Therefore, a velocity profile can be developed whereby the solution velocity increases with increasing distance from the solid surface until it reaches a maximum steady velocity in the bulk solution (Marsden & House, 2009).

Fick (1856) has established that the mass transfer of reactant ions and species through the boundary layer occurs by diffusion which results from the gradient concentration between the reactant in the bulk solution and the lower concentration at the solid surface (driving force). However, it is important to note that the transfer process of reactant is also affected by Brownian motion and the electron tunnelling which increases the net transfer of ions through the boundary layer.

The boundary layer thickness (δ) is defined as the distance from the solid surface to the nearest point at which the velocity equals the steady velocity in the bulk solution (Marsden & House, 2006). The concentration gradient through the boundary layer is described by Fick's law as presented in the equation below:

$$\frac{dn}{dt} = -D_i A \frac{dc}{dx} \quad (2.24)$$

Where:

- dn: number of moles flowing through a plane of surface area (A) during a time dt;
- $\frac{dn}{dt}$: the diffusion driving force (j_d);
- D_i: diffusion coefficient (depending on the size the species, the solution temperature and viscosity)

Fick's equation can also be represented in a more simplified form as given below by Nernst:

$$j_d = D_i A\,(C_0 - C_i)\,/N \quad (2.25)$$

Where:

- N= Nernst diffusion layer thickness
- C_i= concentration of species i in solution
- C_0= concentration of species i at the solid surface

When the concentration of reactant at the solid surface is zero, this means that the chemical reaction is enough to consume all the reacting species, therefore the reaction depends on the mass transfer rate of the reacting species from the bulk solution to the solid surface. However, if the reacting species are not fully consumed at the solid surface, the reaction is limited by the reaction rate and therefore, it is described as a chemically controlled reaction.
In the case where the concentration at the solid surface is zero, the equation (2.25) reduces to:

$$j = -D_i.C_b/N \quad (2.26)$$

And then

$$j = -K_m.C_b \quad (2.27)$$

Where

- C_b=concentration of species i in the bulk solution
- $K_m(= D_i/N)$= mass transfer coefficient which is equivalent to the first-order chemical rate constant.

There are three ways to increase mass transfer of reacting species through the diffusion layer:

- Reduce the diffusion layer thickness;

It is important to note that the diffusion layer depends on the roughness of the solid surface; the viscosity of the liquid; solid and solution flow rates; stirring or mixing rates as well as the degree of turbulence in the bulk solution. The diffusion layer can therefore, be minimized by increasing the solution flow rate and by increasing the shear rate (e.g. better reactor design, use of high shear impellers and baffles in tanks). A system characterised by boundary layers equal or greater than 0.5 mm is classified as poor mixing system; while good mixing systems generally are characterised by boundary layer equal or below 0.01 mm.

- Increase the concentration gradient by increasing solution concentration;
- Increase solution temperature.

Even though increasing temperature has a positive effect on the kinetics, there is a limit at which it reduces oxygen solubility dramatically and therefore, no longer increases the overall reaction rate.

2.4.2.2 *Mass transfer in bulk solution*

Generally well-agitated leaching systems are effective and do not have any problems with mass transfer in bulk solution. However, due to inherent particulate and/or engineering factors, some solutions and slurries have a poor quality of mixing; and the mass transfer in bulk solution becomes a very important parameter. It is therefore, crucial to ensure good mixing in the bulk solution or slurry to maintain homogeneity (e.g., pH, sodium cyanide) and prevent dead zones in the reactor. The mixing must also maximize the transfer of reacting species through the diffusion boundary layer, since this is often the rate controlling factor.

2.4.3 Absorption of gases in liquids

To prevent the absorption phenomenon becoming rate limiting, it is important to maintain, in excess, the concentration of oxygen compared to the rate of consumption (Danckwerts, 1964; Marsden & House, 2009). This can be achieved by using simple gas addition techniques and by replacing the use of air with pure oxygen. However, the rate of oxygen absorption, rather than diffusion, can be the rate-limiting factor for some mass transfer-controlled processes. The gas absorption rate is a function of the following parameters:

- Surface area of the liquid;
- Superficial velocity of gas bubbles;
- Partial pressure of the gas;
- Degree of agitation;

- Temperature;
- Concentration of dissolved oxygen and other species;
- Liquid viscosity.

It is important to note that, the absorption rate of gases (oxygen or air in this case) is increased by increasing the three first factors and decreased by increasing the last four factors. The surface area of the liquid, in contact with oxygen, is a function of the size and number of oxygen bubbles in the system. The smaller the bubbles, the higher the surface area and the higher the number of bubbles produced, the higher the surface area. Therefore, the surface area of the liquid is a crucial parameter in the selection of a sparging system to use for leaching processes involving gas absorption. The number and size of bubbles produced depend on how efficient the sparging system is and how vigorous the mixing is (Marsden & House, 2006).

The superficial velocity of the gas is also a function of the sparging rate and the sparging method. However, the energy required to increase the superficial velocity of bubbles is extremely high. Generally, gases solubility's in liquid are higher at low temperatures, but decreases when the temperature increases as presented in **Figure 2.14**. Compared to the other factors, temperature has less impact on absorption and the operating temperature is selected based on its impact on the reaction kinetics and not based on the maximum solubility.

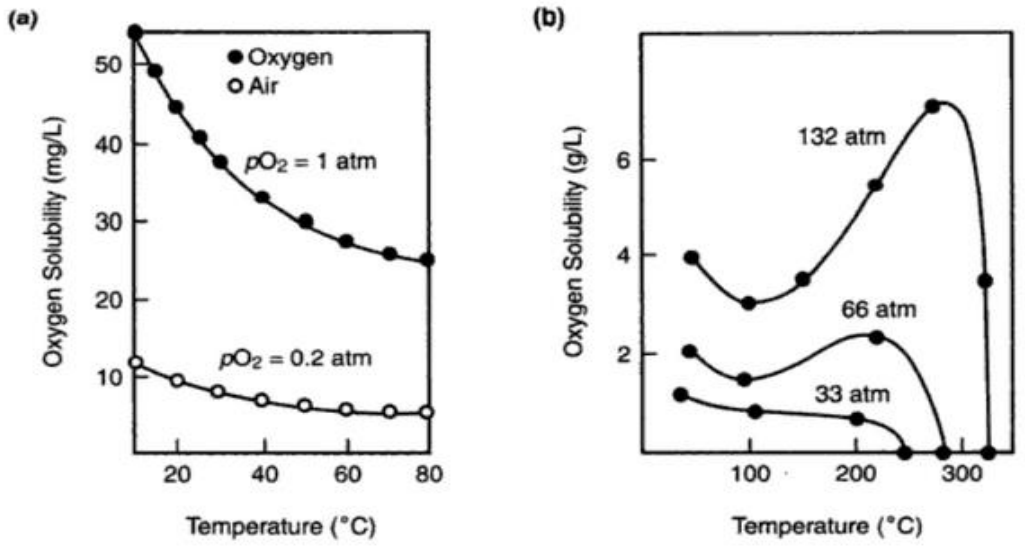


Figure 2.14. : (a) Effect of temperature and gas composition on oxygen solubility in water (b) Effect of temperature and pressure on pure oxygen solubility in water (Hollow, et al., 2005)

The overall driving force for absorption of a gas into a liquid is given by the partial pressure of the gas and the concentration of dissolved gas species. The absorption increases when the partial pressure increases until reaching saturation of the dissolved gas in the liquids (equilibrium liquid-gas), then any increase of the partial pressure will result in slower absorption rate. It is not important to worry about the partial pressure because most cyanidation process are controlled by solid-liquid mass transport rather than partial pressure (Marsden & House, 2009).

It is also important to note that the amount of pure oxygen, or air, used during cyanidation will depend on the absorption kinetics, the efficiency of the mixing system and the gas removal or venting requirements. Therefore, any maximization of pure oxygen or oxygen in air usage will result in minimizing the process cost.

2.4.4 Particulate factors of the slurry

There are in total 5 major factors which control the surface area available to react with the solution phase reactant and therefore, play an important role in the kinetics and the degree of completion of leaching reactions. These factors are presented as follows:

2.4.4.1 *Particle size*

Particle size is one of the main factors affecting the surface area of a mineral particle. The degree of liberation of mineral has, therefore, very crucial impact on the leaching kinetics. The finer the particle the faster the kinetics. Surely the reaction rate per unit of exposed surface area would be the same, it is just that there is more exposed surface area. However, there are two major parameters to consider, the energy required for further comminution and the reagent consumption which also increases when dealing with finer particles. Therefore, it is of importance to ensure optimum liberation of gold from the host rock.

2.4.4.2 *Shape and texture*

Dealing with particles having irregular shapes and rough surfaces amplifies the turbulence of the fluid hydrodynamics around particles. In the case of diffusion-controlled reactions this may affect positively the reaction rate. However, the effect of shape and texture generally have a small impact on the overall kinetics. These factors are only significant in reducing the leaching time of gold particles during ultrafine grinding (Marsden & House, 2006).

2.4.4.3 *Mineralogical factors*

Many factors such as crystal orientation, polycrystallinity and the presence of inclusions, dislocations and impurities affect the reactivity of mineral grains. It has been shown that, generally, minerals present faster kinetics if there are imperfections and many smaller crystals within a mineral grain. The kinetics can also be affected by the presence of other minerals in the ores which may react with reagents in the chemical system. These other minerals such as copper, pyrite and other sulphides are reagent consumers and their reaction may retard the rate of the main reaction (LI, 2009).

2.4.4.4 *Porosity*

Porosity increases the accessibility of the leaching solution allowing access to more gold particles. Therefore, porous ores usually have faster leaching kinetics compared to none porous ores. However, if the reaction rate is too fast, the reagent is consumed before penetrating the particle and, in that case, the surface area is less significant (Marsden & House, 2009).

2.4.4.5 *Effect of competing species*

The kinetics can also be affected by the presence of other minerals in the ores which may react with reagents in the chemical system. As illustrated in section 2.2.2.3, other minerals such as copper, pyrite and other sulphides are reagent consumers and their reaction may retard the rate of the main reaction (LI, 2009). T

2.4.5 Practical parameters affecting the cyanidation process

Several investigations on leaching parameters have been widely undertaken in order to determine and optimize the performance of the cyanidation process (Olyaei, et al., 2014; Hlabangana, et al., 2018). The performance of the cyanidation process of refractory gold ores depends on many physical and chemical variables such as pressure, temperature, concentrations of dissolved oxygen, free cyanide and compounds that react with cyanide, pH, particle size and operating conditions.

2.4.5.1 *Concentration of Oxygen*

Oxygen is one of the important reagents in gold cyanidation as shown in the gold dissolution reactions highlighted below

$$2Au + 4CN^- + O_2 + 2H_2O \rightarrow 2Au(CN)_2^- + H_2O_2 + 2OH^- \quad (2.28)$$

$$2Au + 4CN^- + H_2O_2 \rightarrow 2Au(CN)_2^- + 2OH^- \quad (2.29)$$

The summation of the two partial reactions give the equation (3), known as Elsner equation:

$$4Au + 8CN^- + O_2 + 2H_2O \rightarrow 4Au(CN)_2^- + 4OH^- \qquad (2.30)$$

Ellis and Senanayake (2004) have suggested that the use of air instead of pure oxygen provides a low oxygen concentration in gas which decreases the oxygen solubility and can achieve low overall gold extraction. In 1995, Kondos et al., found that oxygen consumption is markedly higher with the use of pure oxygen than air. Kondos et al., (1995) further concluded that the oxygen consumption depends on the mineralogical compositions of an ore, for example, pyrite-rich ore has a higher oxygen demand than the ore containing albite, quartz and chlorite as the main minerals (Adams; 2016). It has been also shown that oxygen consumption depends on the amount of oxygen gas that can be converted into dissolved oxygen. Oxygen loss is therefore defined as the amount of oxygen that could not be dissolved in the slurry and was lost to the atmosphere (Flatman & Vorster, 2001).

Many factors such as temperature, pressure and ionic strength may affect the oxygen solubility (Ellis and Senanayake, 2004). However, the ionic strength is relatively low and its effect on gas solubility is not important (Ling et al. 1996; Adams. 2016). Therefore, the oxygen dissolution in a solution is mainly affected by temperature and pressure.

Several researchers have concluded that the gold dissolution rate increases with an increase in dissolved oxygen concentration (Marsden and house, 1992; Deschênes et al., 2003; Ellis and Senanayake, 2004; Senanayake et al 2018). However, in 2008 Srithammavut concluded that, at a cyanide concentration level of 104 ppm, high dissolved oxygen concentration did not have a significant effect on gold dissolution. Optimum levels of cyanide and oxygen in solution must be maintained to allow an adequate gold dissolution (Flatman & Vorster, 2001).

2.4.5.2 *Cyanide Concentration*

Many studies on gold leaching have concluded that gold extraction of refractory ores increases with increasing cyanide concentration (Marsden and House, 1992; Kondos et al., 1995; Ling et al., 1996; Wadsworth et al., 2000; Deschênes et al., 2003; Adams; 2016). Ling et al. (1996) have found that the gold dissolution rate was not very sensitive to the change in cyanide concentration at high cyanide levels. This was also found by Deschênes et al. (2003) who concluded that the use of 400-500 ppm NaCN resulted in similar overall gold extractions.

2.4.5.3 *pH*

The gold dissolution of refractory ores is also affected by the pH values prevailing. When the pH increases, the gold dissolution rate is expected to decrease because of the adsorption of OH^- ion onto gold surface that decreases the surface available for cyanide leaching (Kondos et al., 1995; Ling et al., 1996; M.D. Adams; 2016). It is also because of the increase in the rate of competing reactions such as dissolution of sulfides and other reactive species (Adams; 2016).

To control and maintain the pH in the cyanidation process, an addition of an alkali, such as lime (CaO) is required (Ling et al., 1996; Ellis and Senanayake, 2004). Ling et al (1996) have also reported that a high pH level results in lower cyanide consumption and lower gold recovery. In 2004, Ellis and Senanayake reported that at high pH, cyanide leaching is able to minimize the formation of hydrogen cyanide which tends to cause cyanide loss as HCN gas. Parga et al. (2007) have indicated that when the pH increases, the gold extraction for a high-pressure system decrease. This is because Ca ions appear to react with cyanide, inhibiting the main reaction between cyanide and gold, hence the use of alternatives to CaO (Davidson & Sole, 2007).

2.4.5.4 *Particle Size*

Different researchers (Ling et al. 1996, Lima and Hodouin. 2005) have investigated the effect of particle size on gold dissolution and found that a smaller particle size provides a larger contacting surface area between solid and liquid and thus increases the rate of dissolution. However, Adams et al (2016) have reported that the finer the particles, the higher the cyanide consumption and consequently not much improvement in the gold extraction. This may be due to the presence of residual gold in fine occlusions, or in solid solution in the mineral matrix. Ellis and Senanayake (2004) reported that, because of energy consumption, the grinding costs increase with each grinding step. Therefore, the choice of an optimal particle size is critical to the all process. Comminution is very expensive, particularly at the very fine sizes being considered. There is an opportunity to look at an attainable region where additional comminution pays off with additional gold and beyond which further comminution is supported by further gold recovery.

2.4.5.5 *Temperature*

Temperature is an important parameter in the gold leaching phenomenon because it has a significant effect on oxygen solubility and gold dissolution rate. The reaction rates of metals in solution are expected to increase when temperature increases. The viscosity of a liquid decreases when the temperature increases. Consequently, the diffusivities also increase. As the gold dissolution depends on the diffusion rate, therefore, the gold dissolution is expected to increase with increasing temperature (Ellis and Senanayake, 2004; Senanayake et al 2018). However, the gold dissolution in cyanide solution reaches a maximum at 85ºC. Beyond 85ºC, the dissolution of oxygen gas in solution decrease which consequently affects the gold dissolution and therefore, leads to the dissolution of undesirable minerals. That is why ambient temperature is usually required (Adams, 2016). However, for the improvement of gold extraction at high temperatures, operating at high pressure can be implemented (W. Srithammavut, 2008).

2.4.5.6 *Pressure*

As with the temperature, pressure can also improve the gold dissolution in terms of gas solubility. The solubility of gas in an aqueous solution increases when the pressure increases (Ling et al., 1996; Ellis and Senanayake, 2004). Leaching under high pressure conditions can help to treat pyritic refractory gold ores (Fleming, 1992, Srithammavut, 2008).

2.4.5.7 *Slurry Density*

The slurry density normally used for gold leaching is between 35% and 50% of solids. This depends on the particle size, the specific gravity of solids and the presence of minerals that may affect the slurry viscosity (such as clays). The mass transfer of reagents to the ores surfaces increases when the slurry density is low. However, an increase in slurry density can reduce the stoichiometric availability of reagent to exposed gold surfaces and the solids retention time in the reactor (Adams & Wills, 2005; Flatman, et al., 2010; Adams, 2016).

2.4.5.8 *Mixing*

Mixing is one of the key factors in gold leaching because the gold dissolution rate depends on the mode of mixing in the bulk solution and the diffusion layer thickness (Srithammavut 2008). The gold dissolution rate can be improved by increasing the agitation speed since the intense mixing reduces the diffusion layer thickness which then increases substantially the mass transfer rates of cyanide and oxygen (Ellis and Senanayake, 2004). However, as mentioned in section **2.4.2**, increasing the agitation speed has a negative effect on the

absorption of oxygen in cyanide solution. Therefore, the mixing speed must be chosen adequately in order not to affect the absorption process.

2.4.5.9 *Presence of interfering minerals and ions in solution*

The gold leaching rate is usually affected by the presence of many metals and minerals. Most of these metals and minerals are also able to dissolve in alkaline cyanide solution, contributing, therefore, to an increase in cyanide and oxygen consumption. Many researchers, however, have found that some ions enhance the gold dissolution rate (Aghamirian & Yen, 2005; Marsden & House, 2009).

In general, sulphide minerals easily decompose in alkaline cyanide solution. These reactions are characterised by the presence of sulphide ion (S^{2-}) as the principal anion. Once in solution, sulphide ions are strongly adsorbed onto the surfaces of gold resulting in the formation of a passivation layer of sulphide which inhibits further gold dissolution (Kondos, et al., 1995). However, it has been found that the effect of sulphide minerals on gold dissolution depends on the type of mineral and the concentration of oxygen in the solution (Liu & Yen, 1995; Aghamirian & Yen, 2005).

Pyrite, pyrrhotite and chalcopyrite, for example, beside sulphide ions, introduce into solution other cyanicides elements such as iron and copper (Breuer, et al., 2008). Arsenopyrite and galena however, introduce species such as lead (Pb) and arsenic (As) which, when in small amount, contribute to the improvement of the gold leaching rate. It was also found that the concentration of sulphide ions contributing to the passivation of gold in cyanide solution is sensibly decreased with the addition of lead ions (Deschênes & Wallingford , 1995; Deschênes, G. et al., 2000; Senanayake, G., 2008).

2.5 IMPROVEMENT IN THE GOLD CYANIDATION PROCESSES

The extraction of gold from its host mineral using cyanide solution is a method discovered in 1890 by MacArthur-Forrest. This process quickly became a standard method used for recovering gold from most ores worldwide. Almost 44% of the total gold produced in the world is by use of the cyanidation processes (Lakshmanan & Roy, 2016). However, depending on the mineralogy and the grade of gold in the ore, many variations of the cyanidation processes have been developed. All these processes for the recovery of gold from cyanide can be grouped in two main processes, the Merrill-Crowe process and the Carbon adsorption process. It is also important to note that, in each process, numerous leaching reactors have been developed to improve leaching kinetics.

2.5.1 Merrill-Crowe Process

The Merrill-Crowe process is an amelioration of the MacArthur-Forrest process, where additions of vacuums are integrated to remove air in the solution (contribution of Crowe). In addition, zinc dust is also added to the solution in order to precipitate gold by cementation as presented in the following reaction.

$$2Au(CN)^{2-} + Zn^{0} \rightarrow 2Au^{0} + Zn(CN)_4^{2-} \qquad (2.31)$$

Before cementation takes place, a solid-liquid separation step is required to remove the solids particles from the solution. This separation can be done using methods such as counter current decantation (CCD) followed by filtration on horizontal leaf type clarifiers. To improve the solution clarity, another filtration step is required, but this time, using pre-coated filters applying diatomaceous earth. Oxygen or air is then removed from the solution by passing the clear solution through a vacuum de-aeration column. Removing of oxygen and air is then followed by cementation using zinc powder (Angelov & Groudev, 2002). Oxygen is removed from the solution to avoid any passivation of zinc which will result in cessation of gold deposition (Nicol, et al., 1979).

2.5.2 Carbon Adsorption process

In this process, granular coconut shell-activated carbon is widely used for recovery of gold from cyanide solutions. The adsorption process can be applied to clean solutions through fluidized bed adsorption columns, or directly to leached ore slurries by the addition of carbon to agitated slurry tanks, followed by separation of the carbon from the slurry by coarse

screening methods. There are three main processes that use carbon adsorption to recover gold from cyanide solution (Fast & Associates, LLC, n.d.).

2.5.2.1 *Carbon-in-pulp (CIP) process*

The carbon-in-pulp process has become one of the most utilized methods to leach and recover gold. This process comprises two main sections which are the leaching section followed by carbon adsorption section. The completed CIP flow sheet is presented in **Figure 2.15** below.

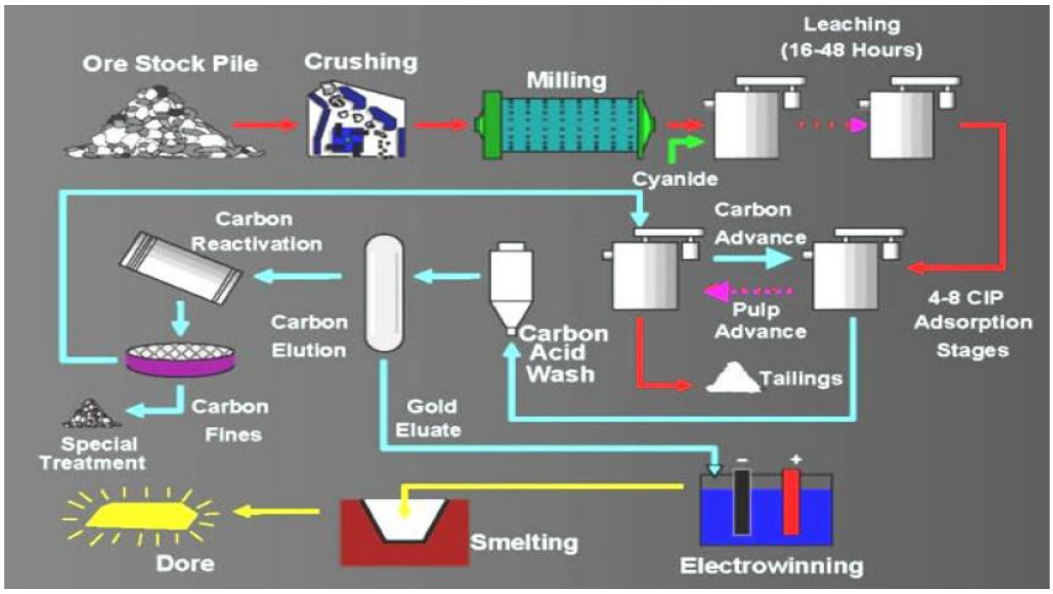


Figure 2.15. : Flow sheet of a modern CIP plant (Fleming, 2004).

2.5.2.2 *Leaching Section*

This section is characterised by parameters such as cyanide and oxygen concentration, pH, slurry density and temperature. In most cyanidation processes, cyanide and oxygen concentration are the rate controlling factors. Therefore, operating at high concentration of oxygen and cyanide improves the leaching kinetics and thus reduces the residence time and increases throughput (Ellis & Senanayake, 2004).

The ore is first passed through the crushing and milling circuit for a reduction in size (typically 80% passing 75μm). After comminution, if dealing with low grade sulphide, the pulp is usually diluted up to 20% solids by mass before flotation, but the flotation step is not included if processing oxide ores. After flotation, the pulp is thickened to increase the pulp density to about 40-50% solid by mass. Lime is then added after thickening to raise the pH to about 10.5-11.5 then cyanide and oxygen, or air, are also added (Stange, 1999). To provide adequate oxygen concentration in the leaching tank, it is important to create many small oxygen bubbles and to disperse them deep enough in the slurry (Ellis & Senanayake, 2004).

A typical CIP leaching section is generally constituted with a series of agitated vessels (six in general), each having a retention time of about four to six hours depending on the type of ores. To ensure a good mixing, the agitated vessels comprise a conventional mechanical agitator, blades as well as a shaft. Pure oxygen or air is injected as small bubbles in the slurry at the lower part of the leaching tank. To reduce the transfer of oxygen from the slurry to air, these vessels are equipped with a cover, which can either be a stationary cover or a floating cover. To maintain an optimum condition in each reactor, a staged addition of reagents is required (Flatman & Vorster, 2001).

De Andrade & Hodouin (2006) carried out an investigative study on a leaching circuit consisting five equal-sized reactors. Based on the gold price and cyanide cost for a gold content higher than 0.5 mg/kg and low cyanide concentration of 250-500 mg/L, the authors recommended the use of a conventional configuration in series. However, the parallel configuration is highly recommended for processes operating at a high cyanide concentration of 750-1000 mg/L and gold content below 0.5 mg/L (de Andrade & Hodouin, 2005).

2.5.2.3 *Adsorption Section*

Due to its efficient properties and high selectivity to adsorb gold, activated carbon or activated charcoal is the most and widely used adsorbent. Activated carbon has large specific area of approximately 1000 m^2/g and strong adsorptive capacity (Marsden & House, 2006). Various types and size of activated carbon can be used. However, most processes often prefer to use granular coconut shell carbon because of its hardness compared to other types available. Besides its high resistance to breakage and abrasion, activated granular coconut also has large loading capacity. The CIP adsorption section is characterised by two important stages:

- Adsorption of the dissolved gold onto activated carbon and;
- Elution of gold from the activated carbon into an alkaline cyanide solution.

Usually, the adsorption process also occurs continuously in a cascade of six large agitated tanks. Each tank has approximately a retention time of about one hour. In the conventional method, each tank is equipped with a mechanical agitator including blades and a shaft. The pulp is then agitated and flows by gravity from one tank to the next. The inlet and outlet of the slurry and carbon in each tank is covered by a screen where carbon is retained in each adsorption stage due to the fact that it is much larger than the ore particles. The fresh or reactivated carbon is reintroduced on the last tank while the slurry is introduced on the first

tank. Activated carbon with the highest gold loading is contacted with the solution having the highest gold concentration in the first tank. The contact between activated carbon and the slurry is done counter currently to maximize the adsorption of gold onto the surface of carbon. The objective in each stage is to load the carbon to a pseudo-equilibrium depending on gold concentration in the solution in each stage. The slurry after adsorption is discharged through the outlet of the last tank to a disposal site for tailings. Activated carbon containing gold, known as loaded carbon, is taken to the elution stage to desorb gold which will further be recovered as solid in the electro-winning process. Before being reintroduced in the adsorption circuit, the eluted carbon must first be regenerated using a strong acid to remove the contaminants.

2.5.2.4 *Carbon-in-leach (CIL) process*

The conventional carbon-in-leach process is just an improvement of the CIP process where the leaching and adsorption sections take place in the same tanks simultaneously. The objective of adding activated carbon directly in the leaching tanks is mainly to avoid the preg-robbing phenomenon when treating ores that contain organic matter and other preg-robbing species such as silicates, graphite and clay (Marsden & House, 2009). Preg-robbing species have the ability to adsorb aurocyanide ions $[Au(CN)_2]^-$ from the solution back to the ore therefore, lowering t the leaching efficiency. The use of a CIL process has the advantage of reducing the capital investment cost compared to a CIP one. The CIL also improves the gold extraction by constantly removing the gold ions from the solution. However, this process also has some disadvantages. One of the biggest challenges is that this process requires a larger carbon inventory resulting in a large tie-up of gold. Carbon losses due to attrition are higher and gold losses due to the loss of fine loaded carbon is also very high.

Due to attrition, CIL generate more, finer, carbon which have high adsorption capacity compared to coarser carbon. However, these finer carbons are lost in the residue and the loaded carbon generated usually has lower concentration in gold compared to the one generated by a CIP process. Therefore, the elution stage of a CIL process will require more carbon to reach the acceptable concentration of gold in solution (Marsden & House, 2006).

A conventional CIL process is usually composed of six agitated vessels, each having a retention time of approximately four hours. The contact between activated carbon and the slurry containing aurocyanide ions and dissolved oxygen in solution is done in a counter-current flow. The carbon is periodically transferred upstream while the leached slurry flows down the cascade. Each tank is equipped with inter-stage screens where the slurry is screened

like in the CIP process. After CIL, the loaded carbon is further stripped and regenerated to restore adsorption activity by renewing the surface.

2.5.3 High pressure and/or elevated temperature cyanidation

In recent investigations, high pressure cyanidation has been presented as a promising technology. This process is a combination of direct oxidation and dissolution of gold simultaneously in autoclave reactors. This technology can even successfully treat pyrite refractory gold ores and concentrates (Parga, et al., 2007). Under these conditions of high pressure and high temperature, many products resulting from oxidation can be generated. It is important to note that oxidation in the autoclaves can also form a porous, but non-protective, elemental sulphur layer on the surface allowing cyanide and oxygen to access the gold that was locked in the ore (Parga, et al., 2012). Sometimes, the elemental layer formed may also result in a non-porous layer inhibiting access of the lixiviants to the underlying metal. Apart from autoclaves, other reactors have been developed to reduce the cost in the high-pressure cyanidation.

2.5.3.1 *The Leachox Process (Aachen reactor)*

The Leachox Process is just the addition, to the conventional process, of new unit process steps such as Imhoflot flotation, ultra-fine grinding of the flotation concentrates and then partial oxidation of sulphides followed by leaching in 4 columns that replace conventional open to atmosphere leach tanks. A new reactor has been recently added to reduce the operating cost of the Leachox process: “Aachen reactor”. This reactor is connected to the leaching columns as shown in **Figure 2.16**.

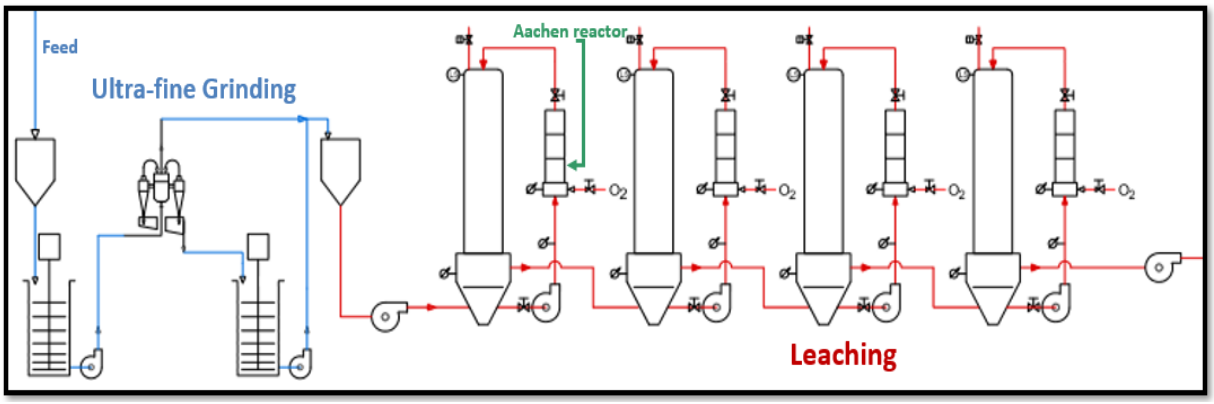


Figure 2.16. : Leaching stage in 4 columns connected to the Aachen reactor (Maelgwyn Mineral Services Ltd, 2009).

The Aachen reactor is designed to improve the leaching kinetics of gold ores by enhancing the dispersion of oxygen gas into slurry. The dispersion of oxygen gas into slurry is basically realized by accelerating the slurry stream at high velocity while adding the oxygen gas into it using a ceramic insert which increases shear rates in the mixing zone. **Figure 2.17** illustrates the principle of operation of the Aachen reactor.

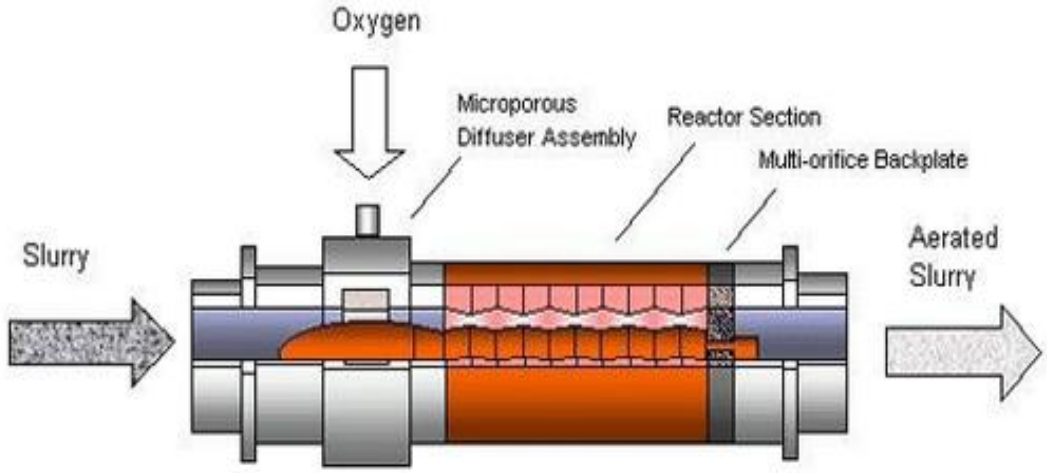


Figure 2.17. : Aachen Reactor –Principle of Operation (Maelgwyn Mineral Services, 2009).

The Aachen reactor can be used to assist open tank leaching processes in order to increase the leaching kinetics. These reactors when combined to the MMS (Maelgwyn Mineral Services) leach columns can reduce sensibly the residence time of any ore compared to the conventional open tank leaching and especially for slow leaching ore (refractory ores).

2.5.3.2 *Jet reactor technology*

One of the most promising reactors developed in high pressure cyanidation is the Jet reactor technology. The Jet reactor technique uses a cross-flow of two ore slurry streams 1 and 2 which are introduced perpendicularly to a separated high velocity stream of cyanide jet as presented in **Figure 2.18** below (Loftus and Lorenzen, 1997). The reaction takes place in an atmosphere of air at atmospheric pressure.

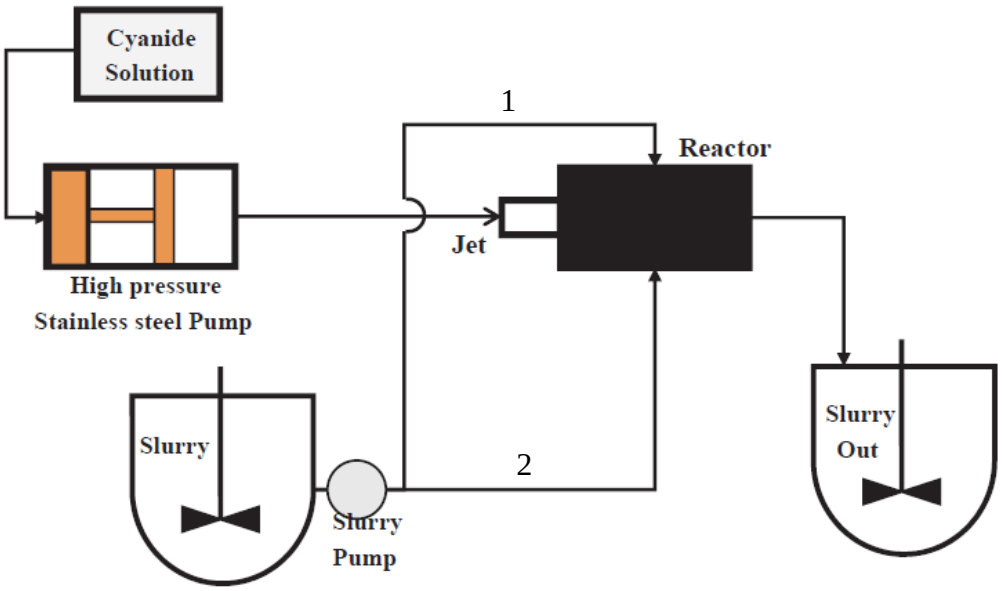


Figure 2.18. : Schematic diagram of the Jet reactor experimental set-up.

Gold ores are mixed with water at 40% solids in the slurry tank while a solution of cyanide is prepared to be equivalent to 1 kg per ton of ore in another storage vessel. A high-pressure reciprocating pump is used to inject the solution of cyanide into the reactor at a pressure around 200 and 300 bar. Using a slurry pump, a cross-flow of two slurry streams is introduced in the reactor, perpendicularly to the high velocity cyanide jet to maximize the contact between slurry and cyanide solution. After being passed through the Jet reactor, the cyanidation process continues in another holding slurry tank (Loftus, et al., 1997).

This process has been shown to improve the leaching kinetics of free milling gold ores. However, apart from the results published on its application to free milling ores, no further developments appear to have been published in relation to its application on refractory gold ores. (Lorenzen & Kleingeld, 2000).

2.5.4 Intensive cyanidation

In the intensive cyanidation process, gold dissolution is done at high cyanide and oxygen concentration and/or high temperature and pressure to improve the gold dissolution rate. Oxygen can be feed in the system as air, pure oxygen or a combination of the two to increase the oxygen partial pressure (Marsden & House, 2006). The conventional methods developed for intensive cyanidation use a high-speed agitator in tank and vat leaching. These conventional methods have shown many challenges due either to excessive wear and high energy requirement for agitation and high loss of fine gold in the vat systems resulting in low

gold recoveries, often between 30% and 60% (Longley, et al., 2003). As a consequence, many researchers have developed new reactors that can use intensive cyanidation in a more efficient and economical way. Reactors such as the ACACIA Reactor and the Gekkos InLine Leach Reactor are widely used in intensive cyanidation with higher gold recoveries (>70%) (Mineral, 2005).

2.5.4.1 *ACACIA Reactor*

The ACACIA Reactor or ConSep ACACIA Reactor is a high efficiency leaching device and promising reactor using the high intensity cyanidation method to achieve very high recoveries (Watson & Steward, 2002). The ConSep Reactor consists of an up-flow fluidized reactor which is designed to produce ideal solid-liquid interaction to maximize the leaching kinetics without any mechanical agitation. The resulting products obtained after this process are in the form of cathode gold which are ready for smelting. It is important to note that the ACACIA reactor has been shown to give very high gold recovery (95-98%). However, this reactor is only effective to treat coarser high-grade gravity gold concentrates, such as Knelson concentrates and it does not operate in a continuous system (Watson & Steward, 2002). **Figure 2.19** describe all the operations taking place in the ACACIA reactor.

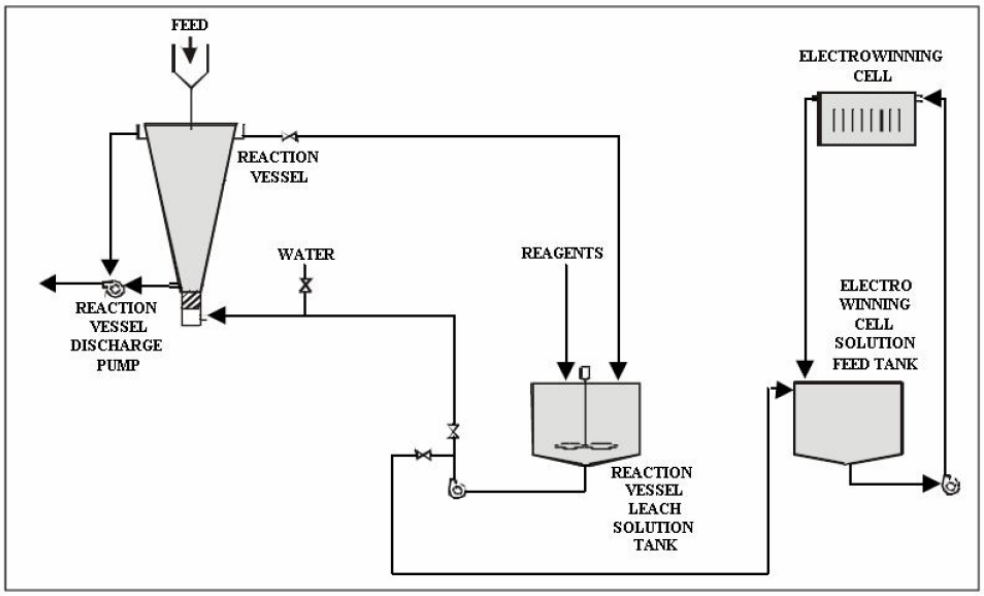


Figure 2.19. : Basic flow sheet of the ACACIA Reactor (Watson & Steward, 2002)

The process starts with the transfer of concentrates from the day storage hopper to the fluidized reactor vessel, where concentrates are first washed with water to remove fines particles. Washing is the most critical stage of this process and it must therefore, be carefully controlled. The presence of fine particles in the leach solution causes many problems during

electrowinning. After washing, gold concentrates are subjected to an up flow of leach solution which is pumped at a flowrate sufficient to fluidize the concentrates. The leach solution used to create the fluidised bed comes from a mixing vessel where the leaching reagents such as caustic solution, concentrated cyanide and other oxidants are added to water. Generally, the completed leaching process takes around 16 hours to achieve gold recoveries of 95-98% (Campbell & Watson, 2003). After completion of leaching, the pregnant leach solution is recovered by simply draining the bottom of the reactor into the leach feed tank. The remaining residues are then washed to remove the residual pregnant solution retained within the solids. The residues are then discharge from the reactor. The pregnant leach solution is then pumped to the electrowinning cells for gold deposition.

2.5.4.2 *The Inline Leach Reactor (ILR)*

The Inline Leach Reactor (ILR) was launched in 1997 by the Gekko system, as the world's first production unit that uses intensive cyanidation. The design of this reactor ranges from a large continuous model treating flotation concentrates, down to small batch units for high-grade coarse gravity concentrates. This reactor is one of the reactors that have been successfully developed in the intensive cyanidation process. Over 100 units of the ILR have been installed in over 40 countries. As presented in **Figure 2.20**, the ILR uses the same principle as the laboratory bottle roll to keep the solids continuously in contact with the solution. The reactor is characterised by a horizontal drum rotating at low speed and two feed tanks in the form of a cone, one for the solids and the other for the cyanide solution. The ILR drum is designed with a set of special baffles and an aeration system for maximum leach performance.

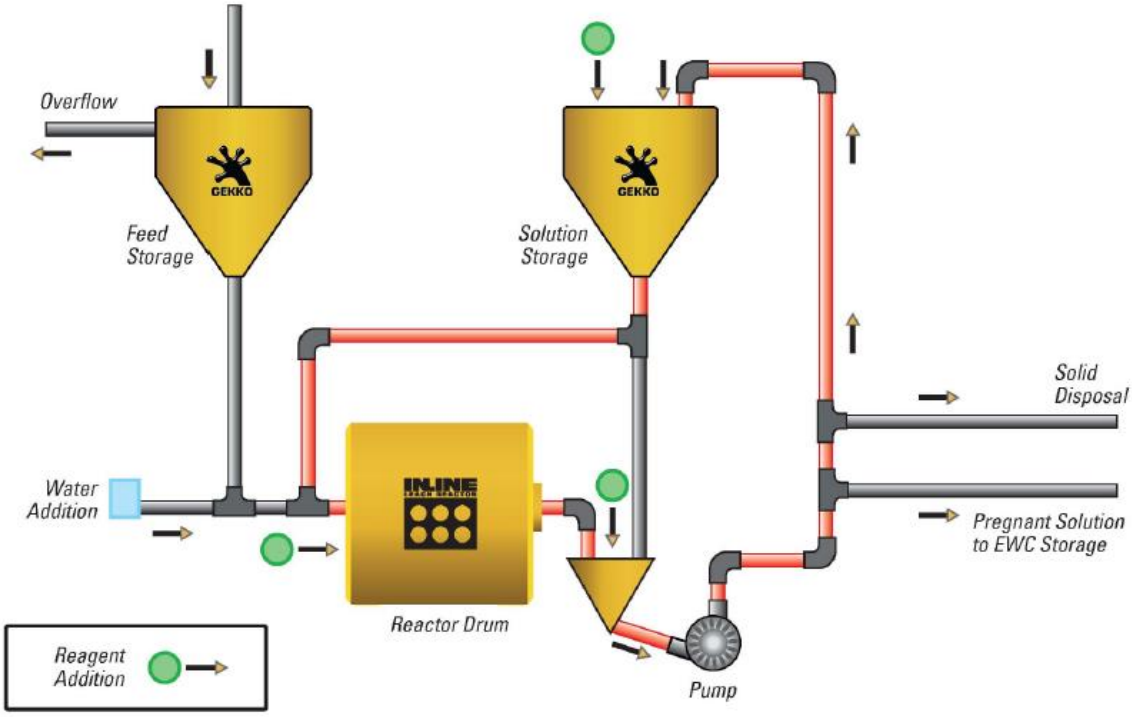


Figure 2.20. : InLine Leach Reactor flowsheet (Longley, et al., 2003)

The solids are fed into the drum while the leach solution passes through the drum carrying fresh reagents which are mixed with the solids as the drum rotates. After reaction, a solid-liquid separation is done on the leached slurry to separate the solids from the pregnant solution. The solids are then washed to recover any entrained pregnant solution. The washed solids are discharged to tails and the dissolved gold is recovered from solution by electrowinning, zinc precipitation or absorption onto carbon or resin. In batch ILRs leaching, solid-liquid separation and washing is performed in the drum and in discrete steps. In continuous ILR systems, the leached slurry discharges continuously from the drum and is separated and washed in a separate CCD or filter (rotary drum filter) and the gold is continuously recovered from solution. The barren solution is then recycled to the drum.

2.6 CAVITATION

Several new technologies and sophisticated methods have been developed, in chemical and metallurgical engineering, with the hope of providing innovative ways to improve the kinetics of some slow chemical processes. One of the most promising development is the use of cavitation. The term cavitation originates from a Latin word ‘‘cavitas’’ which means a hollow space or cavity. Therefore, cavitation can be defined as the phenomenon of formation, growth and collapse of micro-bubbles or cavities in a liquid.

2.6.1 Types of cavitation

The cavitation phenomenon can be classified into four categories depending on the source generating cavities.

- Hydrodynamic cavitation which is produced by pressure variation in a flowing liquid caused by the velocity changes in the system.
- Acoustic cavitation is a result of pressure variation in a liquid when ultrasound waves pass through it.
- Optic cavitation: this type of cavitation occurs when high-intensity laser pulses or light pass through the liquid.
- Particle cavitation: in this case cavitation is caused by elementary particles such protons and neutrinos when high energy particles pass through a liquid.

It has been shown that hydrodynamic and acoustic cavitations are the result of tensions prevailing in a liquid, while optic and particle cavitations are the consequence of local decomposition of energy. Hydrodynamic and acoustic cavitation are the most used methods to generate cavitation in a liquid medium. However, hydrodynamic cavitation, compared to acoustic cavitation, has a high potential in terms of energy efficiency and can be used on a large scale (Arrojo et al 2007). Therefore, this study will only focus on the use of hydrodynamic cavitation and its application.

2.6.2 Hydrodynamic cavitation

Hydrodynamic cavitation is a phenomenon in which rapid variation of pressure in a liquid lead to the formation of small vapor-filled cavities, in places where the pressure is relatively low (low pressure zone). This phenomenon occurs when the local pressure decreases below the saturated vapor pressure of the liquid (Franc, 2006). **Figure 2.21** show the conditions under which cavitation can be generated in a liquid.

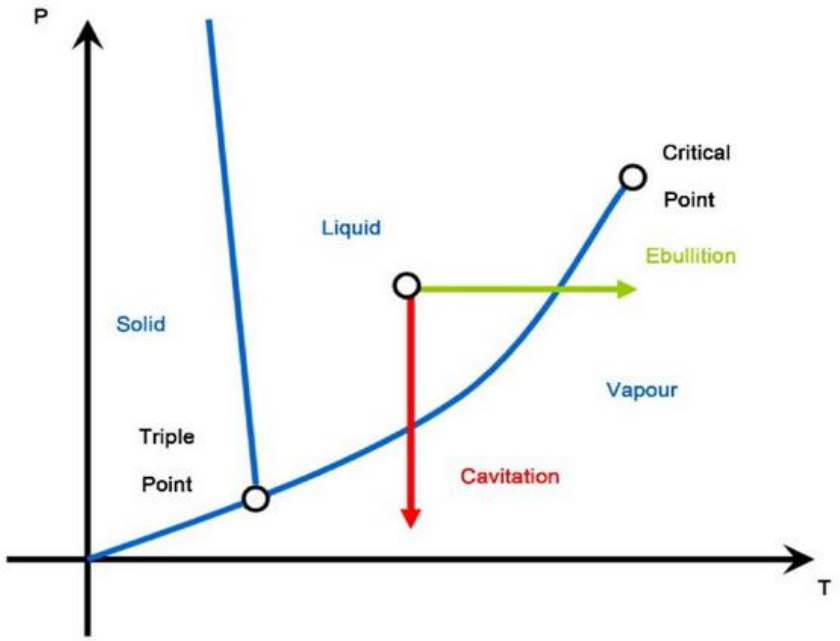


Figure 2.21. : Phase diagram of water near the triple point explaining the liquid-vapor transition during cavitation (from French Wikipedia).

When these cavities formed move from a low-pressure zone to a high-pressure zone, they start collapsing. The generation of bubbles and their subsequent growth and collapse results in a very high energy density and very high local temperatures and pressures at the surface of the bubbles for a very short time.

One of the first and detailed studies of the cavitation phenomenon and the parameters influencing the process was done by Reynold in 1894. In his study, he determined that, the generation of bubbles and the intensity of cavitation mainly depends on parameters such as:

- The geometry of the constriction (geometry of nozzles);
- The flow conditions of the liquid or the scale of turbulence;
- The rate of pressure recovery;
- The local conditions of high temperature and pressures

2.6.3 Mechanism of hydro-cavitation

The hydrodynamic cavitation mechanism can be described in three stages; formation of bubbles, growth and collapsing of the bubbles formed.

- Formation of bubbles in the liquid

There are two ways of producing hydrodynamic cavitation, by mechanical agitation (rotation) of an object through a liquid at a specific rotation speed, or by passing a liquid through a

constricted channel at a specific velocity (Payri, et al., 2013). The condition for cavitation to occur is given by the cavitation number (σ) which is defined as follow:

$$\sigma = \frac{P_a - P_c}{\frac{1}{2}\rho U^2} \quad (2.32)$$

Where:

P_a: the ambient absolute pressure;

P_c: the cavity pressure;

ρ: the mass density of the liquid;

U: the reference speed characteristic of the flow.

The cavitation number at which cavitation begins is called the critical cavitation number. Below this value, cavitation occurs while above, it does not. Therefore, to produce a very large cavitated region, it is required to operate with a cavitation number well below the critical number (Madhu, et al., 2015).

- Bubbles growth

After formation of cavities, due to a relatively low static pressure, bubbles start growing from a small nucleus to many times their original size. The growth continues until bubbles reach their maximum radius size at the point where the static pressure become equal to the partial pressure of the gas. After this stage, bubbles start collapsing because of an increase in the static pressure.

- Bubbles collapse

The size of bubbles, at their maximum radius, is of the order of 100 times the original nuclei size. Consequently, if the original partial pressure of gas in the nucleus was about 1 bar the value of the maximum pressure generated would be about 1010 bar and the maximum temperature would be 4×104 times the ambient temperature (Chakinala, et al., 2008).

On a reaction point of view, the effects of cavitation can be summarised as follow:

(1) Release of local high temperature and pressure, which is useful for reaction rate and mass transport enhancement.

(2) Shock wave generation during the collapse of bubbles decreases thickness of boundary layer in solid– fluid reaction or solid–liquid mass transfer resistance.

(3) Micro-jet impact on solid particles either fragments or cracks the particles, ultimately exposing larger surface area for reaction.

(4) Formation of free radicals enhances nucleophilic reactions.

All these effects coming from the cavitation process can be exploited for the enhancement of mass transfer, rate of reaction and improvement in the overall yield of the physico-chemical transformation (Ladola, et al., 2014).

2.6.4 Application of hydrodynamic cavitation

Hydrodynamic cavitation was first known as a very negative phenomenon which, because of the erosion generated by the collapsing of bubbles or cavities, contributes to the destruction of equipment such as pumps, valves, impellers, tanks and even pipes. However, since this process generates high energy, local pressure and temperature, controlled cavitation can be used to enhance some slow and unexpected reactions (reactions that are not possible under normal conditions) or to improve some industrial processes.

The cavitation process has been used with success in many different processes:

- In water treatment, preparation of nano-emulsions, water disinfection and nanoparticle synthesis (Dular & Petkovšek, 2015). In the treatment of industrial wastewater, induced cavitation can be used in conjunction with the advanced Fenton process (AFP) for the removal of total organic carbon. The combination of the AFP and hydrocavitation usually result in about 60-80% removal of total organic carbon (Chakinala, et al., 2008).
- In mineral processing, the cavitation phenomenon has been mostly applied to flotation (Ahmed & Ahmed, 2013; Royer, et al., 2017) to increase the probability of bubbles formation. Cavitation also produces very tiny bubbles, with diameter from microns down to nano sizes, which increase the contact angle of solids and hence attachment force (Zhou, et al., 2009).
- In leaching, cavitation is used to enhance the leaching kinetics and the leaching recovery of some slow leaching processes. One of the industrial applications reported is the use of ultrasonic cavitation to improve the recovery and enhance the rate of recovery during leaching of uranium. Different types of cavitation reactor schemes are proposed by researchers to improve the leaching kinetics (Ladola, et al., 2014).

In the following section, the investigations focus on the development and application of a reactor using hydrodynamic cavitation to enhance the leaching kinetics and the gold recovery of refractory gold ores. This reactor has the potential to modify the cyanidation process.

2.6.5 Jetleach reactor

The Jetleach reactor (which is different to the Jet reactor described in section **2.5.3.2** above) is a device designed to create and propagate micro-cavitation by impacting two pulp streams against one another at a high velocity. The cavitation process produces bubbles which, once collapsing, propagate stress at the inter-phase bubbles-particles, and increase the local pressure and temperature (Tsaih, et al., 2004). Many changes such as cracks propagation, internal stress or mechanical activation may happen under emission of such extreme energy, and thus result in an increase in the leaching kinetics.

As it can be seen from **Figure 2.22**, the Jetleach reactor is designed to receive two pulp flows (powered against one another at high speed) coming from a Pachuca/stirred tank, via a centrifugal pump. Oxygen gas is added from the top of the impactor and fills the inner tube. Before being impacted, the two pulps pass through two constrictions (nozzles) at a high velocity that generate the formation of micro-bubbles (micro-cavitation) in the pulp. Despite the surface polishing of ores particles, the effects of collapsing bubbles release high shocks of energy that may breaks the matrices or generate stress in ore particles. After passing through the Jetleach reactor, the pulp is returned to the agitated tank.

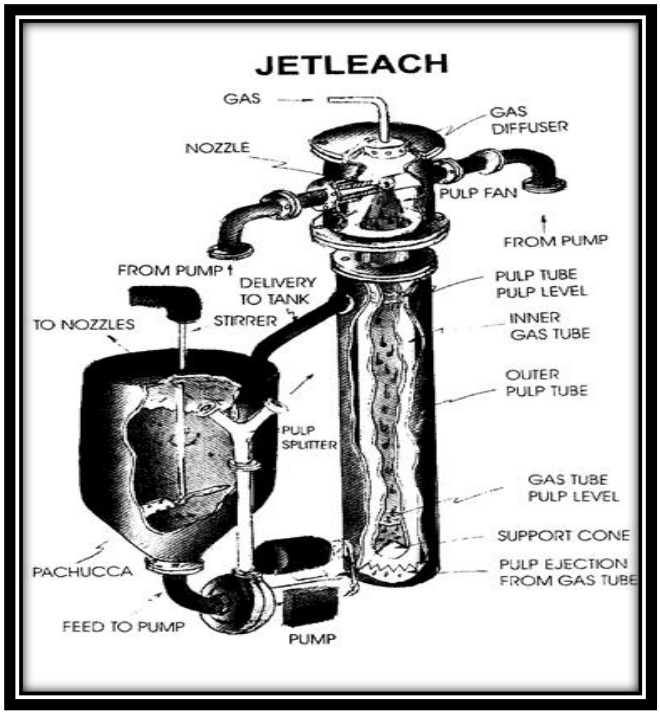


Figure 2.22. : the Jetleach reactor connected to a Pachuca (GRMS report, 1997).

2.6.5.1 *Characteristics*

The Jetleach reactor is constituted by an assemblage of two co-axial and vertical tubes with different diameters. The small cylinder (gas-filled tube) is fixed to the impactor and placed inside the big cylinder.

There are two important characteristics pertaining to the Jetleach reactor;

- Opposing nozzles that direct the incoming pulp flow on a collision course to provide a zone of attrition before converting into a "Bernoulli fan", and
- A gas-filled tube through which the comminuted pulp falls before being expelled from the reactor via a comparatively fast-flow annulus.

Figure 2.23 and **2.24** represent the external and internal view of the impactor of the Jetleach reactor.

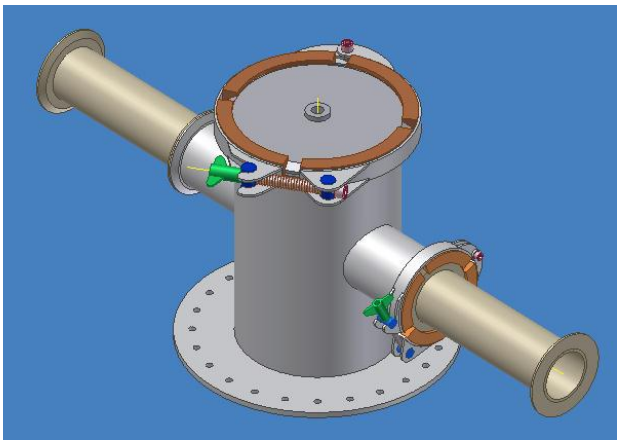


Figure 2.23. : External View of the Impactor

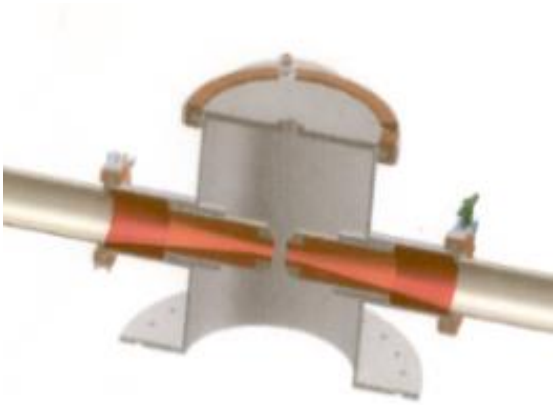


Figure 2.24. : Internal View of the Impactor

The nozzles are designed in a way to maximize production of micro-cavities in the liquid component of the slurry. The velocity of impact, at the convergence of the two jets, is a product of the pumping rate and the nozzle design. The pressure of oxygen in the gas tube is a product of the height of the tube, and the difference between the pulp level in the inner gas tube and the outer pulp filled pipe.

2.6.5.2 *Setup description*

In operation, the Jetleach reactor receives a pulp feed, from a stirred tank, via a centrifugal pump. The Jetleach reactor comprises of a central pressurized tube, completely filled with oxygen, through which the pulp stream falls. Oxygen gas is added from the top of the impactor and fills the inner tube. Before being impacted, the two pulps, coming from the agitated tank, pass through two constrictions (nozzles) at a high velocity that generate the formation of micro-bubbles (micro cavitation) inside the pulp. After being impacted, the resulting pulp droplets fall down the tube in an atmosphere filled with oxygen in order to maximize the contact between oxygen and cyanide solution. Upon reaching the bottom of the tube the pulp emerges from the gas column and rises in the surrounding space of an outer tube before flowing back into the agitated tank. Typically, the pulp flow rate, through the reactor, is at least three times the rate of pulp flow through the plant. In the case of a batch leach operation this ratio is higher.

2.7 Summary

The literature review has covered the causes of refractoriness and the pre-treatments methods, the chemistry of gold cyanidation including the thermodynamic and kinetics consideration, the improvement that has been made in the cyanidation process of refractory ores and an overall knowledge on cavitation and its application in industry. The next chapter discusses the materials and methods that were used in this research.

CHAPTER 3 MATERIALS AND METHODS

3.1 Introduction

This research focuses on investigating the performance of the Jetleach reactor on improving the leaching kinetics and the gold recovery of refractory ores, compared to the conventional methods used in this research (bottle roll and leaching in agitated vessel). This chapter discusses the preparation of the materials, reagents, experimental setups that were used as well as the analytical and experimental methods that were involved in this study to achieve all objectives assigned.

3.2 Experimental

3.2.1 Materials characterization

Three different types of samples were involved in this study. One of the samples was from DRD Gold Company in South Africa. The sample consisted of high-grade concentrates obtained after flotation of old gold tailings at the Ergo plant. The other two samples consisted of rougher flotation concentrates from the Diorites (DIO) and Meta-volcanic (MVO) gold deposits from West Africa.

3.2.1.1 *Sample from Ergo tailing plant*

The flotation concentrate sample from Ergo plant was submitted to Mintek for a mineralogical analysis where the following methodology was adopted. First, X-ray diffraction (XRD) was used to identify the mineral phases that are present in the Ergo flotation concentrate, based on their crystalline structural properties. After XRD, the flotation concentrate was subjected to heavy liquid separation (HLS) at a separation SG of 3. The floats (SG <3) represent light silicates and oxides. The sinks (SG >3) represent sulphides, free gold and heavy silicates & oxides. This process concentrates the gold, thus improving the probability of locating enough gold grains for significant results.

The float and sink fractions of the flotation concentrate were then screened at 25 and 10 microns to allow a far more accurate assessment of gold nature and deportment. The size fractions of sinks and floats were analyzed for gold and total sulphur at the Ergo assay laboratory.

QEMSCAN analyses were also done to determine the deportment of gold within the flotation concentrate sample, with specific emphasis on gold speciation, gold grain size distribution, gold liberation, exposure and gold association.

3.2.1.2 *Samples from West Africa*

The two samples from West Africa (Diorites and Meta volcanic gold ores) were submitted to Suntek for a mineralogical analysis. X-ray diffractometer (XRD) and automated mineralogical analysis was used to study the mineralogy of the ore. A Panalytical X'pert Pro diffractometer, that employed Co-radiation, was used to collect the XRD patterns. The data was then interpreted using the Panalytical High-Score Plus analytical software and the PAN-ICSD database (Panalytical-Inorganic Crystal Structure Database).

The automated mineralogical analyses consisted of modal analysis, particle map analysis and gold grain mapping using an MLA (Mineral Liberation Analyzer). SEM-EDS spot analysis (Scanning Electron Microscopy coupled with Energy Dispersive Spectrometry) were used to obtain the mineral composition. Two 90°-cut polished sections were prepared from each sample for the modal analysis. Ten normal polished sections were prepared from the concentrate samples for the gold searches.

3.2.2 Reagents

In this study, sodium cyanide ($NaCN$) was used as the main leaching reagent whilst calcium oxide (CaO) was used to control the pH values. Pure oxygen gas was used as the oxidizing agent during pre-aeration and cyanidation. Silver nitrate and oxalic acid were used for cyanide and lime titration, respectively. All these reagents were of analytical grade (AR), which are known as chemical substances of enough purity to be used for laboratory and general purposes according to International standards (ASTM®, 2012; Grades of chemicals, 2008). Granular activated carbon with a particle size of 1.7-3.3 mm was used to prevent any preg-robbing phenomenon from occurring. The reagents used in this study were all purchased from Merck and Sigma Aldrich, except for oxygen gas which was purchased from AFROX. All reagents were used as received.

Distilled water was used to prepare all solutions and slurries that were involved in this study.

3.3 Chemical analysis

The gold content in the solution was determined by wet chemical analysis method using atomic absorption spectrometry (AAS) and verified by inductively coupled plasma-atomic emission spectroscopy (ICP-AES).
All leach residues were analyzed by fire assay and all results were verified using atomic absorption spectrometry (AAS) after digestion of the solid material sample in aqua-regia.

3.4 Methods

To achieve all assigned objectives, it was important to first understand the mineralogy by doing a complete gold characterization of the samples involved in this work. The mineralogical analysis revealed that all samples had high pyrite contents. Therefore, to reduce the amount of cyanide used, a pre-aeration stage was undertaken before cyanidation.

The cyanidation process started with a comparative leaching study between the Jetleaching method and the conventional methods here represented by bottle rolling and leaching in an agitated vessel. After comparing the three processes, investigations were focused only on the Jetleach reactor by studying the effect of physical and chemical parameters. This investigation was done by first varying one factor at a time to see the effect each parameter had on the process, thereafter a designed set of experiments was done to evaluate the interactions effects of parameters on the gold recovery.

The leaching investigations were then followed by understanding what impact cavitation had on solid particles which could justify the improvement observed in terms of the leaching kinetics and gold recovery. These investigations were completed by doing a particle size analysis to verify if any size reduction was happening and a SEM analysis to detect any presence of cracks or cavities on the surface of solid particles.

The final stage of this research was to investigate how cavitation was generated in the Jetleach by isolating one of the nozzles of the Jetleach in a transparent tube reactor which was designed to simulate the impact in the Jetleach reactor and by using high-speed photography to capture the formation of cavitation.
The **Figure 3.1** below presents a flow diagram summary of all the operations stages that were necessary to achieve the objectives assigned in this project.

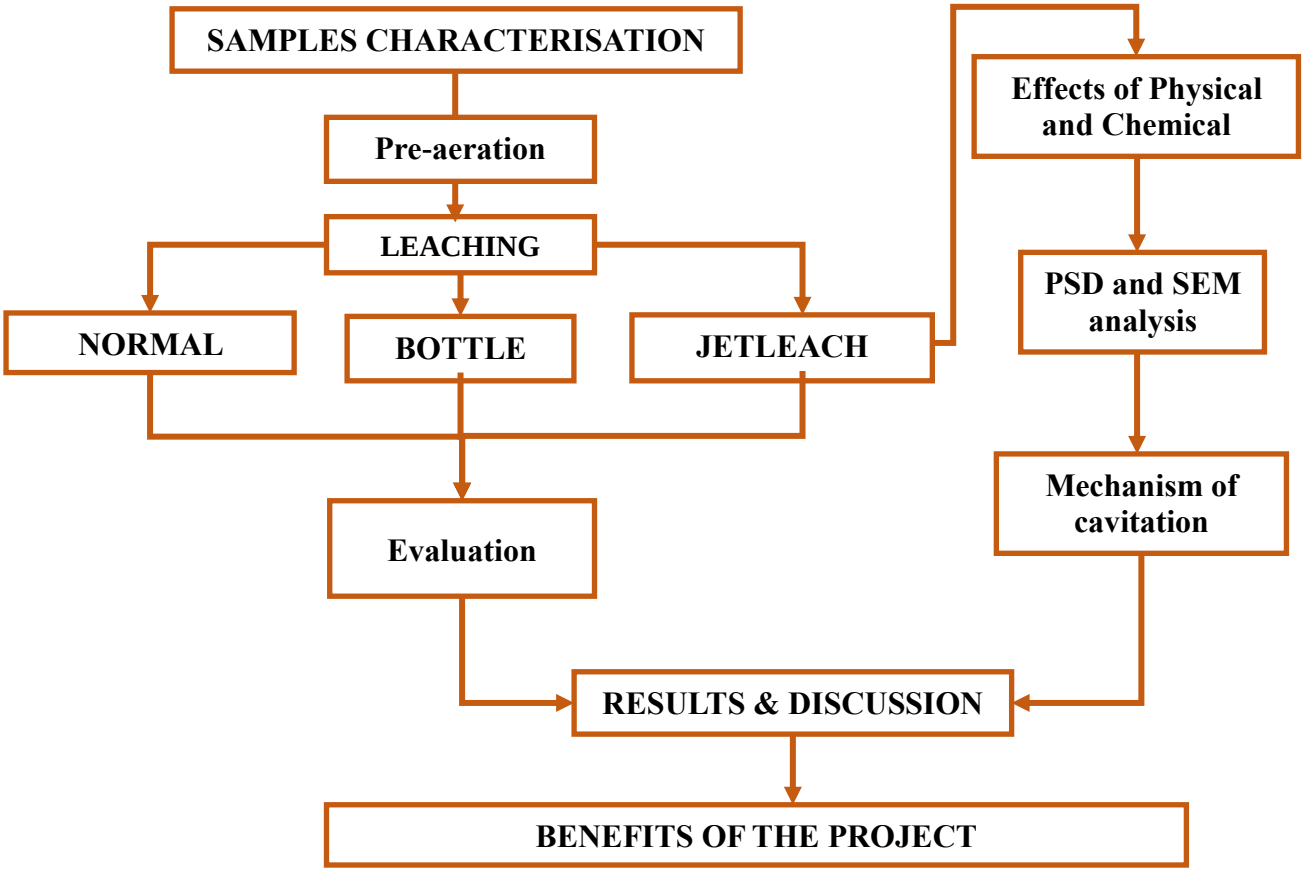


Figure 3.1: Operations stages necessary to achieve the objectives assigned

3.4.1 Comparison between conventional leaching methods and Jetleaching method on refractory gold ores

This investigation was divided into three stages as presented below:

3.4.1.1 *Preliminary tests (pre-aeration)*

In these preliminary tests, the objective was to investigate if pre-aeration could help to reduce cyanide consumption by passivating pyrite and other sulphidic materials. The choice of this method was not only because it is environmentally friendly but also because it contributes to reducing the overall cost of processing refractory ores compared to other pre-treatment methods used in industry which are energy and time consuming (as presented in chapter 2, section **2.2.2.2**).

Tests were performed on slurries of each sample at 40% solid weights ratio. These tests were conducted in a laboratory sized Jetleach setup with a capacity of 20 liters as presented in **Figure 3.4.** Generally the pre-aeration period takes around 8 to 24h in order to oxidize the majority of iron (II) into iron (III) and the duration depend on the type of ore (Ellis &

Senanayake, 2004; Marsden & House, 2006). In this study, pre-aeration was done by supplying 25 KPa of pure oxygen from a gas cylinder tank over a period of 20 hours. During the first 5 hours, samples were taken every 30 minutes, then at 8, 12, 14, 18 and 20 hours to measure the redox potential (Eh), the pH of the slurry as well as the concentration of dissolved oxygen. Stability of the system was observed when the Eh of the slurry was constant.

Two liters of each aerated-slurry were then subjected to cyanidation in an agitated leaching vessel as presented in **Figure 3.2** below. The pH was maintained between 10.5 and 11.5 (to avoid the decomposition of cyanide into HCN which is a very toxic gas), cyanide concentration at 5kg/T and oxygen flowrate at 30 ml/min. The amount of cyanide used in this investigation was based on the diagnostic leaching done by Mintek as well as the actual amount used at Ergo plant. It was reported that such high cyanide demand is connected to the high concentration of sulphide (mostly pyrite) in the ore. Another two liters of each slurry, but this time not pre-aerated, were also subjected to direct cyanidation using the same conditions and same setup. After a leaching period of 24 hours, samples were collected then filtered using a filter press, to separate the residue from the solution. The residues were washed twice using distilled water before they were dried for 24 hours in the oven at a temperature of 60℃. The dried samples were analyzed for gold content using fire assay (see section **3.3**). Ten milliliters of each solution were titrated for free cyanide using a standardized solution of silver nitrate and diphenylcarbazide as indicator. Free lime was determined using oxalic acid solution and phenolphthalein as indicator.

3.4.1.2 *Comparison of different leaching methods*

Three different leaching methods were involved in this investigation; the bottle rolling method, the normal leaching method in an agitated vessel and the Jetleaching method. All three setups are presented in the sections below. Before cyanidation, all three samples (Ergo, DIO and MVO) were first subjected to a pre-aeration period of 20 hours using 25 kPa of pure oxygen. Parameters such as pH, cyanide concentration and solid percentage used in this set of experiments were chosen based on the set points at the Ergo plant.

- ***Bottle rolling method***

Tests were conducted using ore slurries at 40% solid weight ratio which consists of 534 grams of each representative ore and 800 ml of distilled water in a 5 litre bottles. For over 30 minutes after pre-aeration, the slurry was preconditioned using lime ($Ca(OH)_2$) to raise the

pH and maintain it between 10.5-11.5. Then sodium cyanide was added as the main lixiviant at a concentration of 5 kg/ton of ore. Bottle rolling rate was kept constant at 35 rpm in all tests. It is important to note that no activated carbon was used when processing the two samples from West Africa (DIO and MVO) since there was no preg-robbing happening. However, back loading phenomenon was observed when dealing with the Ergo flotation sample; therefore, activated carbon at 20 g/l was required to prevent the preg-robbing phenomenon. The bottle roll experiments were all done in batch lots. Therefore, cyanidation tests were carried out for 15, 30, 45, 60, 105, 120 minutes and 4, 8- and 24-hours intervals. After cyanidation, samples were filtered, using a filter press. The residues and the solutions collected underwent the same analysis methods as presented in section (**3.3**).

For this experiment, a set up consisting of two rolling bottles and a bottle roller was used as presented in **Figure 3.2**.

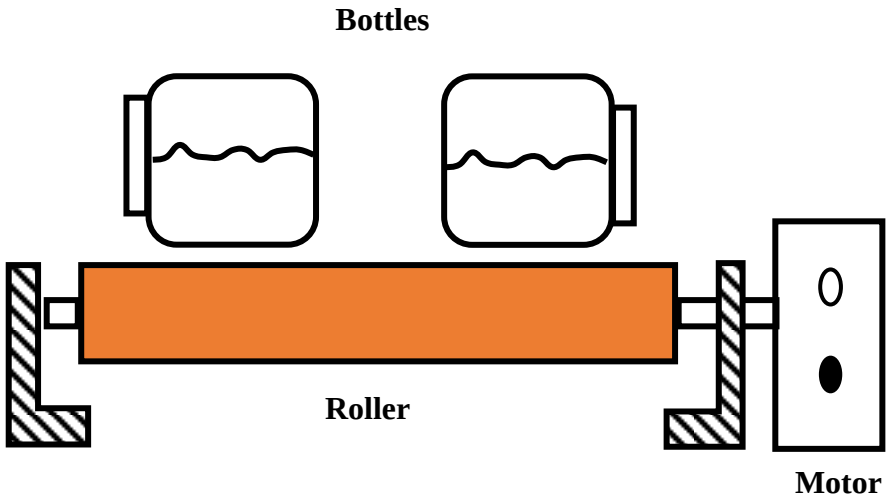


Figure 3.2: Set-Up for the bottle rolling experiments

- ***Normal leaching in an agitated vessel***

The normal leaching tests were conducted in a five liter agitated reactor equipped with pH, Eh and DO meters. All tests were done using the same conditions as for the bottle rolling tests. However, these tests were conducted in a continuous process and the mixing speed was maintained at 500 rpm. Pure oxygen gas was provided directly into the leaching reactor at a flow rate of 30 ml/min using a porous sparger in glass (to avoid contamination). The cyanidation process was carried out for 24 hours and samples were collected after every 15 minutes for 2 hours and at 4, 8- and 24-hours intervals. The collected samples were filtered, using a filter press. The residues and the solutions collected were analyzed as presented in

section (**3.3**).The experimental setup used for these tests is presented in **figure 3.3** below. This setup is consisted of an agitated leaching vessel, equipped with pH, Eh and DO meters. During these experiments, pure oxygen gas was directly fed into the leaching vessel using a small gas pipe. The pipe was connected to the oxygen bottle via a regulator to control the oxygen flow rate.

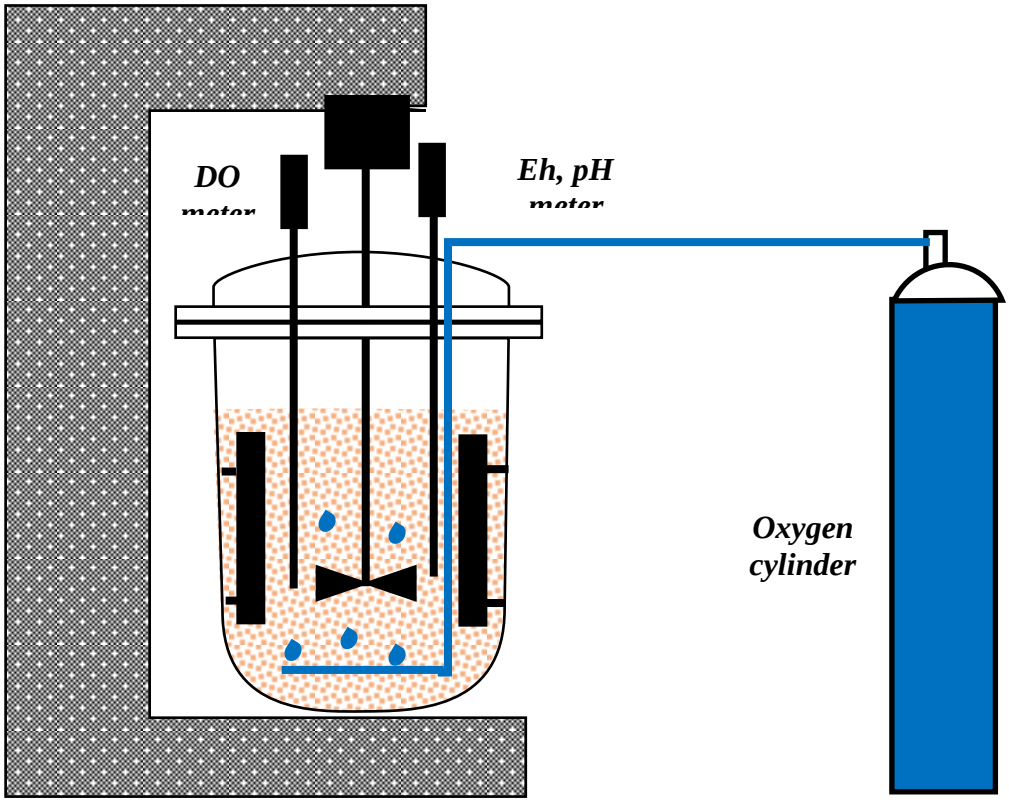


Figure 3.3: Set-Up for the normal leaching experiments

- ***Jetleaching method***

The conventional leaching experiments were followed by the Jetleach experiments. The tests conditions used in the normal and bottle rolling methods were also used for the Jetleach tests. The pressure of the slurry pump was maintained at 10 MPa, the nozzle diameter was kept fixed at 1 cm whilst the space between the nozzles was fixed at 0.8 cm. The experimental setup employed during the test program with the Jetleach reactor is the same as presented in the literature review. The setup consisted of an agitated leaching vessel with a capacity of 50 liters, which was connected to the Jetleach reactor via a slurry pump. The pulp, coming from the agitated tank, was fired into the impactor at high velocity via two opposing nozzles. After

being impacted, the resulting pulp droplets fall down the tube in an atmosphere filled with oxygen in order to maximize the contact between oxygen and cyanide solution. The Jetleach reactor was designed with a special oxygen diffuser directly placed in the impactor. Upon reaching the bottom of the tube, the pulp emerges from the gas column and rises in the surrounding space of an outer tube before flowing back into the agitated tank. (**See Figure 3.4**):

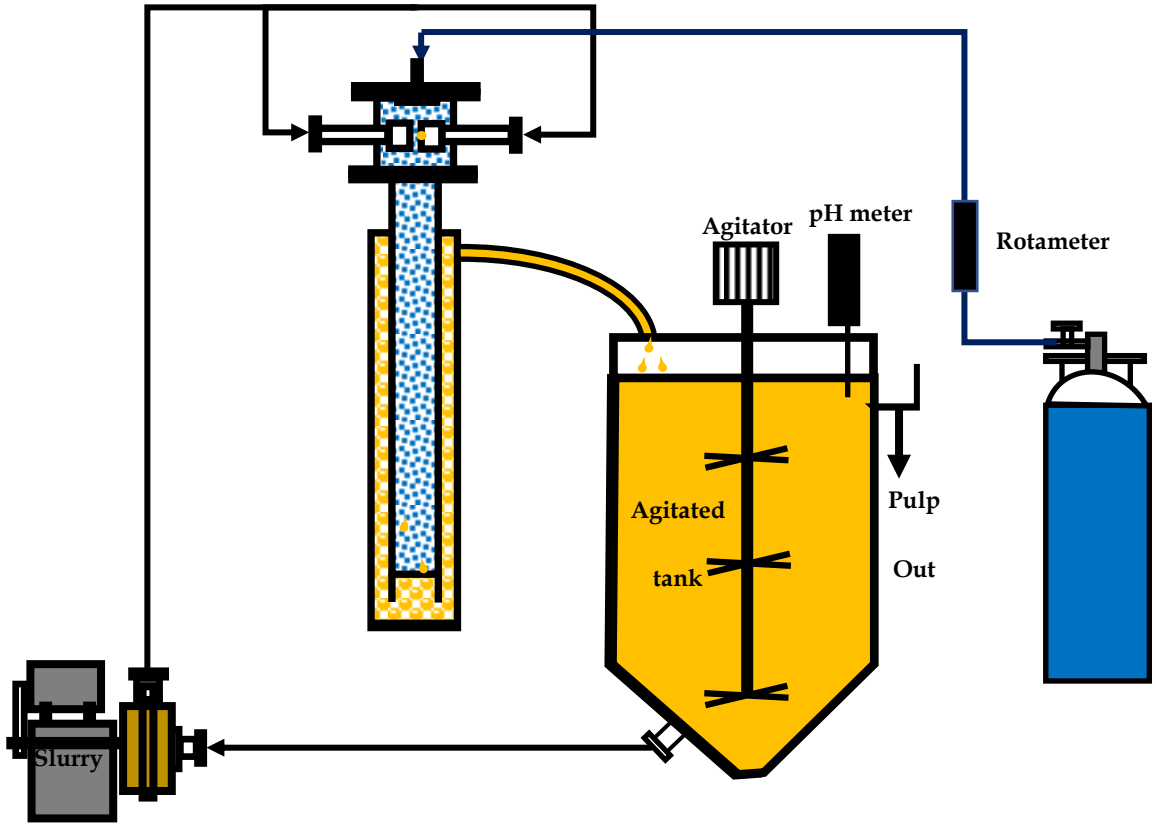


Figure 3.4: Set-Up for Jetleach Experiments

3.4.1.3 *Evaluation of the potential benefits of using the Jetleach process*

This investigation was done based on the results obtained from the comparison between the Jetleach method and the conventional methods which are represented by the bottle rolling method and the normal leaching method. The points such as the revenue generated in term of gold recovery, the throughput to process, the reagents consumption and the energy savings were considered in this investigation.

3.4.2 Effect of physical and chemical parameters on the Jetleach process

3.4.2.1 *One factor at a time*

A one factor at a time set of experiments was done to understand the effect of each individual parameter on the gold recovery. As presented in section (**2.4.5**), many parameters influence the rate of dissolution of gold in a cyanidation process mainly parameters such as, the solution composition (cyanide concentration, pH and concentration of other cyanicides elements), the redox potential (oxidant concentration), the contact surface area of gold particle linked to the particle size, temperature, slurry density, pressure and mass transfer rate or mixing.

However, in this investigation, a number of these parameters were ignored since they could not be changed or they cannot be directly controlled.

- Temperature: this factor was considered constant since many plants are operating under atmospheric condition. Therefore, there is little that can be done to control this factor. Although, when using autoclaves or other high temperature reactors, this factor will play a very important role.
- pH: there is a very small operational pH window where the reduction of oxygen and the oxidation of gold can simultaneously occur. For a pH above 12, cyanide consumption will necessarily increase. At pH below 9.5, cyanide will decompose by hydrolysis; this might even produce a very toxic gas HCN. Therefore, the pH was considered constant at one of the values between 10.5 and 11.5.
- Surface area or particle size: this can either be function of the grinding methods used or the mineralogy (gold occurrence, grain liberation, grain exposure, grain mineral association). For a specific type of ore and a specific milling method, this factor can also be ignored since it is practically constant for a plant.
- Mixing speed of the agitated tank: this parameter was also considered constant since it was not directly connected to the Jetleach reactor. This was kept at 500 rpm as in the normal leaching method.

Therefore, the only parameters that were studied during these investigations were: the solid percentage (or slurry density), the pressure of the pump, the space between nozzles for the Jetleach reactor, oxygen flowrate and cyanide concentration. The experimental parameters are as presented in **Table 3.1** below:

Table 3.1 : Parameters range for experiment

Parameters	Solid percentage (%)	Pump pressure (*MPa*)	Space between nozzles (*Cm*)	Cyanide concentration (*Kg/T*)	Oxygen flowrate (*ml/min*)
Runs at different solid percentage	17, 30, 40, 46	10	0.8	5	30
Runs at different pressure	40	5,10, 15, 20	0.8	5	30
Runs at different space between nozzles	40	20	0.5; 0.8; 1.2	5	30
Runs at different cyanide concentration	40	20	0.5	4.6; 4.8; 5.2	30
Runs at different oxygen flowrate	40	20	0.5	4.8	10; 20; 30; 40

In this set of experiments, each parameter was investigated on its own and for each parameter studied, the best value obtained was kept constant in the next set of experiments. Samples were once again collected at the same intervals as previously presented in section **3.4.1.2**. Residues and solutions were analyzed for gold content as presented in section **3.3** .

3.4.2.2 *Interaction between parameters*

To understand the interaction between the parameters, a two-level factorial design was developed using Design Expert 11. The model involved five factors and is presented in **Table 3.2** below:

Table 3.2 : Levels of factors involved in the two-levels DOE

Factors	Levels	
	Low (-)	High (+)
Pump pressure (MPa)	5	20

Space between nozzles (Cm)	0.5	1.2
Solid percentage (%)	30	46
Oxygen flowrate (ml/min)	10	40
Cyanide concentration (kg/t)	4.6	5

For the same number of factors or parameters, the software Design-Expert gives a choice of different experimental design to use. The choices appear in color; white squares symbolize full factorials requiring 2^k runs for k (the number of factors) from 2 to 9. The other choices are colored like a stoplight: green for go (2^{k-1} runs), yellow for proceed with caution (2^{k-2} runs), and red for stop (2^{k-3} runs), which represent varying degrees of resolution. The choice of a specific design to use depends on the objectives to achieve, but also the amount of sample and the cost required per experiment (reagent, transportation and other factors).

The Jetleach setup used in all these experiments required a large amount of sample per run (10-20 kg) depending on the slurry density. A full two-level design of experiment involving five parameters requires 32 runs in total, which would have required an equivalent of almost 640 kg of sample to just determine the significant figures. It was then crucial to find a way to reduce the number of runs but without affecting the significance of the experimental design used. Therefore, instead of a full two levels design, a green design was selected to evaluate the interaction between these five parameters. The green design only requires 16 runs to achieve a good determination of the significant factors.

3.4.3 Effect of cavitation on solid particles

As presented in the characterization of the Ergo sample, almost 40% of gold particles are locked either in pyrites, silicates, arsenopyrite or other sulphides minerals. Normal cyanidation methods cannot reach gold particles that are locked. However, cavitation phenomenon generated in the Jetleach can reach the locked gold by producing micro bubbles or micro-cavities which once collapsing generate cracks and cavities on the surface of solids particles allowing cyanide solution to penetrate and leach gold particles that were locked in pyrite and arsenopyrite.

To investigate the effect of cavitation on the solid particles, two analyses were required. The SEM analysis was done on the residue after Jetleaching to visualize the presence of cracks and cavities on the surface of solid particles. The particle size analysis was also performed on the Ergo samples before and after passing through the Jetleach reactor to verify if there was any comminution of the solid particles. The PSD analysis was done on each representative sample using the Malvern Mastersizer. The Malvern uses a laser diffraction particle size analyzer, which delivers rapid and accurate particle size distributions for both wet and dry dispersions.

3.4.4 Mechanism of cavitation

To understand the mechanism of cavitation, generation and collapsing of bubbles, a special apparatus was made by isolating one of the nozzles used in the Jetleach reactor in a tube reactor. As presented in **Figure 3.5**, the design consists on a transparent reactor (tube in Perspex) in which water is impacted at a very high velocity to simulate the impact generated in the impactor of the Jetleach reactor. A high-speed camera was placed outside the reactor to capture the cavitation phenomenon that takes place in the reactor. In these sets of experiment, the focus was more on capturing how cavitation is generated and the parameters influencing the phenomenon. Therefore, the only parameter studied in these set of experiments was the effect of the solution flowrate on the cavitation zone.

It is important to note that water with different colorations was used instead of slurry as in the leaching set of experiments in order to have a better visual observation of any cavity formed.

The cavitation setup consisted of a transparent tube reactor where the solution was passed at high velocity through a nozzle specially designed to generate micro-cavitation (see **Figure 3.5** below). After passing through the transparent reactor, the solution returns to the holding tank.

The setup was equipped with a flow meter and a valve before the flow meter to control the flow passing through the nozzle.

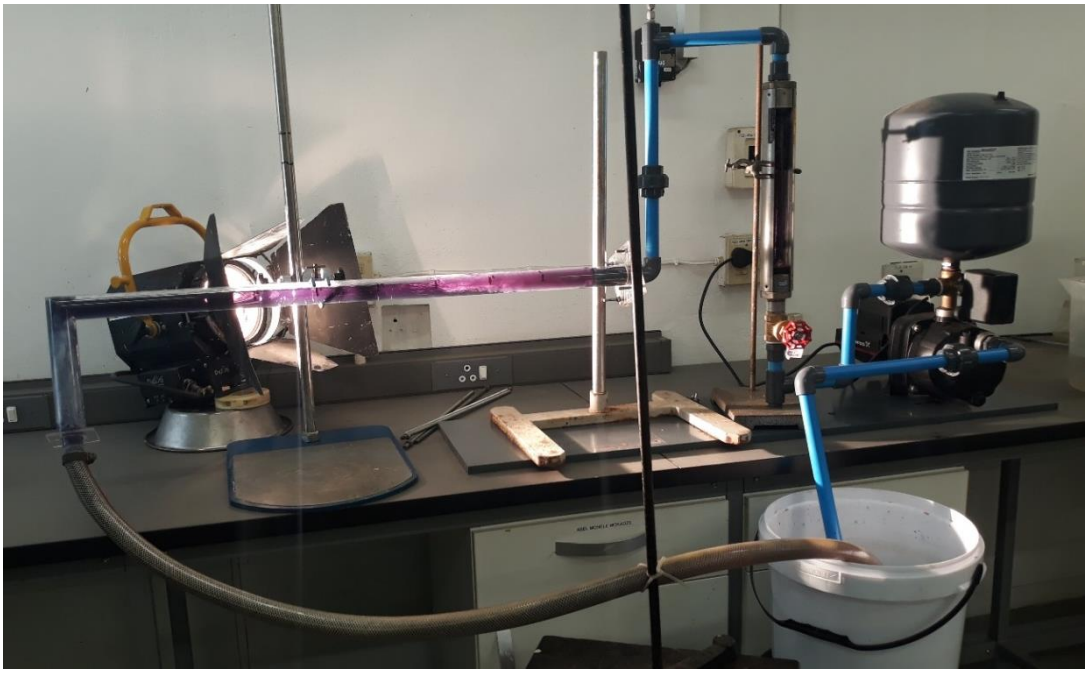


Figure 3.5: Setup to study the mechanism of micro-cavitation

3.4.5 Experimental Design

The experimental design indicating the methods, test conditions, samples tested and the number of replicates for each experimental test used in this work and discussed in the preceding sections is presented in **Table 3.3** below.

Table 3.3 : Experimental design

Test type	Methods used	Test conditions	Samples tested	Replicates
Preliminary tests (pre-aeration + cyanidation)	• Oxidation • Normal leaching	• Eh • pH • Dissolved oxygen	• DIO • MVO • Ergo	2
Comparison of different leaching methods	• Bottle rolling • Normal leaching • Jetleaching	• Same conditions for all three methods (pH, CN, Oxy and Leaching time)	• DIO • MVO • Ergo	2
One factor at a time experiments (OFAT)	• Jetleaching	• Solid percentage • CN concentration • Oxygen flowrate • Space between nozzles • Pump pressure	• Ergo	2
DOE experiments: Identification of influential parameters	• Jetleaching	• Solid percentage • CN concentration • Oxygen flowrate • Space between nozzles • Pump pressure	• Ergo	2
Impact of cavitation on solid particles	• Jetleaching	• SEM analysis • PSD analysis	• Ergo Jetleach residue	2
Visualization test (cavitation)	• Jetleach simulator	• High speed photography	• Water with different colours	3

The agitation speed for the normal leaching and the stirred tank connected to the Jetleach was kept at 500 rpm while the bottle roller speed was kept at 35 rpm

3.5 Data Analysis

The data was obtained as described in the foregoing sections of this chapter. The data obtained was used to determine relationships between the desired responses (gold extraction) and the parameters tested. The gold extraction was calculated as a percentage of the gold in the solution to that in the feed sample. The interactions between parameters, identifications of significant factors and determination of the optimum conditions were done using the software Design-Expert 11. This software makes it possible to see what, if anything, emerges as statistically significant and how to model the results most precisely. It also offers a wide selection of graphs that help identify standout effects and visualize the results.

3.6 Summary

This chapter has covered the type of materials involved in this work, reagents, methods, experimental design, data collection and data analysis of the results. The experimental results and discussions are discussed in the subsequent chapters of this dissertation.

CHAPTER 4 CHARACTERIZATION OF REFRACTORY GOLD ORES

4.1 Introduction

Refractory gold ores are ores which give low gold recovery during a normal cyanidation process. As presented in chapter 2, section (**2.2.1**)**,** there are five major causes of the refractoriness of gold ores. Gold particles can be physically locked, chemically locked, in association with reactive gangue, the ore can contain carbonaceous or silicates materials which might re-adsorb the gold in solution; or the ore can contain some ionic species which might passivate the surface of gold particles and therefore inhibit the reaction. It is, therefore, important to do a complete mineralogical investigation in order to understand the type of ore that will be processed and the type of leaching configuration (CIL or CIP) adequate to treat these ores.

4.2 Results and discussions

4.2.1 Ergo sample

4.2.1.1 *XRD analysis*

The XRD results revealed that most of the sample predominantly consisted of quartz and pyrite, in the proportion of 45.13% and 36.33% respectively. The XRD results in term of relative abundance is presented in **Table 4.1** whilst the detailed XRD analysis is presented in **Table 4.2**.

Table 4.1 : X-ray diffraction results (Relative Abundance)

	Compound Name	Formula	Relative Abundance
	Quartz	SiO_2	Predominant
	Pyrite	FeS_2	Major
	Chlorite	$(Mg,Fe)_6(Si,Al)_4O_{10}(OH)_8$	Minor
	Muscovite	$KAl_2(Si_3\ Al)O_{10}(OH,F)_2$	Trace
	Pyrophyllite	$Al_2Si_4O_{10}(OH)_2$	Trace

Predominant (>50 mass %), Major (20-50 mass %), Minor (20-5 mass %) and Trace (< 5 mass %)

Table 4.2 ***: Detailed X-ray diffraction results***

Mineral	Chemical Formulae	Mass%
Quartz	SiO_2	45,13
Pyrite	FeS_2	36,33
Muscovite	$KAl_2(Si_3Al)O_{10}(OH,F)_2$	5,34
Chlorite	$(Mg,Fe^{2+})_5AlSi_3Al_2O_{10}(OH)_8$	4,11
Pyrophyllite	$Al_2Si_4O_{10}(OH)_2$	4,07
Goethite	$Fe^{3+}O(OH)$	2,01
Rutile	TiO_2	0,67
Biotite	$K(Mg,Fe{+}{+})_3[AlSi_3O_{10}(OH,F)_2$	0,46
K-feldspar	$KAlSi_3O_8$	0,28
Plagioclase	$(Na,Ca)(Si,Al)_4O_8$	0,41
Diopside	$CaMgSi_2O_6$	0,18
Chalcopyrite	$CuFeS_2$	0,38
Arsenopyrite	FeAsS	0,33
Other sulphides		0,13
Other		0,17
Total		100

"Other sulphides" include galena and sphalerite and "Other" includes titanite, apatite, monazite, dolomite, calcite and garnet

4.2.1.2 *Gold speciation*

The results of the gold speciation presented in **Table 4.3** show that gold occurs primarily in two forms, native gold and electrum which is gold combined with silver in different proportions. These results also show that over 70% of the gold present in the sample is native gold and less than 30% is electrum.

Table 4.3 ***: Gold speciation results***

Species	Ergo Conc. Sinks	
	Area%	Mass%
Electrum	26.0	29.17
Gold	74.0	70.83
Total	**100.0**	**100.00**

4.2.1.1 *Gold grain size distribution*

The particle size distribution was done on two different screens (25 and 10 microns) as presented in **Table 4.4** and **Table 4.5**. Results in Table 4.4 show that 35.49% of the particles are bigger than 25 microns, 36.31% between 25 and 10 microns and 28.21 fewer than 25 microns. **Table 4.5** shows the gold and total sulphur contained in each size fraction of the flotation concentrate.

Table 4.4 ***: Particle size distribution of flotation concentrate***

Particle size	Flotation concentrate
+25 microns	35.49%
+10 microns	36.31%
-10 microns	28.21%

Table 4.5 ***: Assay by size fraction***

Size fraction	Flotation concentrate gold g/t	Flotation concentrate total sulphur %
+25 microns	2.73	19.39
+10 microns	2.31	23.13
-10 microns	2.05	5.11

4.2.1.2 *Gold liberation*

The gold liberation by grade shown in **Table 4.6** and **Figure 4.1** shows that almost 44% of the gold present in the flotation concentrate are locked, 12.82% are low middlings, 29.52% high middlings while only 13.29% are liberated.

Table 4.6 ***: Ergo Conc. Sinks-Liberation by Grade (Discrete)***

Fraction	Locked			Low Middlings		High Middlings			Liberated		
	<= 10%	<= 20%	<= 30%	<= 40%	<= 50%	<= 60%	<= 70%	<= 80%	<= 90%	< 100%	100%
+25 µm	78.04	0.00	0.00	0.00	10.28	11.68	0.00	0.00	0.00	0.00	0.00
-25/+10 µm	14.61	0.00	0.00	0.00	12.81	52.13	0.00	0.00	0.00	20.45	0.00
-10 µm	13.38	23.57	0.00	17.83	1.91	4.46	0.00	9.55	19.11	0.00	10.19
Combined	40.78	3.59	0.00	2.72	10.10	28.06	0.00	1.46	2.91	8.83	1.55

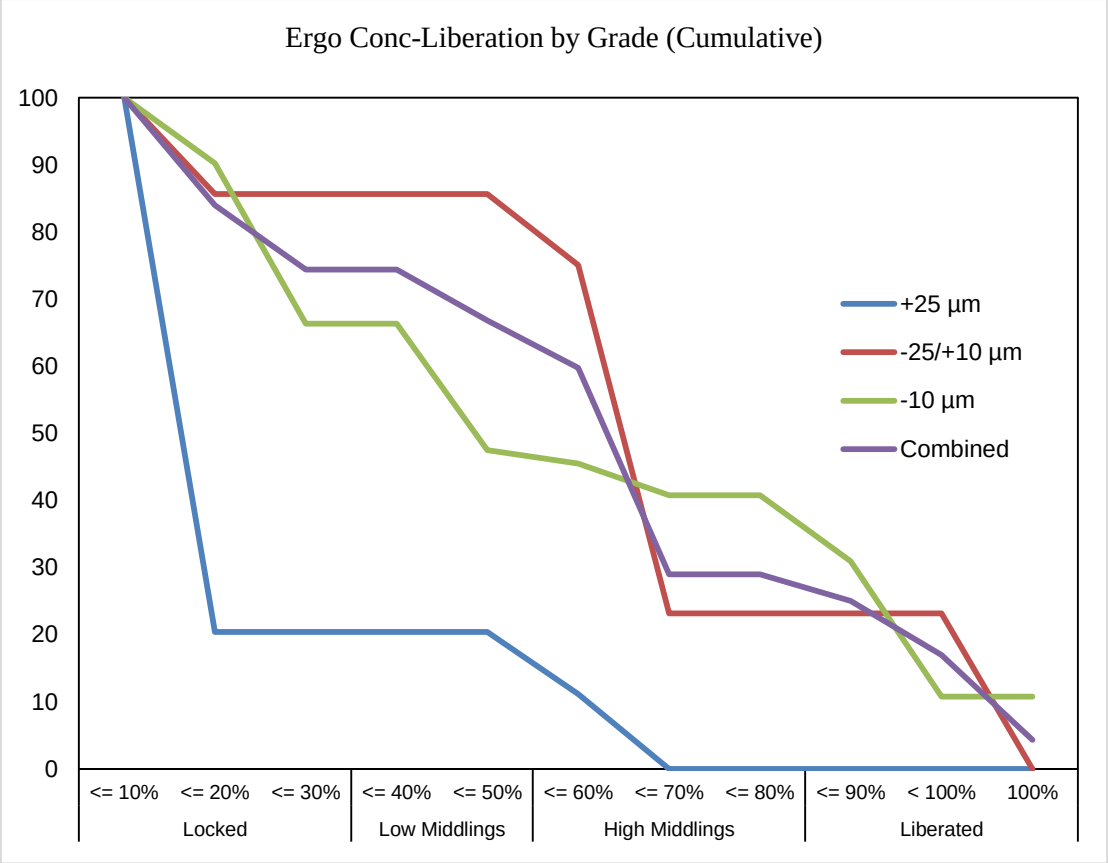


Figure 4.1 : Gold liberation by grade

4.2.1.3 *Gold grain mineral association*

The gold association with different mineral is presented in **Table 4.7** below. This Table shows that 25.4% of gold is present as free milling gold, 44% is associated with sulphides (pyrite representing 24.07% and 20% representing other sulphide). However, more than 23% of gold is associated with silicates.

The EDS spectra and the BSE image of different particles were done using the QEMSCAN. These results revealed that gold exist in different degree of liberation depending on the mineral association. It also shows how most gold particles are locked in pyrite, arsenopyrite and silicate. Results from the QEMSCAN analysis are presented in the appendix A.

Table 4.7 ***: Gold association (details and synthesis)***

Mineral	Ergo Conc.
	Gold
Free Surface	25,37
Arsenopyrite	5,19
Mixed Cu-Fe-S phase *	8,33
Pyrite	24,07
Pyrrhotite	5,19
Other Sulphides*	1,48
Microcline	2,04
Plagioclase	0,37
Quartz	5,37
Fe Silicate	2,96
Other Silicates*	12,78
Other Oxides	0,19
Rutile	0,00
U-bearing phases (Uraninite and Coffinite)	6,67
Monazite	0,00
Total	100,00

Association type	Flotation concentrate %
Free gold	25.4
Sulphides	44.2
Silicates	23.5
Oxides	0.2
Uranium minerals	6.7

4.2.2 Samples from West Africa

The two samples from West Africa (Diorites and Meta volcanic gold ores) were submitted to Suntek for a mineralogical analysis. X-ray diffractometer (XRD) and automated mineralogical analysis was used to study the mineralogy of the ore. A Panalytical X'pert Pro

diffractometer, that employed Co-radiation, was used to collect the XRD patterns. The data was then interpreted using the Panalytical High-Score Plus analytical software and the PAN-ICSD database (Panalytical-Inorganic Crystal Structure Database).

The automated mineralogical analyses consisted of modal analysis, particle map analysis and gold grain mapping using an MLA (Mineral Liberation Analyzer). SEM-EDS spot analyses (Scanning Electron Microscopy coupled with Energy Dispersive Spectrometry) were used to obtain the Mineral compositional. Two 90°-cut polished sections were prepared from each sample for the modal analysis. Ten normal polished sections were prepared from the concentrate samples for the gold searches.

4.2.2.1 *XRD analysis*

The XRD results are presented in **Table 4.8** below. The mineralogical analyses revealed that pyrite is present at 10-20% in both ores (DIO and MVO), while quartz is present at 10-20% in the DIO and 20-30% in the MVO. The XRD histogram presented in **Figure 4.2** indicate the presence of mineral such as pyrite, calcite, dolomite and other minerals constituting the two samples.

Table 4.8 ***: XRD of Diorites and Meta-volcanic gold sample***

Mineral	Formula	Mineral abundances (%)	
		DIO	MVO
Quartz	SiO_2	10-20	20-30
Plagioclase	$(Ca, Na)(Al, Si)_4O_8$	10-20	10-20
Chlorite	$(Fe, Mg)_5Al(Si_3Al)O_{10}(OH, O)_8$	20-30	10-20
Dolomite	$CaMg(CO_3)_2$	3-10	10-20
Mica	$KAl_2(Si_3Al)O_{10}(OH, F)_2$	10-20	10-20
Calcite	$CaCO_3$	3-10	3-10
Pyrite	FeS_2	10-20	10-20
Rutile	TiO_2	<1	<1

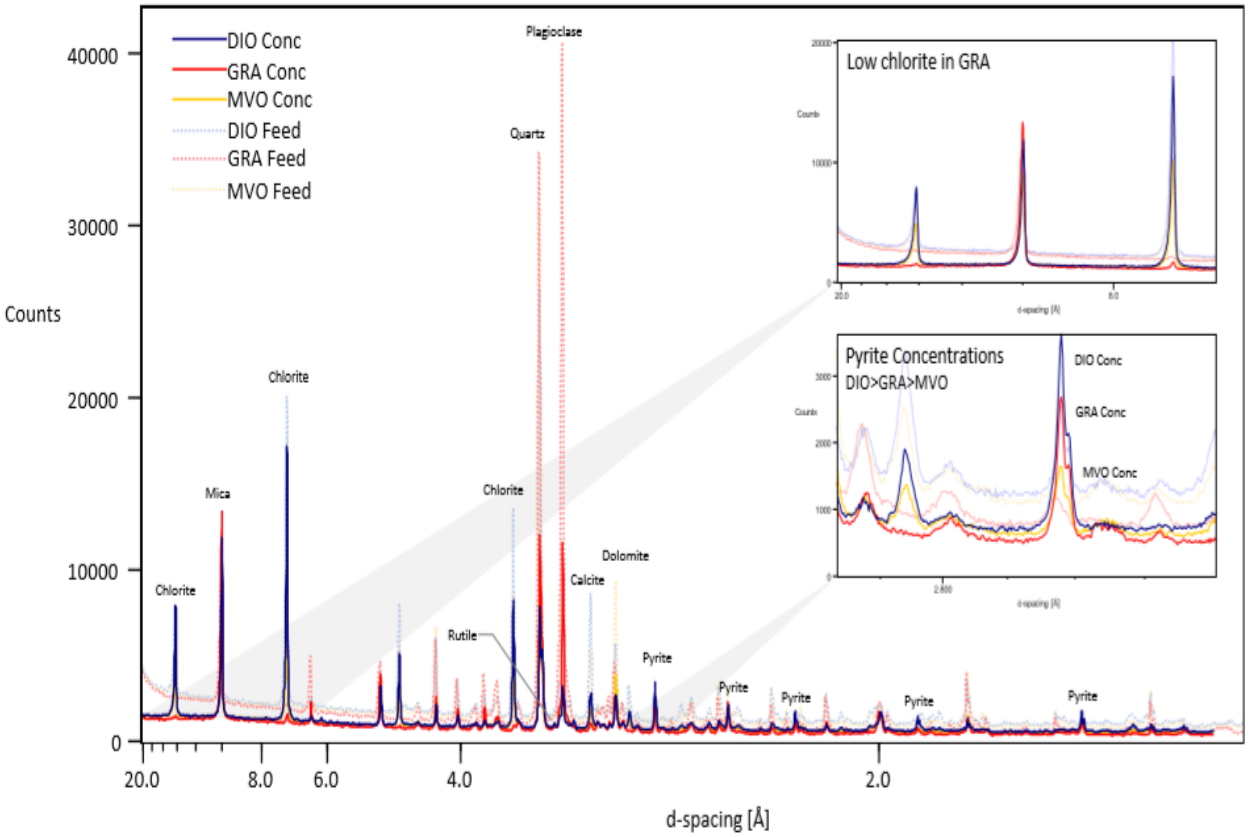


Figure 4.2 : X-ray diffractograms of the feed and concentrate samples.

4.2.2.2 *Automated Mineralogy / MLA Modal Analysis*

Modal analysis was done on the two flotation concentrate samples as shown in **Table 4.9** below. The results corroborate the XRD data, which indicated the presence of quartz (~16-22%), plagioclase (~10-16%), mica (~16-22%), chlorite (~13-19%) and ankerite/dolomite (~0-2%) and pyrite (~11-23%) as the major minerals in the rougher concentrate samples.

Table 4.9 ***: Results of the Modal Analysis***

Mineral	Approximate Formula	Mineral Abundance (%)	
		DIO	MVO
Quartz	SiO_2	16.31	21.26
Plagioclase feldspar	$(CaNa)(Al,Si)_4O_8$	11.56	15.25
Mica	$KAl_2(Si_3Al)O_{10}(OH,F)_2, K(Mg,Fe)_3AlSi_3O_{10}(OH,F)_2$	16.75	21.95
Chlorite	$(Fe,Mg)_5Al(Si_3Al)O_{10}(OH,O)_8$	18.98	13.08
Other Silicates	$CaTiSiO_5, ZrSiO_4$	0.05	0.09
Total Silicates		**63.65**	**71.63**
Pyrite	FeS_2	23.42	10.52
Arsenopyrite	$FeAsS$	0.36	0.86
Other Sulphides	$PbS, CuFeS_2,\ Cu_{12}As_4S_{13}$	0.18	0.18
Total Sulphides		**23.96**	**11.56**
Fe-oxide	Fe_2O_3, Fe_3O_4	0.16	0.12
Rutile	TiO_2	0.53	0.56
Chromite	$FeCr_2O_4$	0.00	0.09
Total Oxides		**0.69**	**0.77**
Ankerite	$Ca(Fe,Mg,Mn)(CO_3)_2$	6.59	8.97
Calcite	$CaCO_3$	2.87	2.97
Dolomite	$CaMg(CO_3)_2$	0.61	1.62
Total Carbonates		**10.07**	**13.56**
Apatite	$Ca_5(PO_4)_3(OH,F,Cl)$	0.08	0.16
Monazite	$(Ce,La,Nd,Th)PO_4$	0.31	0.67
Total Phosphates		**0.39**	**0.83**
Barite	$BaSO_4$	0.01	0.01
Native Copper	Cu	0.05	0.34
Other		1.15	1.31
Total		**100.00**	**100.00**

4.2.2.3 *Automated Mineralogy | MLA Gold Deportment*

The results of the gold deportment show that gold occurs primarily in the form of native gold with a negligible proportion of gold occurring in Petzite. The MLA results have identified two forms of native gold, namely low Ag gold (avg. ~5.4% Ag) and high Ag gold (avg. ~12.7% Ag). The SEM-EDS analysis of 39 gold grains from all two samples indicated that

the distribution of Ag is variable (~2 to 18%). SEM photomicrographs, accompanied by MLA particle maps and EDS spectra, of selected gold grains are shown in **Figure 4.3** below.

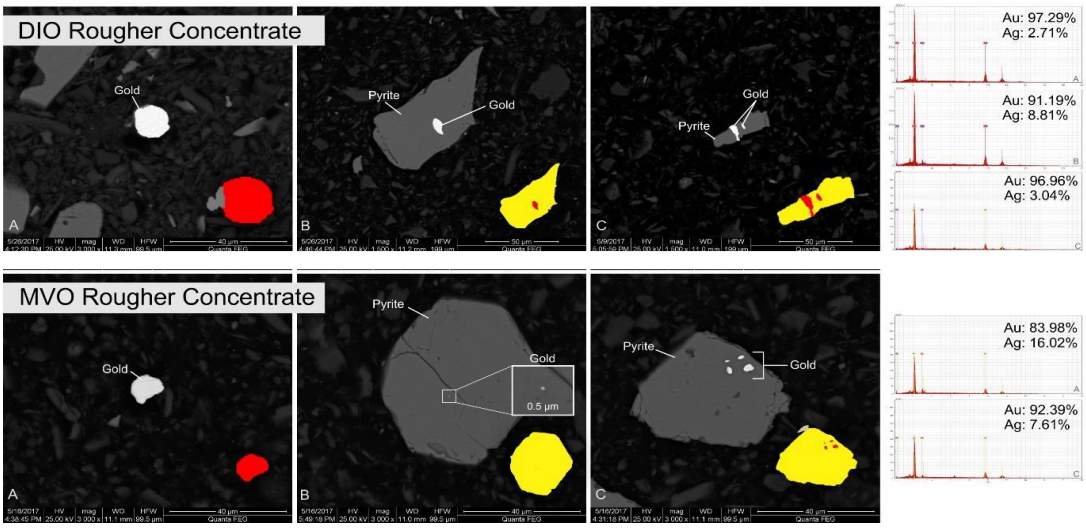


Figure 4.3 : SEM photomicrographs, MLA particle maps and EDS spectra of selected gold grains.

4.2.2.4 *Gold grain size distribution*

The gold grains size in all two samples were very fine-grained (<20 µm) as shown in **Figure 4.4** below. Most of the grains range between 2 and 14 µm in size (~88-93%).

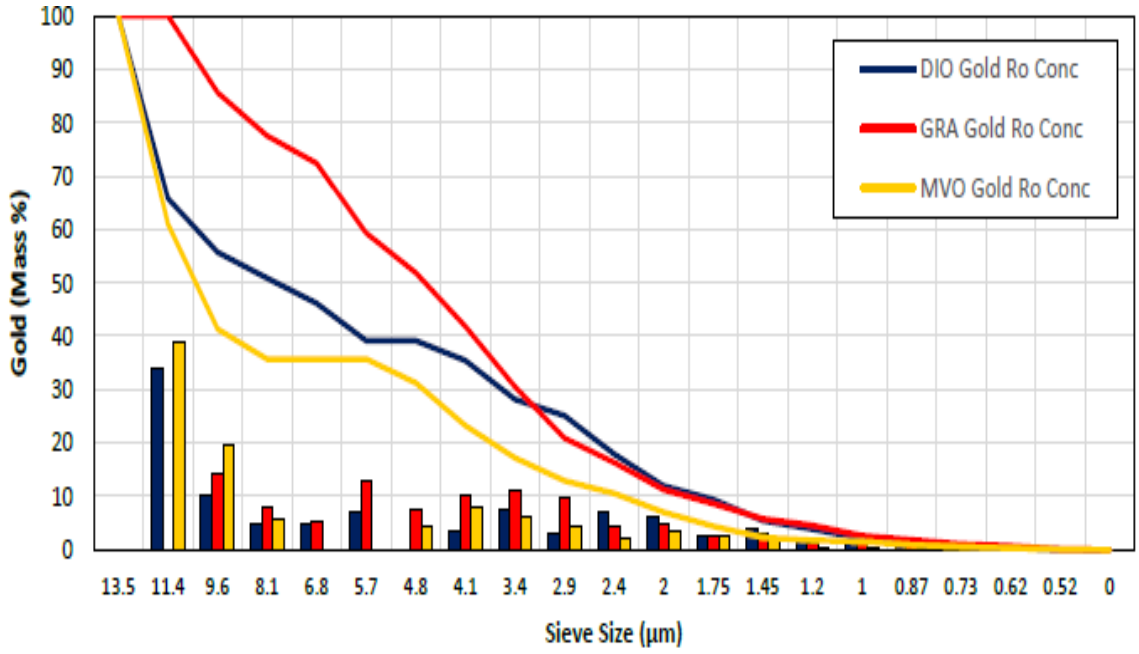


Figure 4.4 Grain size distribution data of gold (discrete and cumulative).

4.2.2.5 *Gold liberation*

Results obtained from the SEM photomicrographs accompanied by the MLA particle maps analysis indicating the liberation characteristics of gold revealed that there was a relatively high proportion of locked gold (~23-51%), a low proportion of middlings gold (~3-26%) and a variable amount of liberated gold (~23-75%). The refractoriness of these ores is mainly because gold is locked and associated with labile sulphides and other sulphides present in the ore. It is important to note that more gold particles were locked into pyrite in the MVO sample (~17%) compared to the DIO sample (~25%). However, the size distribution of the pyrite reveals that gold occurs in two main modes as presented in **Figure 4.5** below:

1. Numerous fine-grained gold grains (<4 µm), accounting for approximately a third of the gold mass, occurring as locked and enclosed gold within pyrite and other sulphides (type I).
2. A few relatively coarse-grained gold grains (>4 µm), accounting for most of the gold mass, occurring as liberated and middlings gold with elevated degrees of exposure (type II).

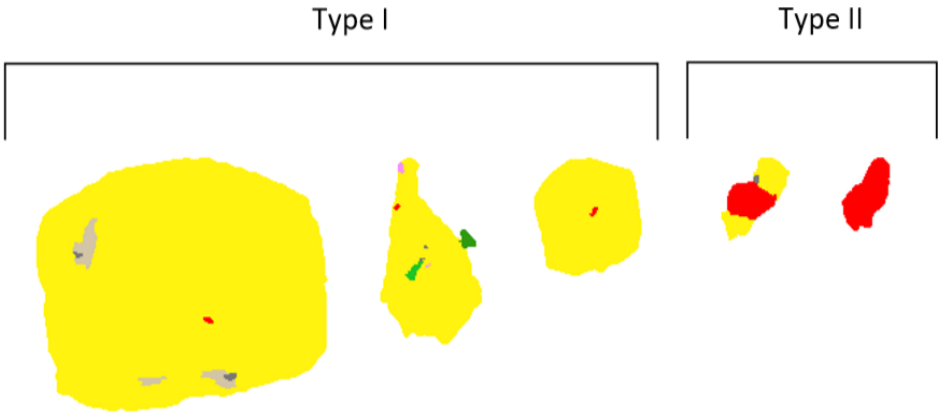


Figure 4.5 : Modes of gold occurrence.

4.2.2.6 *Gold grain mineral association*

The gold mineral association represented in **Table 4.10**, shows that pyrite is the major mineral in association with gold and ranges from ~85 to 96%, however associations with silicates and arsenopyrite were recorded in the MVO sample (~2% and ~6%, respectively).

Table 4.10 ***: Gold mineral associations (%)***

Mineral	Rougher Concentrate	
	DIO	MVO
Silicates	1.06	2.40
Pyrite	96.18	85.15
Arsenopyrite	0.21	6.01
Other sulphides	0.26	4.08
Rutile	0.29	0.00
Dolomite/ankerite	0.00	1.21
Monazite-(Ce)	0.00	0.00
Other	2.02	1.16
Free Surface	-	-
Total	100	100

4.3 Summary and Conclusion

Three gold flotation samples were involved in these investigations. One from Ergo plant in South Africa and the other two samples (DIO and MVO) are from West Africa. The mineralogical analysis on the Ergo sample shows that almost 44% of the gold particles present in the flotation concentrate are locked, 12.82% are low middlings, 29.52% high middlings while only 13.29% are liberated. This investigation also showed that 25.4% of gold is present as free milling gold, 44% is associated with sulphides, with pyrite representing 24.07%. However, more than 23% of gold is associated with silicates.

For the DIO and MVO samples, a large proportion of gold grains are locked (23-51%), a low proportion are middlings (~3-26%) and a variable amount of liberated gold (~23-75%). The refractoriness of these ores is mainly due to the locked gold and gold associated with labile sulphides and other sulphides present in the ore. The gold mineral associations of DIO and MVO shows that pyrite is the major mineral in association with gold and ranges from ~85 to 96%, however less than 6% of the gold particles were in association with silicates and arsenopyrite.

This chapter has covered the material characterization of the three samples involved in this work and it has revealed that all three samples contain a high concentration of pyrite and other sulphide minerals, therefore, the next chapter focuses on the comparison between the Jetleaching method and the conventional methods used to leach refractory gold ores as well as the potential benefits generated by the use of the Jetleach.

CHAPTER 5 COMPARISON BETWEEN CONVENTIONAL LEACHING METHODS AND JETLEACHING METHOD ON REFRACTORY GOLD ORES

5.1 Introduction

As presented in chapter 3, this project involved three different samples, two samples from West Africa (DIO and MVO) and one sample from Ergo in South Africa. The mineralogical analysis of all the three-flotation concentrates have revealed that they contain a very high proportion of pyrite and other sulphidic material. Pyrite is considered as a cyanicides during gold leaching. The presence of pyrite and other sulphidic material substantiated the necessity of pre-aeration to prevent reaction of these elements with cyanide during the leaching period hence reducing cyanide consumption. Therefore, these comparison tests were first preceded by preliminary tests which consisted of evaluating the effect pre-aeration on the cyanide consumption.

The pre-aeration stage was done by monitoring the variation of the pH, Eh and dissolved oxygen in the slurry. This stage was then followed by cyanidation in an agitated vessel to evaluate the effect of pre-aeration on cyanide consumption. All cyanidation tests were done at a cyanide concentration of 5kg/t, oxygen flowrate of 30 ml/min, pH: 10.5-11.5 and a slurry solid percentage of 40% by weight.

Many leaching methods have been developed to improve the leaching kinetics and the gold recovery from refractory gold ores. However, there are two main methods used to conduct cyanidation in the laboratory. The two methods generally used are the bottle roll method and leaching in agitated vessel. Therefore, after the pre-aeration test, the next stage was to compare the performance of the Jetleach reactor to the conventional leaching methods, here represented by the bottle roll and leaching in agitated vessel or normal leaching. In order to have an accurate comparison, all experiments were done under the same conditions. The cyanide concentration was kept at 5kg/t, oxygen flowrate at 30 ml/min, pH: 10.5-11.5 and slurry solid percentage at 40% by weight. The two additional parameters of the Jetleach, pump pressure and space between nozzles, were also kept constant at 15 MPa and 0.8 Cm, respectively.

The leaching stage was then followed by the evaluation of the potential benefits the use of the Jetleach reactor can generate when introducing in a conventional cyanidation process.

5.2 Results and discussions

5.2.1 Pre-aeration

It can be seen in **Table 5.1** and **Figure 5.1** that the Eh observed for the Ergo sample started with a negative value of -112 mV, and then increased gradually as the oxidation process continued until the system stabilized at an Eh of 98 mV. However, when dealing with the two samples from West Africa (DIO and MVO), the Eh was already positive, probably because the samples might have partially oxidized due to the long time spent before being delivered at Wits for the test work.

It can be seen from **Figure 5.2** that the pH of all three samples was a bit acidic at the end of the pre-aeration process and this could be an indication of a certain amount of sulphide minerals present which oxidized forming sulphuric acid. The insignificant change in pH after 5 hours can be an indication of a passivating layer being formed around the sulphide minerals thereby reducing the rate of decomposition of sulphides into acid. It can also be seen from **Figure 5.3** that by using oxygen to oxidize Fe (II) into Fe (III), the concentration of dissolved oxygen in the slurry also augments the pre-aeration process.

Table 5.1 : Pre-aeration process of slurry before cyanidation

Time	pH			Eh (mV)			DO (mg/L)		
	Ergo	DIO	MVO	Ergo	DIO	MVO	Ergo	DIO	MVO
0 min	6,5	7,19	7,92	-112	75	42	6,53	5,04	5,32
30 min	6,45	6,89	7,71	-94	90	79	8,63	6,35	7,54
1 hour	6,42	6,86	7,32	-20	103	83	9,94	7,53	8,45
1h30 min	6,29	6,8	6,94	-15	105	91	11,05	8,43	10,12
2 hours	6,2	6,71	6,82	-1	111	102	12,25	7,88	11,21
2h30 min	6,18	6,36	6,58	5	130	110	11,78	9,21	10,75
3 hours	6,18	6,32	6,34	16	123	112	10,16	9,32	9,22
3h30 min	6,14	6,27	6,3	21	127	124	10,88	10,54	9,82
4 hours	6,14	6,2	6,17	27	129	131	10,55	11,97	9,53
4h30 min	6,11	5,98	6,02	34	130	134	13,52	12,21	12,74
5 hours	6,06	5,74	5,76	69	135	137	14,1	13,42	13,03
8 hours	5,9	5,52	5,45	83	138	139	12,94	13,23	13,22
12 hours	5,82	5,23	5,29	95	138	140	11,13	13,31	13,61
14 hours	5,8	5,23	5,03	97	139	140	13,99	12,77	11,87
16 hours	5,8	5,23	5,01	98	139	140	13,06	12,81	11,03
20 hours	5,8	5,22	5,01	98	139	140	14,89	12,31	12,09

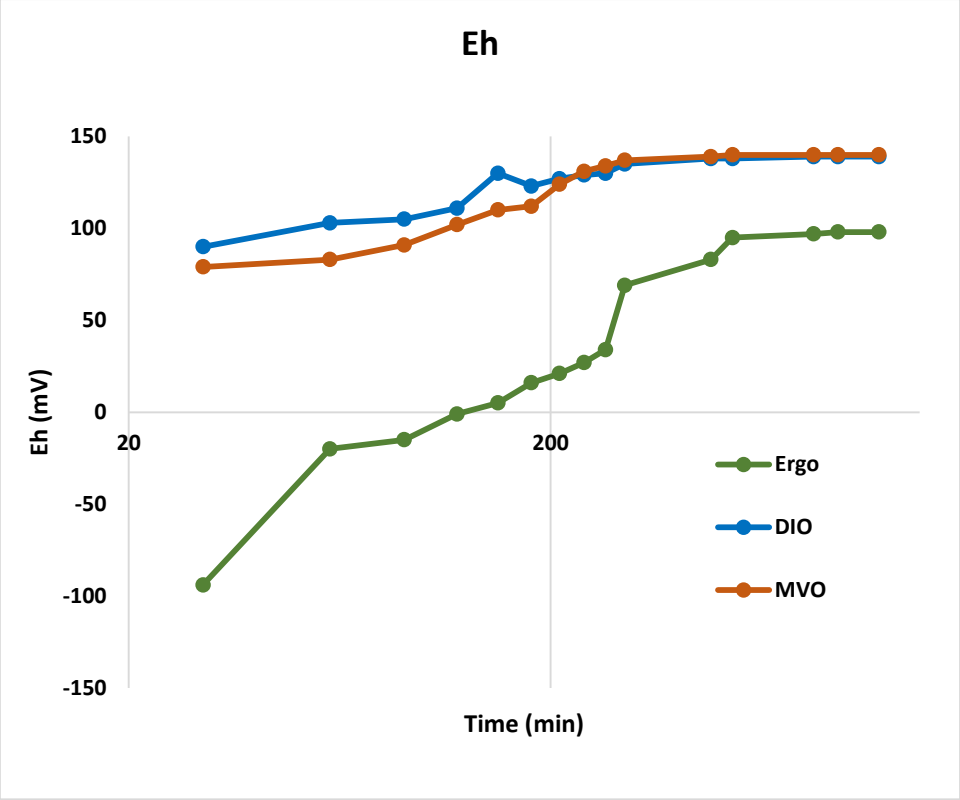


Figure 5.1 : Variation of the Eh during pre-aeration on the Ergo sample

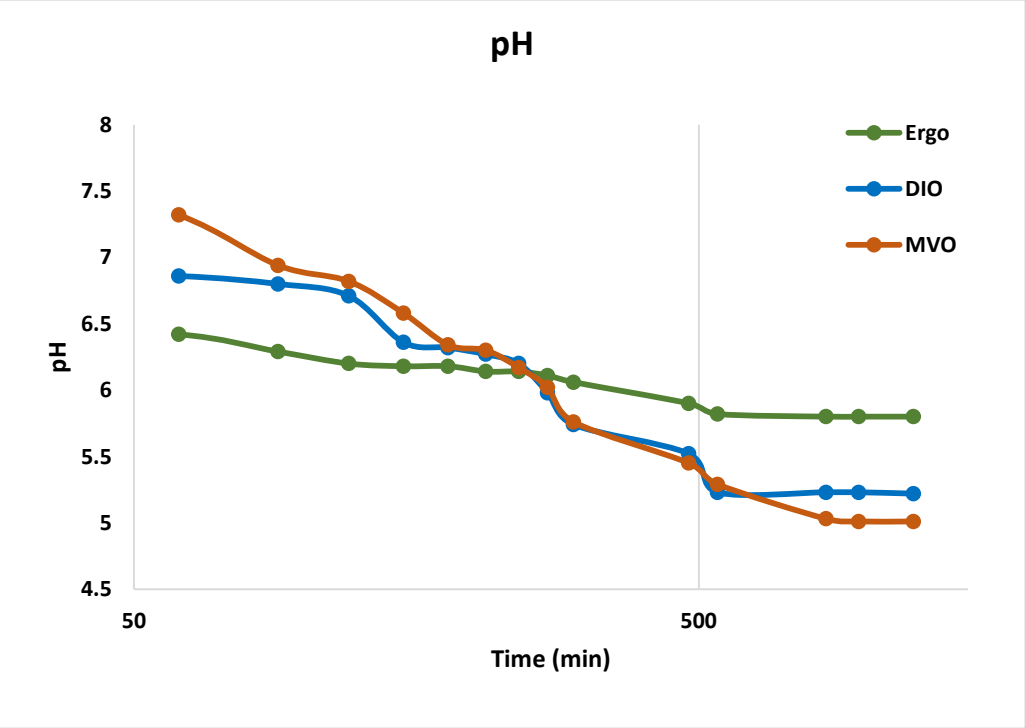


Figure 5.2 ariation of pH during pre-aeration

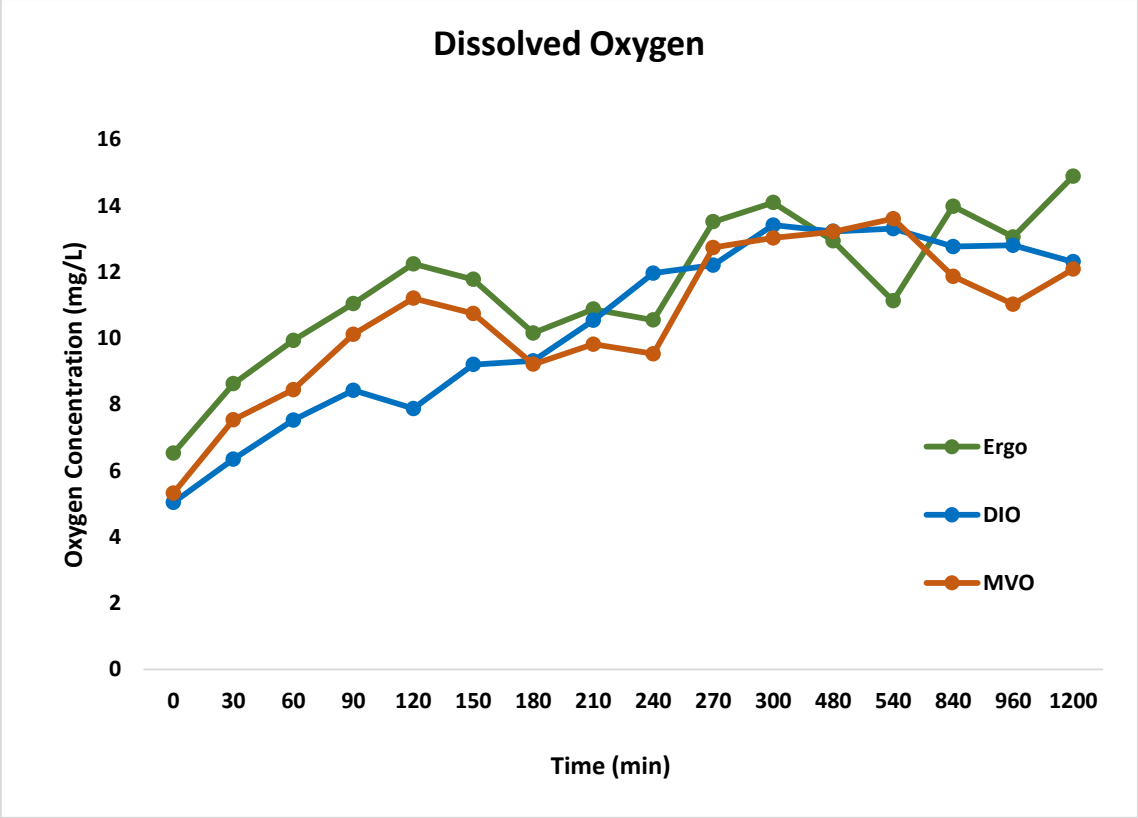


Figure 5.3 : Variation of the oxygen concentration during pre-aeration

The effect of pre-aeration on cyanide consumption can be seen in **Table 5.2** below. The results show that cyanide consumption for all three samples decreased when the slurry was aerated before cyanidation. The amount of cyanide consumed without pre-aeration was 4.97 Kg/t for the Ergo sample, 4.23 Kg/t for the DIO and 4.21 Kg/t for the MVO. When aeration is done prior to cyanidation, the CN consumed decreased to 4.82, 3.7 and 3.69 Kg/T for the Ergo, DIO and MVO, respectively. These results confirm that indeed pre-aeration creates a passivation layer on the surface of pyrite and other sulphides, therefore, reducing their reactivity with cyanide. Pre-aeration seems to have no effect on the gold recovery, almost the same gold recovery was obtained on the sample with and without pre-aeration. This is because the objective of pre-aeration is to target pyrite particles in order to passivate them and render them not reactive to cyanide. However, this treatment does not have any effect in term of gold liberation (Jara & Bustos, 1992; AYDIN , et al., 2015).

Table 5.2 : Effect of pre-aeration on gold recovery and cyanide consumption

Type of sample	Cyanide consumption (Kg/T)		Gold recovery (%)	
	Without pre-aeration (direct cyanidation)	With pre-aeration	Without pre-aeration (direct cyanidation)	With pre-aeration
Ergo sample	4.97	4.82	59.23	59.31
DIO sample	4.23	3.7	76.41	76.40
MVO sample	4.21	3.69	81.7	81.68

5.2.2 Leaching

Results obtained when comparing the Jetleach methods to the conventional methods on the two samples from West Africa and on the Ergo sample from South Africa are presented below.

5.2.2.1 *Samples from West Africa*

- ***Diorite sample (DIO)***

As can be seen from **Figure 5.4**, gold recovery reached 72.3% in 15 minutes with the Jetleach while the conventional and bottle rolling methods gave 19.22% and 17.81%, respectively. After 24 hours of leaching, gold recoveries of 76.42% and 65.27% were obtained with the conventional and the bottle rolling methods, respectively while only 90 minutes was required to reach more than 80% recovery with the Jetleach reactor. After 24 hours of leaching, the Jetleach reactor showed an improvement of almost 8% and 19% compared to the conventional and the bottle rolling methods, respectively.

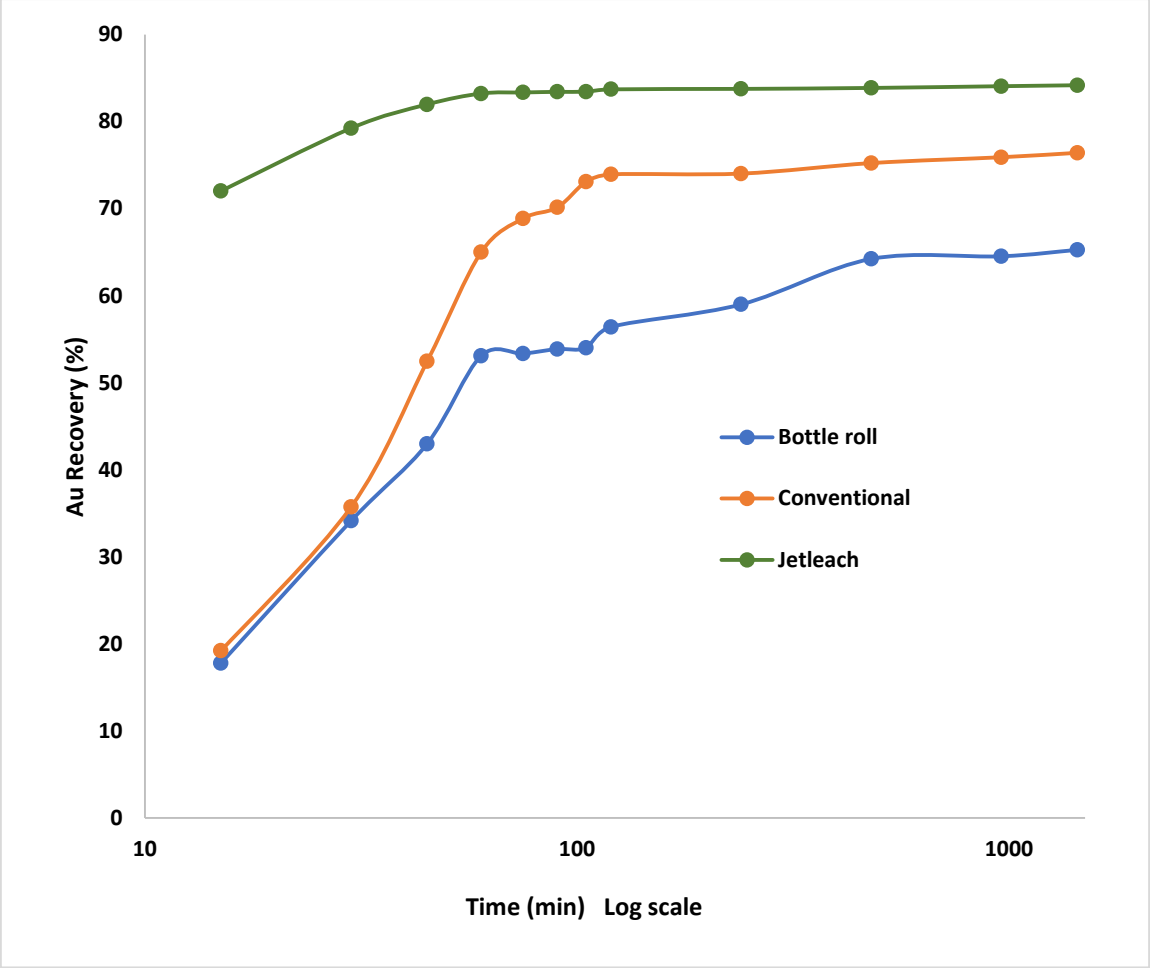


Figure 5.4 : Comparative Trends in Gold Recovery for the DIO sample

- ***Meta-volcanic sample (MVO)***

Figure 5.5 shows the results obtained for MVO samples. It can be seen from the figure that for the Jetleach, only 90 minutes was required to give a gold recovery of over 80% while the conventional and bottle rolling methods gave 75.0% and 67.3%, respectively. Gold recovery of 82.93% was obtained after only 2 hours of leaching using the Jetleach reactor. After 24 hours leaching, a maximum gold recovery of 81.70% was obtained with the conventional method and 74.36% with the bottle roll whilst 91.28% gold recovery was obtained using the Jetleach reactor. This represent a gold recovery improvement of almost 10% and 17% higher compared to the conventional and bottle rolling methods respectively.

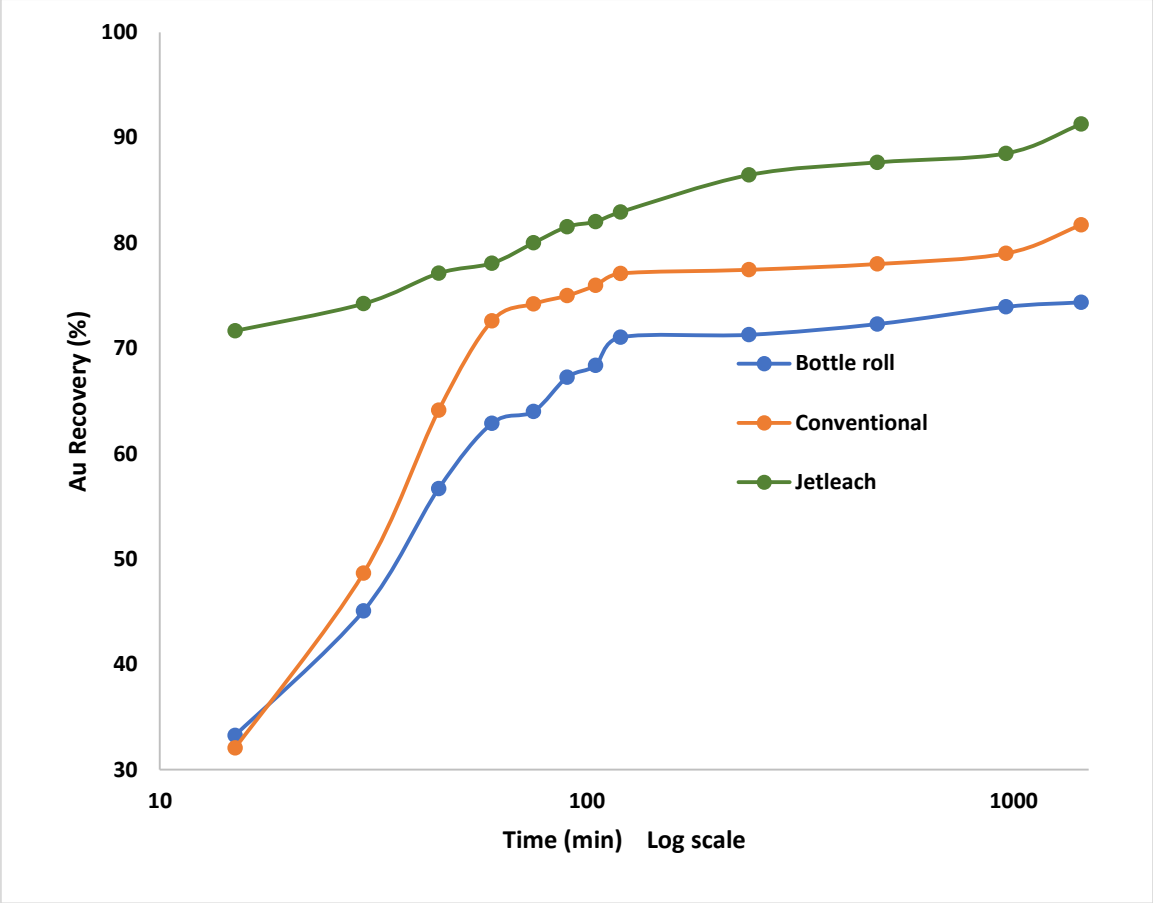


Figure 5.5 : Comparative Trends in Gold Recovery for the MVO Sample

The difference in leaching kinetics between the DIO and MVO samples can be explained by the mineral liberation results which revealed that more gold particles were locked into pyrite in the MVO sample compared to the DIO sample. 25% of gold in the DIO sample is locked into pyrite while only 17% for the MVO sample. This would explain why, in the first hour, we have faster leaching kinetics in the DIO compared to the MVO.

5.2.2.2 *Ergo sample*

When doing the cyanidation tests on the Ergo sample, back loading (preg-robbing) was observed in all three leaching methods (bottle rolling, conventional leaching and Jetleach) as presented in **Figure 5.6**. For the three leaching methods, the gold recovery increased in the first 60 minutes and reached a maximum of 69.74%, 36.48% and 39.37% for the Jetleach, conventional leaching and bottle roll, respectively. After that, the preg-robbing phenomenon become more visible and the gold recovery fluctuated abnormally. This preg-robbing phenomenon observed with the Ergo sample can be associated with the presence of silicate

mineral in the ores. This is because silicates and carbonaceous materials behave as activated carbon and adsorb the gold already in solution (Dunne, et al., 2012).

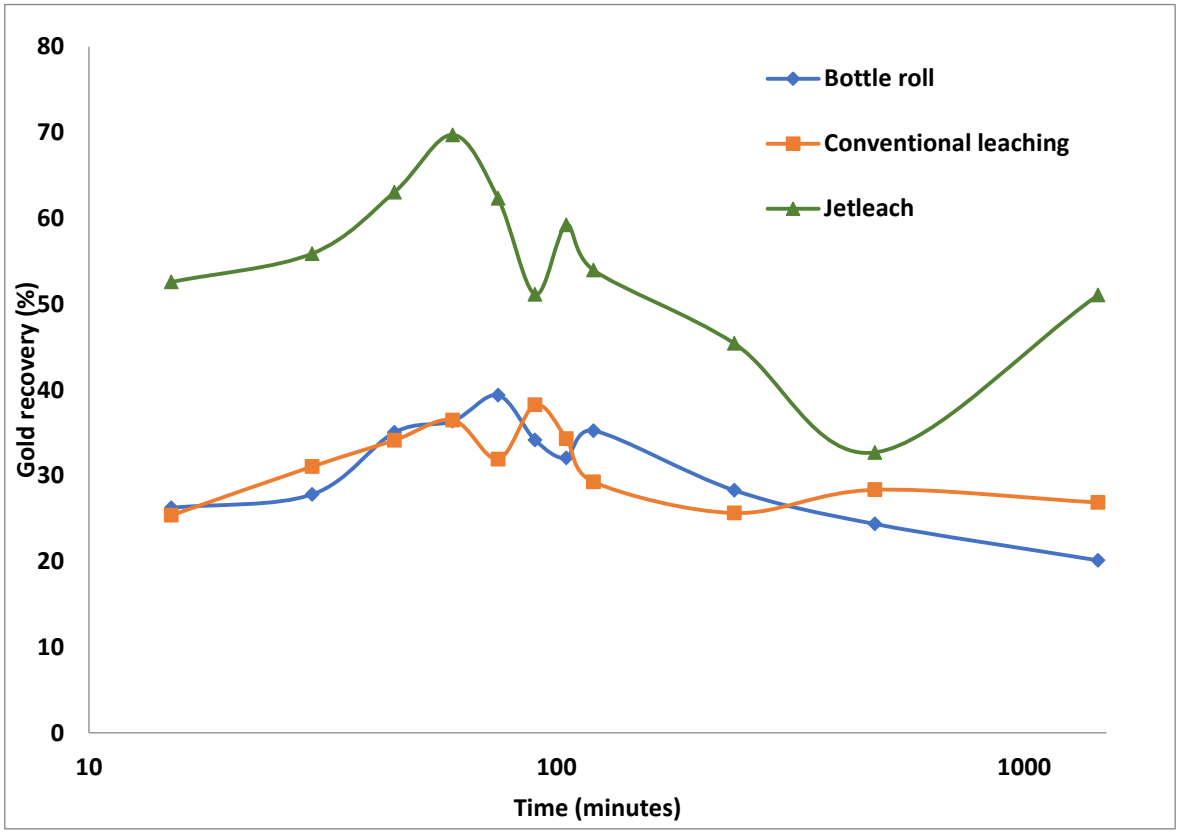


Figure 5.6 : Comparative Trends in Gold Recovery without addition of activated carbon

- ***CIL configuration for the Jetleach reactor***

It has been shown by many researchers that the CIL is the best practical way to prevent preg-robbing (Deschênes, et al., 2003; Adams & Wills, 2005; Marsden & House, 2006; Adams, 2016). This is achieved by adding activated carbon directly to the slurry during the leaching section. The use of activated carbon to prevent the preg-robbing phenomenon was easily achieved for the normal leaching and the bottle rolling experimental setups. However, it was challenging to adapt the Jetleach setup from a CIP process to a CIL process, because of the high-pressure impact of the two streams which was causing the activated carbon to be crushed to very fine particles. This resulted in gold loss due to the entrainment of finer activated carbon in the leach residues.

To overcome this challenge, an activated carbon holding filter was designed. The filter was designed in such a way that the size of the opening of the holes on the filter only allowed the slurry to pass through while retaining the activated carbon inside. This filter could therefore, prevent activated carbon from being entrained and crushed by the Jetleach impactor. The holding filter was then placed in the agitated tank as shown in **Figure 5.7**.

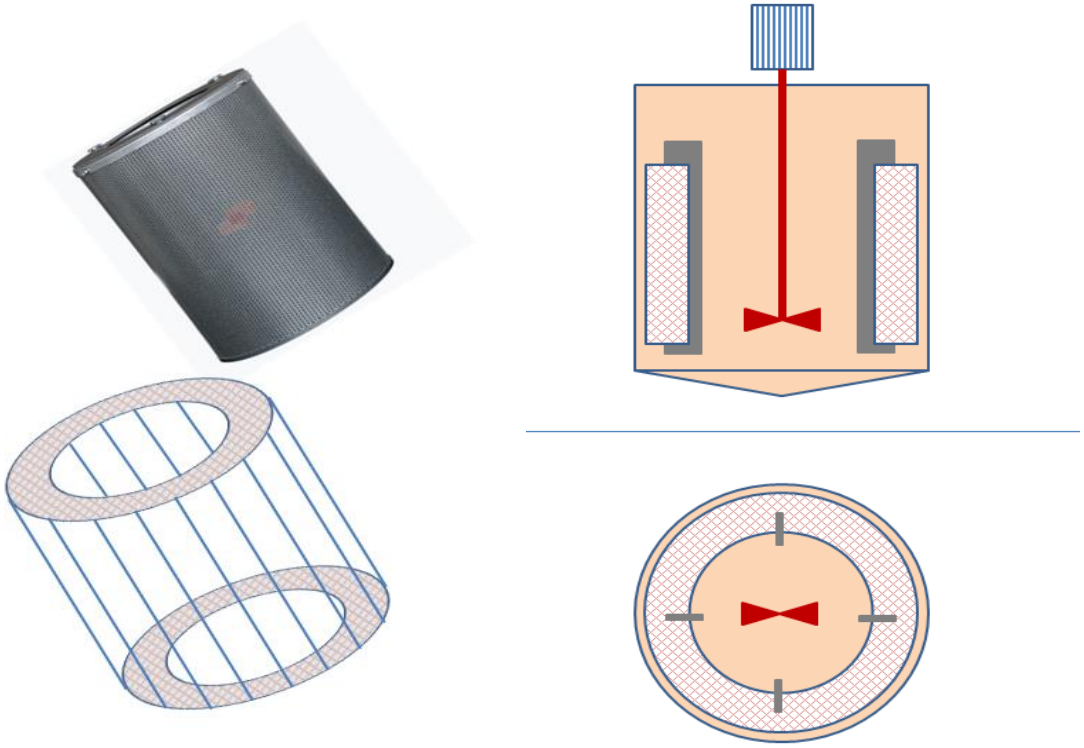


Figure 5.7 : Holding filter for activated carbon

Details of the design of this filter are confidential as there is a patent application pending for this technology. After the design and the construction of the holding filter, the same experiments were done but this time with the process running as a CIL circuit.

It can be seen from **Figure 5.8** that gold recovery reached 52.58% in 15 minutes with the Jetleach reactor while the conventional and bottle rolling methods gave 25.37% and 26.25%, respectively. After 24 hours of leaching, gold recoveries of 59.23% and 56.59% were obtained with the conventional and the bottle rolling methods, respectively while only 45 minutes was required to reach more than 60% recovery for the Jetleach reactor. After 24 hours of leaching, the Jetleach reactor shows a recovery of 72.85% which is an improvement of almost 13.62% and 16.27% compared to the conventional and the bottle rolling methods, respectively. The gold recovery was flat around 75%, this can be explained by the presence

of solid solution gold which could not be liberated by the cavitation mechanisms involved in the Jetleach reactor technology.

The comparison of these three different methods shows that the Jetleach reactor can improve the leaching kinetics and the gold recovery of refractory gold ores by more than 12% compared to the conventional and bottle rolling methods. The results presented in Table 18 also show that the Jetleach reactor can also decrease dramatically the leaching time from 24h to less than 2h while still giving a 10% higher gold recovery compare to the two methods.

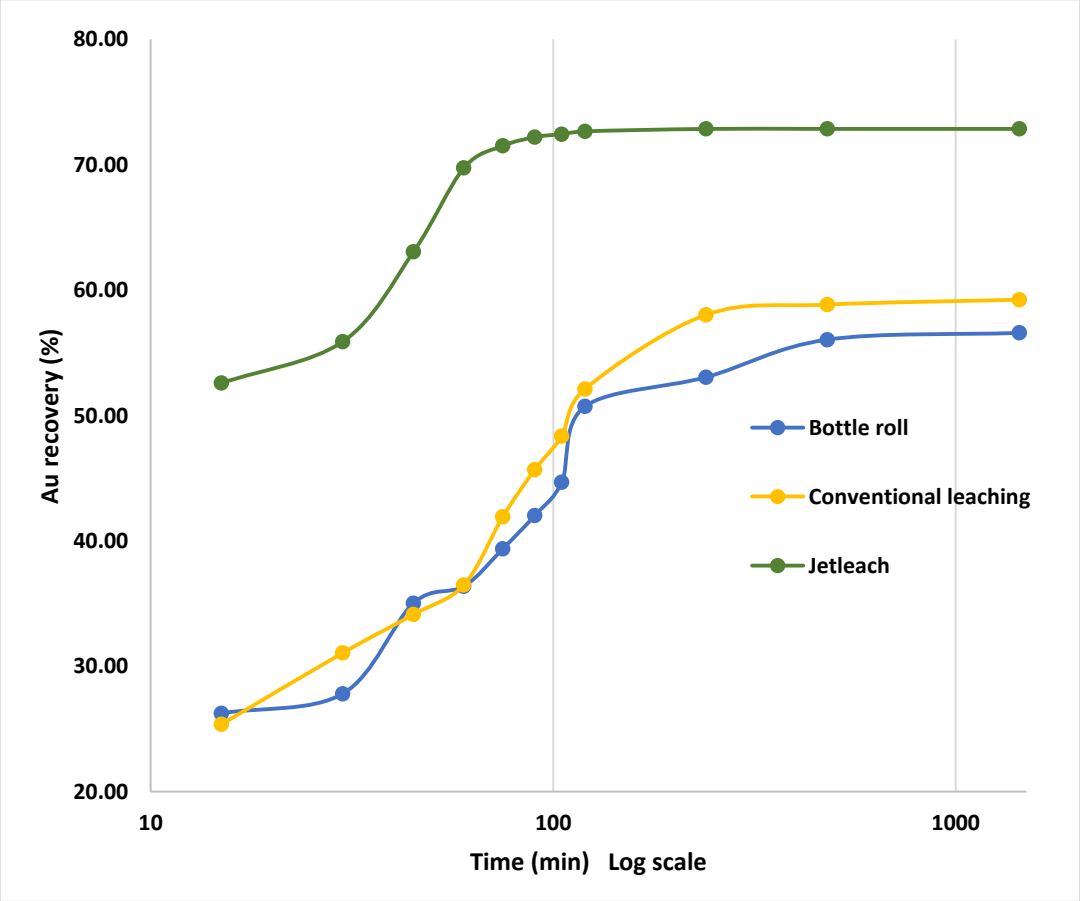


Figure 5.8 : Comparative Trends in Gold Recovery with addition of activated carbon

5.2.3 Potential benefits of using the Jetleach process

There are many potential benefits which might come from the use of the Jetleach reactor:

5.2.3.1 *High gold production per unit of ore processed*

It has been shown in one of the internal reports from DRD Gold that Ergo plant process around 60 thousand tonnes of pyrite concentrate (at 2.38g/t gold) per month. An overall

leaching gold recovery of 64% means that 57.12 kg of gold per month is lost to final residue. At R 720 000 per kilogram (gold price on the 18th of October 2019) this is R 41.1 million revenue lost per month. Therefore, an increase of 1% gold recovery will represent a gain of R 1.02 million in revenue per month. It was shown in experiment that the Jetleach reactor could improve the gold recovery by at least 10% after a leaching period of 24 hours. This would therefore imply that this reactor can generate around R 10.2 million per month, which will represent R 123.3 million per year.

5.2.3.2 *High throughput*

It was also shown that the Jetleach reactor could give a gold recovery of 71% after a leaching period of only 2 hours and this represent an improvement of almost 8%. For a plant which processes 500 tons of ores (feed to cyanidation) with a recovery of 64% as in the case of Ergo plant, over a period of 24 hours and using the conventional leaching methods, this plant will only treat a maximum of 500 tons of ores. However, if the Jetleach is integrated in the cyanidation process, the plant will only need 2hours to process the same amount of ore (500 tons) while keeping an improvement of almost 8% gold recovery. Therefore, the plant will be able to process around 6000 tons of ore instead of 500 tons per day.

5.2.3.3 *Low reagents consumption*

A comparative reagent consumption was done between Ergo plant and the Jetleach reactor. In this investigation, cyanide consumption and oxygen consumption were investigated. Results from this study (as shown in **Table 5.3**) show that the use of the Jetleach reactor can help to reduce the cyanide consumption from 5kg to 4.6 kg/t while still having greater gold recovery compared to the conventional method used on the plant. The oxygen consumption was also reduced by almost 50%. This is because in conventional processes, a large amount of oxygen is lost in the atmosphere since reactors are usually opened to the atmosphere and therefore, not 100% of the oxygen injected in the leaching tank has enough residence time to be converted from oxygen gas into dissolved oxygen. However, since the Jetleach process is a closed system, oxygen gas has enough residence time to react and be dissolved in the slurry. This is also the reason why high concentration of dissolved oxygen was obtained with the Jetleach reactor than in normal conventional leaching.

Table 5.3 : Overall reagents consumption

Methods	Cyanide addition	Oxygen addition	Au recovery
Ergo plant	5kg/t	5-8kg/t	54-62%
Conventional leaching	5kg/t	5.3kg/t	59.23%
Bottle roll	5kg/t	-	56.59%
Jetleach	5kg/t	2-3kg/t	74.73%
	4.8kg/t		74.47%
	4.6kg/t		72.31%

5.2.3.4 *Smaller leaching tanks required*

Since it was demonstrated in the previous section how the throughput can be increased by using the Jetleach reactor, the size of leaching tanks can also be reduced to process the same amount of ore per day as presented in **Figure 5.9** below. The size and number of the leaching tanks are directly connected to the leaching residence time. There are three main parameters affecting reactor dynamics for a Continuous Flow Stirred Tank Reactor (CFSTR), these are: the flow rate (Q), the residence time (T) and the dilution rate (D). In the case of a leaching process, the flow rate can be defined as the volume of slurry that is processed per unit of time. The residence time is the time it takes for a certain volume of slurry to pass through the leaching section and achieve the required objectives. These flow rate and the residence time are connected as presented in equation (5.1).

$$Q = {}^{V_T}/_{T} \qquad (5.1)$$

$$V_T = n * V \qquad (5.2)$$

V_T : the total volume, V: the volume of one leaching tank and n: the number of leaching tanks

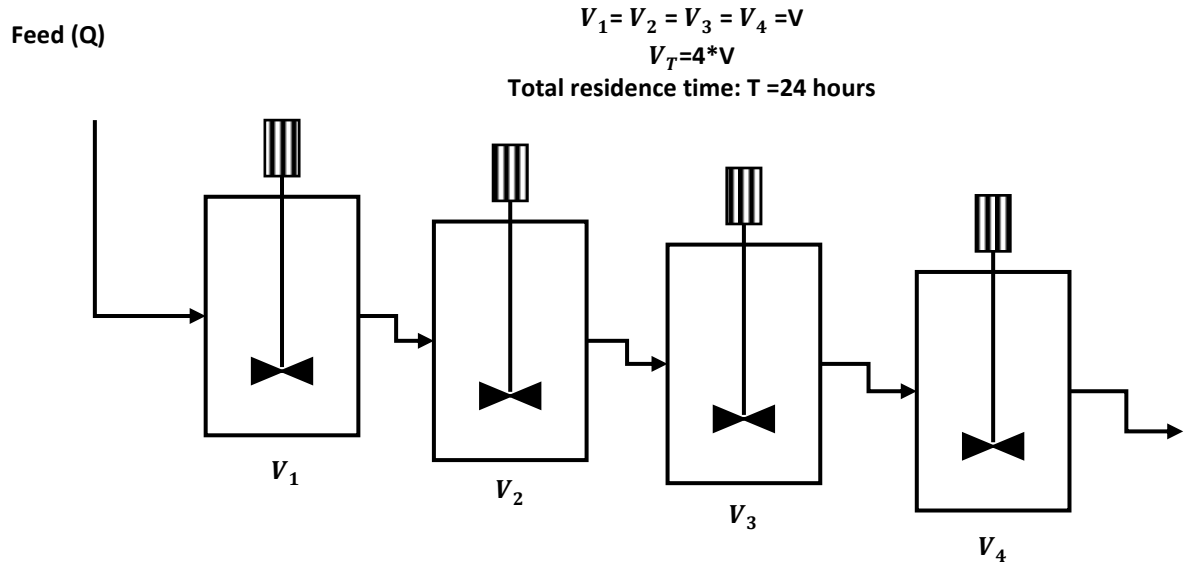


Figure 5.9 : First example of a leaching circuit with four reactors (A)

Apart from the high throughput, there are two more benefits that can be generated when the residence time is dramatically reduced like in the case of the Jetleach reactor:

- As presented in **Figure 5.10**, the size of the actual leaching tanks can be reduced into smaller tanks but will still be processing the same amount of material.

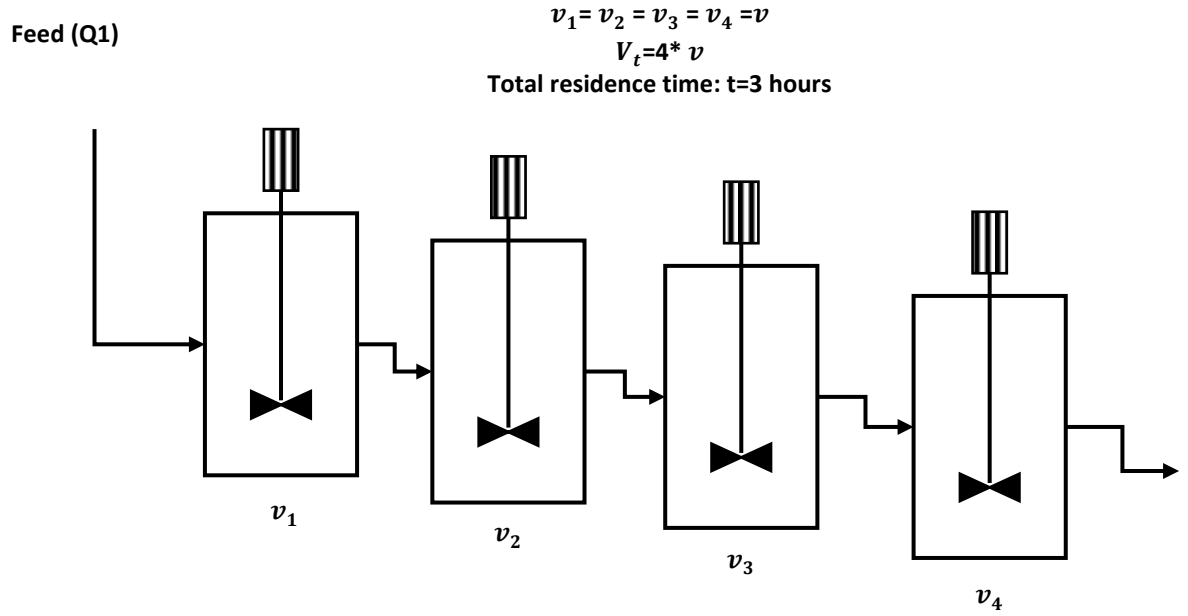


Figure 5.10 : Second example of a leaching circuit with four reactors (B)

$$Q1 = {}^{V_t}/_{t} \quad \text{and} \quad Q = {}^{V_T}/_{T} \qquad (5.3)$$

If processing the same amount of slurry at the same solid percentage, this will mean that $Q1 = Q$, consequently:

$$V_t/_t = V_T/_T \qquad (5.4)$$

$With: t = 3h,$

$T = 24h,$

$V_t = 4 * v \ \ and$

$V_T = 4 * V$

Equation (5.4) can be written as follow:

$$(4 * v)/_3 = (4 * V)/_{24} \rightarrow \boldsymbol{v = V/8}$$

- The number of tanks required can be reduced accordingly.

$$(n1 * v)/_3 = (n * V)/_{24}$$

If V is equal to 12 Liters and n equal to four as presented in **Figure 5.9**, then n1 (which represent the new number of tanks for a residence time of 3 hours) can be equal to:

$n1 = 1$ for $v = 6\ liters,$

$n1 = 2$ for $v = 3\ liters,$

$n1 = 3$ for $v = 2\ liters,$

However, there are also many other parameters to consider before deciding to reduce the size or number of leaching tanks.

5.2.3.5 *Energy savings*

The fact that the Jetleach reactor can reduce the leaching residence time means that the energy required to process the same amount of ore for 24 hours using conventional methods, will be reduced to almost 3 hours with the Jetleach method. However, it is important to also investigate the power consumption of the slurry pump in the Jetleach process.

5.3 Summary and conclusion

In this investigation, pre-aeration was used as a pre-treatment method for all three samples before cyanidation. The objective was to see if pre-aeration could reduce the amount of cyanide required for gold leaching. Pre-aeration was done by supplying pure oxygen at 25 KPa directly in the slurry for a period of 20 hours each.

Results have shown that the use of pre-aeration as a pre-treatment method could reduce the cyanide consumption by almost 0.1 Kg/t for the Ergo sample, 0.53 Kg/t for the DIO sample and 0.52 Kg/t for the MVO sample. This can be explained by the fact that during pre-aeration, iron (II) is oxidized into iron (III) resulting in the formation of a passivating layer on the surface of pyrite therefore, reducing its reactivity to cyanide.
After finding that the pre-aeration process can reduce cyanide consumption, all cyanidation experiment involved in this research were preceded by a pre-aeration stage of 20 hours before leaching.

From the leaching experiments, the Jetleach reactor has been shown to improve the gold recoveries compared to the two other leaching methods. On the DIO sample, the Jetleach reactor was able to improve the gold recovery by almost 8% and 19% compared to the conventional and bottle rolling method, respectively, while on the MVO sample, the improvement was about 10% compared to the conventional (stirred tank) method and 17% compared to the bottle rolling.

On the Ergo sample, the improvement of gold recovery was over 12% compared to both two conventional methods. It is important to note that when dealing with gold ore that presents any preg-robbing phenomenon as shown with the Ergo sample, the use of activated carbon is required. However, an activated carbon filter holder is required for the Jetleach to prevent carbon particles for being crushed in the Jetleach reactor.
For all samples, the gold recoveries obtained after only 120 minutes of leaching, using the Jetleach reactor, are at least 2% higher compared to the recoveries obtained, after 24 hours of leaching, using the two other conventional leaching methods.

It has been shown that the integration of the Jetleach reactor in the cyanidation process can generate many benefits. Some of the benefits are; high throughput due to the reduction of the leaching time, reduced amount of reagent required, greater profitability due to increased gold production per unit of ore processed; smaller leach tanks requirements, reduced number of

leach tanks and energy savings in terms of leaching time. However, energy saving may be limited when replacing tank stirring with Jetleach process due to the energy required for pumping of the slurry. All these benefits can contribute to the reduction of the overall processing cost of refractory gold ores as well as the capital necessary to start a new leaching section.

The next chapter investigates the effect of physical and chemical parameters on the Jetleach processing of refractory gold ores.

CHAPTER 6 INVESTIGATING THE EFFECT OF PHYSICAL AND CHEMICAL PARAMETERS ON THE JETLEACH

6.1 Introduction

There are two main ways of evaluating the effect of parameters on a specific process. One is known as a one-factor-at-a-time (OFAT) approach, which varies only one parameter or factor at a time while keeping others constant. The other method is known as the design of experiments (DOE), which is a statistically designed experiments that vary several factors simultaneously. A comparison between the two methods has shown that a designed experiment is more effective in determining the effect of interaction of parameters on a response than an OFAT. However, many investigations done in engineering and scientific area often use the OFAT experiments probably because it is simple and does not require many statistical calculations. The advantages of using a designed experiment over the one-factor-at-a-time experiment can be presented as follows:

- DOE provides a large amount of information for fewer resources involved (materials, reagent, experiment, time, etc.). This can be of major importance in industry, where experiments can be very costly and time consuming.
- The effects of each factor can be estimated more accurately. DOE involves more observations to estimate an effect, which results in higher precision and reduced variability. All observations involved in designed experiment are used to estimate the effect of each factor and each interaction, while only two of the observations in an OAFT experiment are used to estimate the effect of each factor.
- Interactions between factors can be systematically estimated with DOE, while this cannot be done with the OFAT experiment. Investigations done without designed experiments often result in a hit-and-miss scattershot sequence of experiment which could have been avoided with a statistical designed experiment.
- DOE improves the prediction of the response in the factor space by reducing the variability of the response estimated in the factor space. Therefore, optimization becomes more efficient because the optimal condition (or solution) are searched for over the entire factor space.

In this work, all two ways of evaluation of the effect of factors were investigated. The study using DOE was done using the software ‘‘Design Expert 11’’as a research tool to identify the significant factors that affect the cyanidation process of refractory gold ore using the Jetleach reactor.

6.2 Results and discussions

6.2.1 One-factor-at-a-time (OFAT) experiments

6.2.1.1 *Effects of solids percentage*

These experiments were run at a pH values of 10.5-11.5, cyanide concentration: 5kg/T, space between nozzles 0,8Cm, pump pressure 15MPa and oxygen flowrate of 30mL/min. It can therefore, be seen from **Figure 6.1** that a maximum gold recovery of 76.5% was obtained when using a very dilute slurry of 17% solid. This figure also shows that the gold recovery decreases gradually from 76.5% to 73.63% then to 72.01% as the solid percentage increases from 17% to 30% then to 40%, respectively. However, a drop of almost 12% in the gold recovery was observed when increasing the solid percentage from 40% to 46%. This huge drop in gold recovery can be explained by the fact that cavitation depends on the density of the fluid used. The higher the slurry density used the harder it is to generate micro-cavitation in the slurry (Zhou, et al., 2009; Payri, et al., 2013).

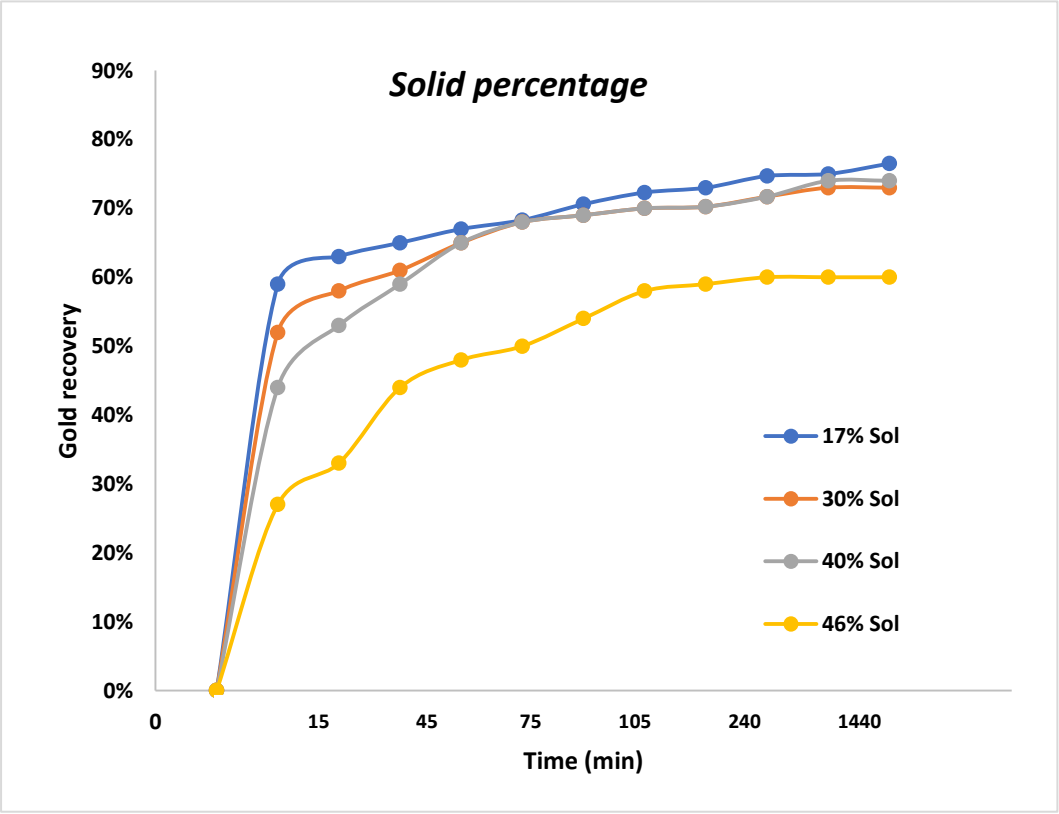


Figure 6.1 : Effect of solid percentage on gold recovery (Ergo sample)

During this set of experiments, the highest gold recovery was obtained at a solid percentage of 17%. However, it is practically difficult and costly for an actual plant like Ergo to operate at a solid percentage lower than 30%. Therefore, a solid percentage of 40% was selected and used in the next experiments.

6.2.1.1 *Effects of cyanide concentration*

The effect of cyanide concentration on the gold recovery is presented in **Figure 6.2**. As observed from literature, it was expected that cyanide concentration would have a significant effect on the gold recovery and the leaching kinetics. However, results from these experiments revealed something different. The range of cyanide concentration chosen in this set of experiment (base on the plant set point) seemed not to affect the gold recovery as expected. Gold recoveries of 72.3, 74, 74.3 and 74.8% were obtained at a cyanide concentration of 4.6, 4.8, 5 and 5.2 Kg/T, respectively. It can be seen from **Figure 6.2** that cyanide concentration only affected the leaching kinetics in the first 2 hours, but the overall gold recovery after 24 hours for the three highest cyanide concentration remained almost the same (between 74 and 75%). These results can be justified by the fact that the driving force in the Jetleach reactor is no longer cyanide concentration, but mostly the cavitation bubbles produced in the impactor. Therefore, in the next set of experiments cyanide concentration was kept at 4.8 kg/T.

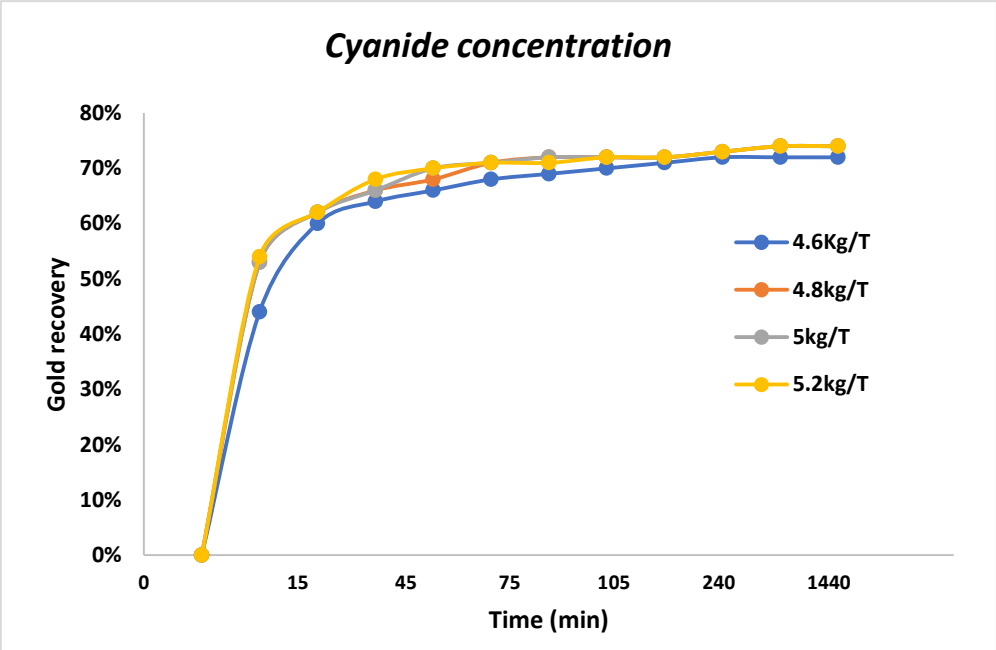


Figure 6.2 : Effect of cyanide concentration on gold recovery (Ergo sample)

6.2.1.2 *Effects of space between nozzles*

These sets of experiments were run at a pH: 10.5-11.5, cyanide concentration: 4.8kg/T, pump pressure of 15MPa, solid percentage of 40% and oxygen flowrate of 30mL/min. As it can be seen from **Figure 6.3**, the gold recovery slightly increases as we decrease the space between the nozzles. An improvement of almost 1% was obtained when reducing the space between nozzles from 1.2 cm to 0.5cm. However, the general leaching profile is not much affected by the change of the spacing between nozzles. A close analysis of the kinetics aspect of the three curves plotted below revealed that, a slight increase of the leaching kinetics was observed when reducing the space between nozzles. This slight increase in the leaching kinetics and the gold recovery can be explained by the fact that the change of the space between nozzles for the intervals used in this investigation was too little to have any significant effect on the energy released during the cavitation phenomenon. It is also important to note that this parameter was very difficult to change because any variation was affecting the vortex generated during the impact of the two slurry streams. Therefore, it was difficult to re-center the vortex in the middle of the Jetleach impactor. The next experiments were run at a space between nozzles of 0.5cm since this was the one that gave the highest gold recovery.

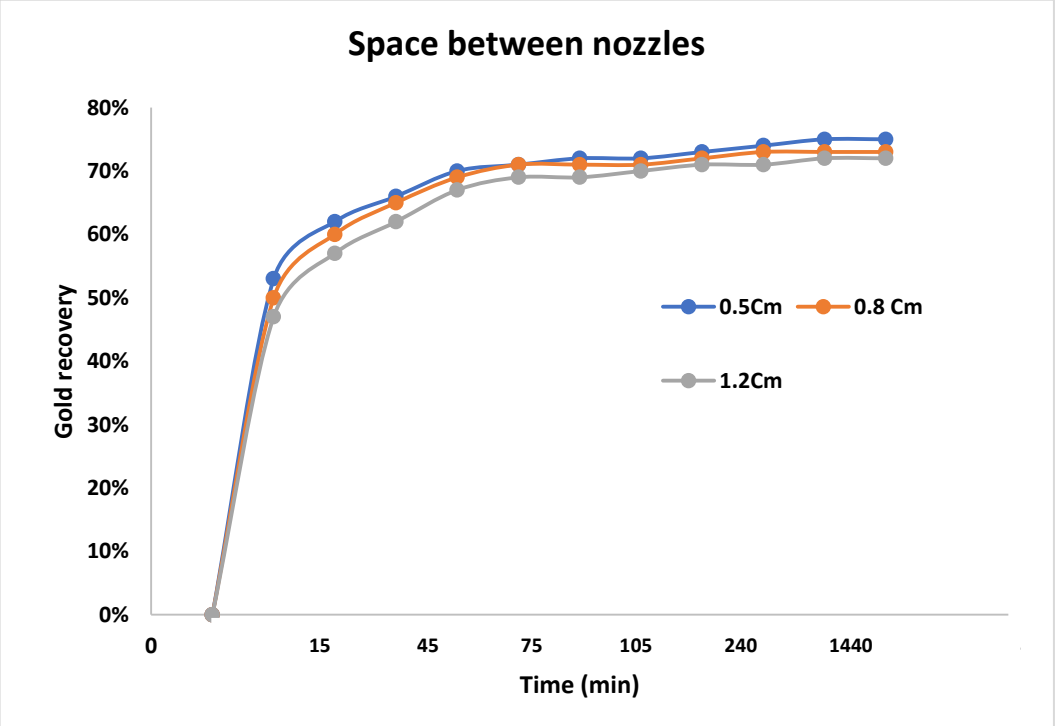


Figure 6.3 : Effect of the spacing between nozzles on gold recovery (Ergo sample)

6.2.1.3 *Effects of oxygen flowrate*

These experiments were run at a pH: 10.5-11.5, solid percentage of 40%, cyanide concentration: 4.8kg/T, pump pressure of 15MPa and space between nozzles of 0.5 cm. As presented in the literature review, oxygen concentration is one of the most critical parameters in the cyanidation process.

Results obtained from these experiments revealed that oxygen flowrate has a significant effect on the gold recovery. As shown in **Figure 6.4**, the gold recovery increased when increasing the flowrate of oxygen. The concentration of dissolved oxygen in the slurry also increases with an increase of the oxygen flowrate. A very low gold recovery of 45% was observed when running the Jetleach at an oxygen flowrate of 10 ml/min, while gold recoveries of 63, 74 and 76% were obtained at oxygen flowrate of 20, 30 and 40 ml/min. It was observed that the concentration of dissolved oxygen in the slurry reached a maximum of 11.23, 13.72, 16.88 mg/L and 17.15 mg/L at flowrates of 10, 20, 30 and 40 ml/min, respectively. These results can be explained by the fact that the gold dissolution rate increases with an increase in dissolved oxygen concentration (Deschênes & Wallingford , 1995; Deschênes, et al., 2003; Ellis & Senanayake, 2004; Senanayake, G., 2008; Senanayake , et al., 2018). However, at a cyanide concentration level higher than 104 ppm (like in the case of this study), high dissolved oxygen concentration does not have a significant effect on gold dissolution (Senanayake , et al., 2018). This is the reason why a slight improvement of gold recovery was also observed at oxygen flowrate of 30 and 40 ml/min. Therefore, in the next experiments the oxygen flowrate was kept at the value of 40 ml/min.

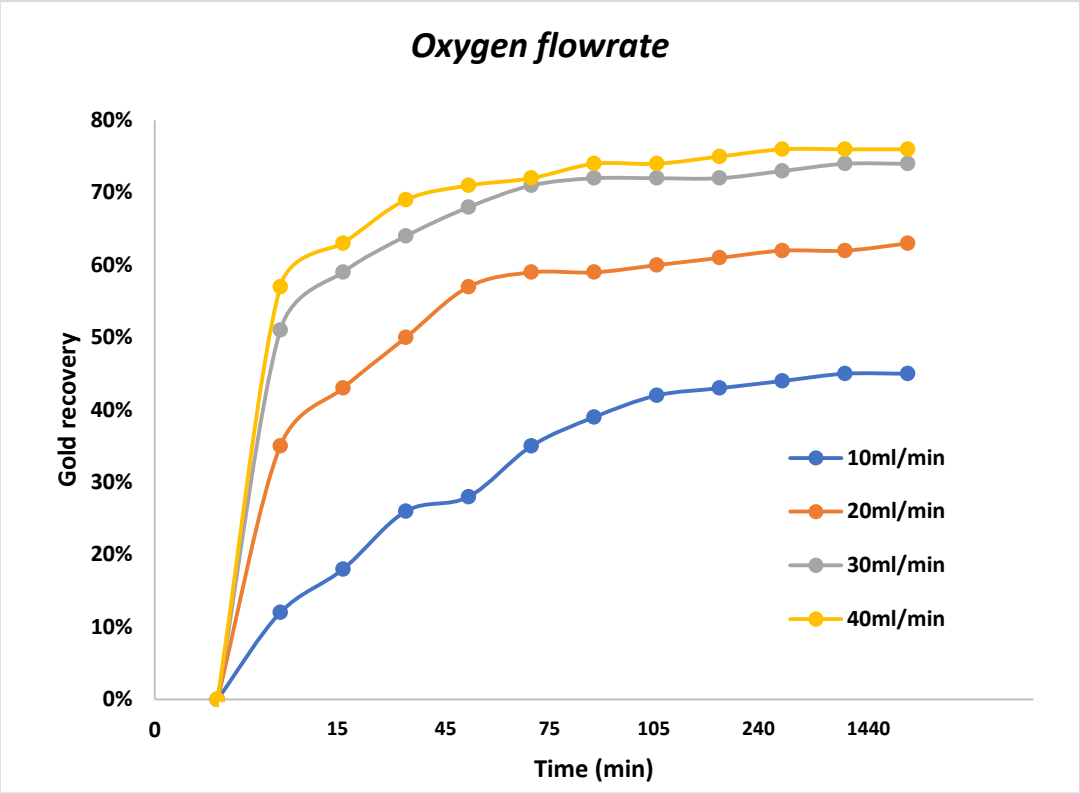


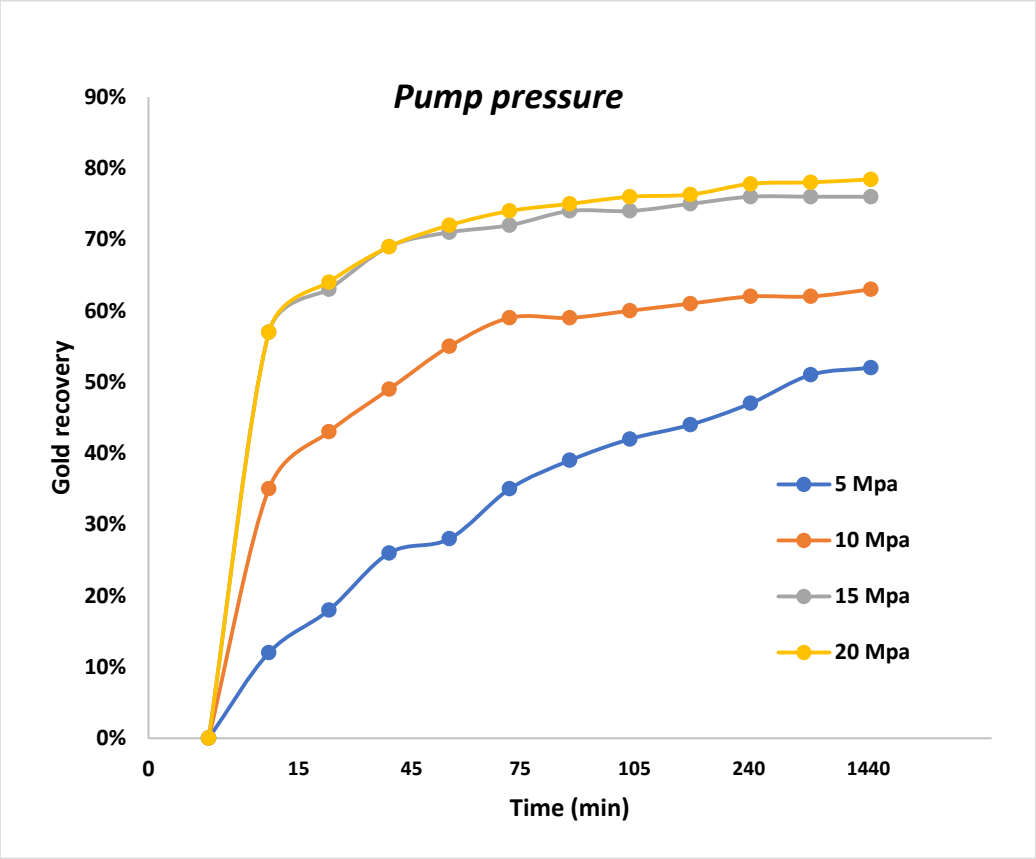
Figure 6.4 : Effect of oxygen flowrate on gold recovery (Ergo sample)

6.2.1.4 *Effects of pump pressure*

These experiments were run at a pH: 10.5-11.5, solid percentage of 40%, cyanide concentration: 4.8kg/T, oxygen flowrate of 40 ml/min and space between nozzles of 0.5 cm. It can be seen from **Figure 6.5** that the reaction is very fast within the first 15-20 mins. at 15 and 20MPA. For instance, you have 57% recovery for the 15 and 20MPa at 15minutes whereas it takes 75 minutes to get 59% recovery at 10MPA and 1440 minutes to only achieve 52% with 5MPA. This shows that higher the pump pressure increases the reaction kinetics. The reason of different shapes of curves plotted below is also connected to the reaction kinetics. The different shapes can be explained by the fact that less cavities are generated in the slurry when the pump pressure is decreased. Since the generation of cavitation bubbles in the slurry is the major cause of faster leaching kinetics and improvement in gold recovery, therefore, a decrease of the number of cavities generated as well as the reduction of the collision force between the two streams of slurry will also result in a decrease of the kinetics and the gold recovery. The stationary phase observed after 2 hours of leaching for the curves at 15 and 20MPA can be explained by the fact that the remaining gold in the solids were

probably extremely locked in their matrix such as silicates that even cavitation at these high pressures was not able to expose to cyanide solution.

Figure 6.5 : Effect of pump pressure on gold recovery (Ergo sample)



6.2.2 Interaction between parameters (DOE)

For this set of experiments, statistical Design of Experiments (DOE) was used to study the interaction effects between different parameters involved in the cyanidation process of refractory gold ores using the jetleaching process. This experimental design consists of a simultaneous combination of several factors influencing the process which results in better understanding of the general process (Barrentine, 1999). The software Design-Expert 11 was used in order to change several factors in a systematic way so as to ensure a reliable and independent study of the main factors and their interactions.

Design–Expert is a statistical software package from Sat-Ease Inc. that is specifically dedicated to performing design of experiment (DOE). Design–Expert offers comparative tests between factors, screening, characterization, optimization, robust parameter design, mixture designs and combined designs (Tanco, et al., 2008). This software provides test matrices for screening up to 50 factors. Design-Expert is equipped with analysis of variance (ANOVA) which help to establish the statistical significance of factors. It is also equipped with graphical tools helping to identify the impact of each factor on the desired outcomes and reveal abnormalities in the data. The main intention with this designed experiment was to identify the key factors that affect the desired goal to achieve a high gold recovery and the interactions among the factors. Leaching experiments were carried out at low and high factor levels as presented in **Table 6.1** below. The factors investigated included: solid percentage, cyanide concentration, space between nozzles, pump pressure and oxygen flowrate.

Factors that influence the dissolution of gold in cyanide solution have been studied and identified by previous researchers using various leaching methods (Deschênes, et al., 2003; Ellis & Senanayake, 2004; Marsden & House, 2006; Haque, 2007; Marsden & House, 2009; Gonzalez-Anaya, et al., 2011; Asamoah, et al., 2014). Therefore, the choice of factors was based on past experience in the cyanidation process of refractory gold ores. However, the choice of levels was based on the set point used at Ergo plant.

It is important to note that although a parameter such as the agitation rate may have an influence on the response, it was held constant at 500 rpm because it is of no particular interest in the current study.

The design of experiment showing the interaction between different parameters can be seen as presented in **Table 6.1**. The design consist of a two levels design (green design) involving all five parameters at the same time as presented in chapiter 3, section (**3.4.2.2**).

Table 6.1 : design of experiment to evaluate the significants parameters

			Factor 1	Factor 2	Factor 3	Factor 4	Factor 5	Response 1
Std	Block	Run	A: Pump pressure	B: Space between nozzles	C: Solid percentage	D: Oxygen flowrate	E: Cyanide concentration	Gold recovery
			MPa	Cm	%	ml/min	Kg/t	%
3	Run	3	20	0.5	30	10	4.6	37.4
5	Run	8	5	1.2	30	10	4.6	31.2
9	Run	13	5	0.5	46	10	4.6	33.5
15	Run	2	20	1.2	46	10	4.6	42.1
17	Run	6	5	0.5	30	40	4.6	58.3
23	Run	7	20	1.2	30	40	4.6	76.0
27	Run	10	20	0.5	46	40	4.6	63.8
29	Run	9	5	1.2	46	40	4.6	52.7
1	Run	15	5	0.5	30	10	5	37.0
7	Run	5	20	1.2	30	10	5	49.5
11	Run	16	20	0.5	46	10	5	42.1
13	Run	11	5	1.2	46	10	5	33.2
19	Run	14	20	0.5	30	40	5	78.6
21	Run	12	5	1.2	30	40	5	52.4
25	Run	1	5	0.5	46	40	5	45.9
31	Run	4	20	1.2	46	40	5	56.8
4	Rep	18	20	0.5	30	10	4.6	37.2
6	Rep	25	5	1.2	30	10	4.6	31.6
10	Rep	20	5	0.5	46	10	4.6	33.1
16	Rep	22	20	1.2	46	10	4.6	42.3
18	Rep	28	5	0.5	30	40	4.6	58.2
24	Rep	27	20	1.2	30	40	4.6	76.7
28	Rep	19	20	0.5	46	40	4.6	64.0
30	Rep	21	5	1.2	46	40	4.6	53.1
2	Rep	31	5	0.5	30	10	5	37.3
8	Rep	32	20	1.2	30	10	5	49.1
12	Rep	24	20	0.5	46	10	5	41.6
14	Rep	23	5	1.2	46	10	5	33.4
20	Rep	17	20	0.5	30	40	5	79.3
22	Rep	30	5	1.2	30	40	5	52.2
26	Rep	26	5	0.5	46	40	5	45.7
32	Rep	29	20	1.2	46	40	5	57.1

It can be seen from the analysis of variance (ANOVA) presented in **Table 6.2** and the pareto chart presented in **Figure 6.6 below** that among all five parameters, only three are significant; the oxygen flowrate, pump pressure and the solid percentage. However, it can also be seen that three interactions were significant as well: interaction between the pump pressure and the oxygen flowrate; interaction between the solid percentage and the oxygen flowrate; and finally the interaction between the solid percentage and the cyanide concentration. ANOVA for selected factorial model **(Response: Gold recovery)**

Source	Sum of Squares	df	Mean Square	F-value	p-value	
Block	0.0001	1	0.0001			
Model	29.83	9	3.31	61.52	< 0.0001	significant
A-Pump pressure	6.29	1	6.29	116.80	< 0.0001	significant
B-Space between nozzles	0.0001	1	0.0001	0.0012	0.9724	
C-Solid percentage	1.29	1	1.29	23.91	< 0.0001	significant
D-Oxygen flowrate	20.22	1	20.22	375.18	< 0.0001	significant
E-Cyanide concentration	0.0030	1	0.0030	0.0565	0.8145	
AD	0.2407	1	0.2407	4.47	0.0467	significant
AE	0.1212	1	0.1212	2.25	0.1485	
CD	0.8246	1	0.8246	15.30	0.0008	significant
DE	0.8457	1	0.8457	15.69	0.0007	significant
Residual	1.13	21	0.0539			
Cor Total	30.97	31				

The **Model F-value** of 61.52 implies the model is significant. There is only a 0.01% chance that an F-value this large could occur due to noise. **P-values** less than 0.0500 indicate model terms are significant. In this case A, C, D, AD, CD, DE are significant model terms. Values greater than 0.1000 indicate the model terms are not significant.

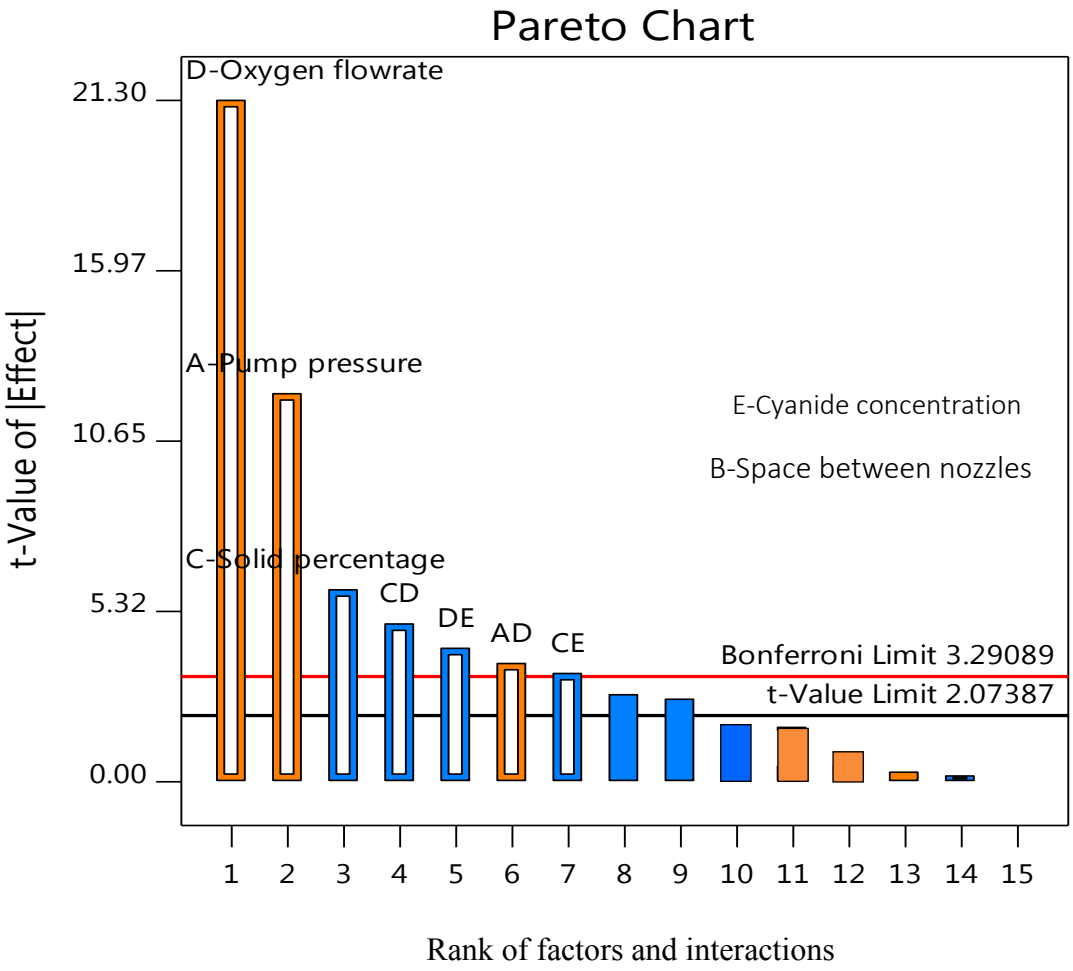


Figure 6.6 : Pareto chart showing significants factors (Design Expert 11)

The fitted model between significant factors and the response was developed to illustrate the dependence of the response on the significant factors. The model is expressed as presented below:

$$R = 49.06 + 6.38X_A - 3.19X_C + 11.13X_D + 1.94X_{AD} - 2.63X_{CD} - 2.25X_{DE}$$

Where R is the gold recoery.

The effect of the three significant factor (oxygen flowrate, pump pressure and solid percentage) on the gold recovery is presented as a cubic interaction between the significant factors in **Figure 6.7**. It can be seen from **Figure 6.7** below that high gold recovery, around 76%, was obtained when operating at high pump pressure (20MPa), high oxygen flowrate (40 ml/min) and low solid percentage (30%).

It can be seen from **Figure 6.8** that cyanide concentration and the space between nozzles do not have a significant effect on the response which is the gold recovery. The pump pressure

and the oxygen flowrate have a positive significant effect; while the solid percentage have a negative significant effect. A positive significant effect simply mean that any increase of the factor results in an significant increase of the response and any decrease of the factor results in a significant decrease of the response value. Therefore, a negative significant effect is the opposite of the positive significant effect.

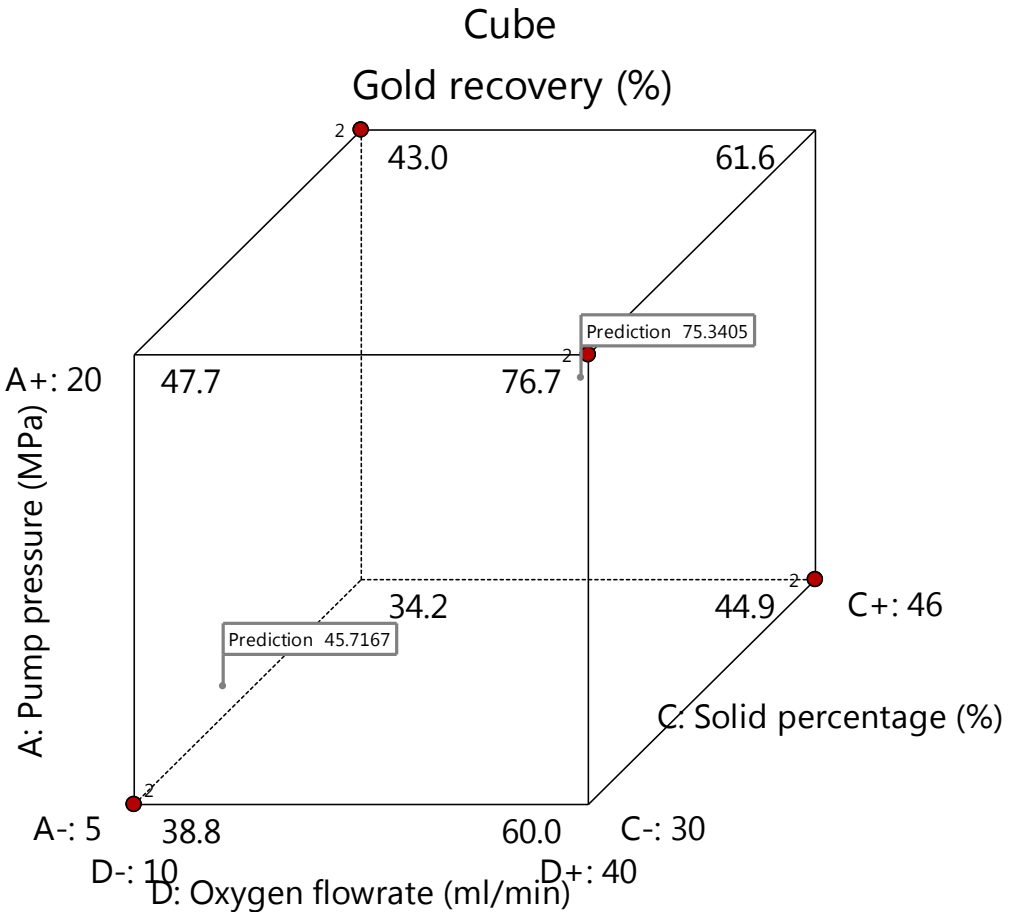


Figure 6.7 : Cubic representation of the interaction between pump pressure-oxygen flowrate and solid percentage

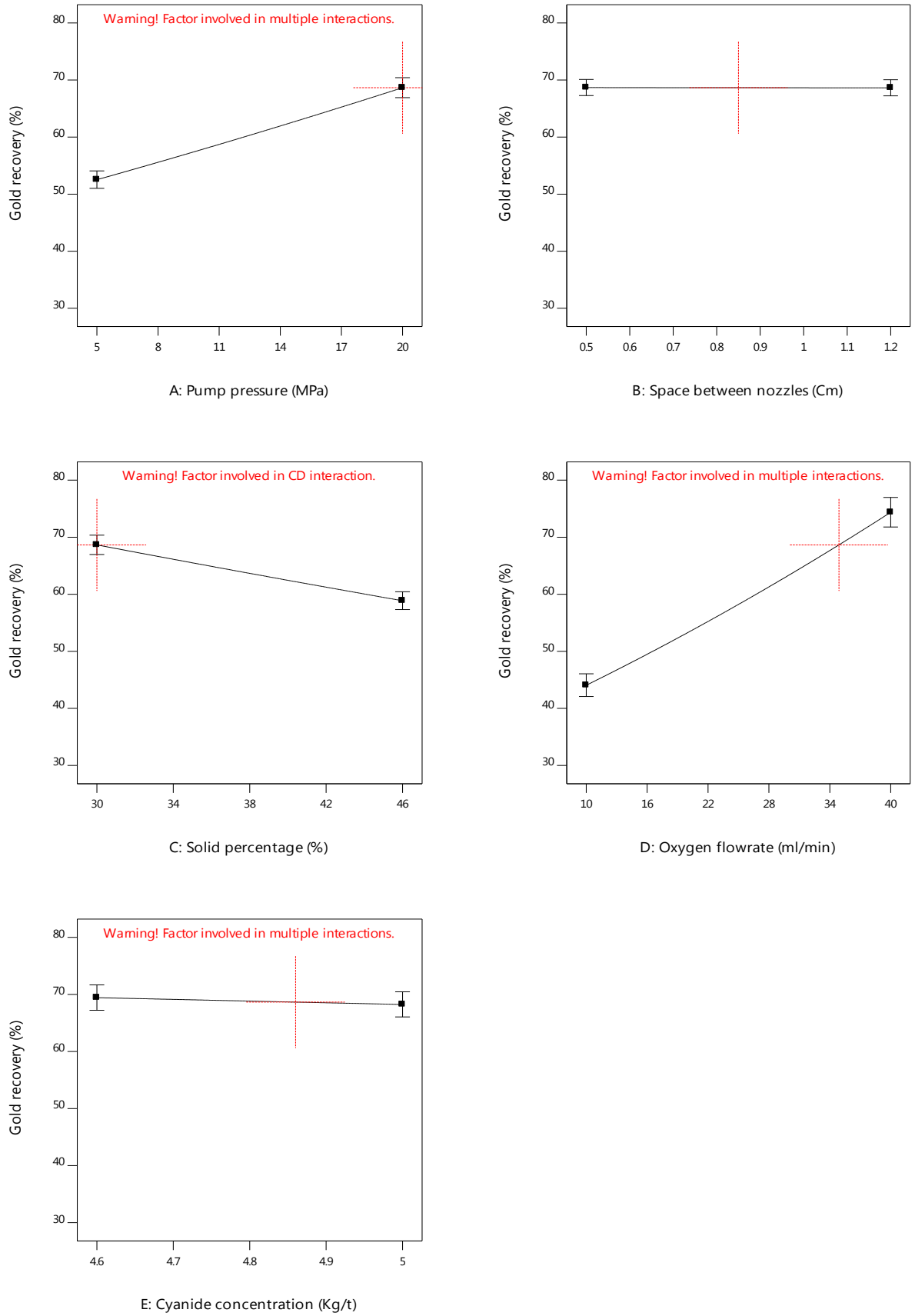


Figure 6.8 : Effect of pump pressure, space between nozzles, solid percentage, oxygen flowrate and cyanide concentration on the gold recovery

However, the effect of each significant interactions between parameters (AD, CD and DE) are presented in **Figure 6.9**, **Figure 6.10** and **Figure 6.11**, respectively. The effect of the interaction between the oxygen flowrate and the pump pressure is presented in **Figure 6.9**. It can be seen from this figure that if the oxygen flowrate and the pump pressure are increased, the gold recovery also increases until reaching a gold recovery of almost 80% which was obtained at the maximum value of pressure and oxygen flowrate (20MPa and 40ml/min, respectively). This figure also show that the oxygen flowrate as well as the pump pressure have a positive effect on the gold recovery. The positive effect of the oxygen flowrate on the the gold recovery can be explained by the fact that at higher cyanide concentration, as in the case of this study, the gold recovery increases when the concentration of dissolved oxygen also increases (Deschênes & Wallingford , 1995; Ellis & Senanayake, 2004). The positive effect of the pump pressure is connected to the increase in the number of cavities generated during the impact in the Jetleach reactor. Therefore, the combinasion of the two parameters also result in a positive effect on the gold recovery. This is the reason why the highest was obtained at the maximun values of the two parameters (pump pressure and oxygen flowrate).

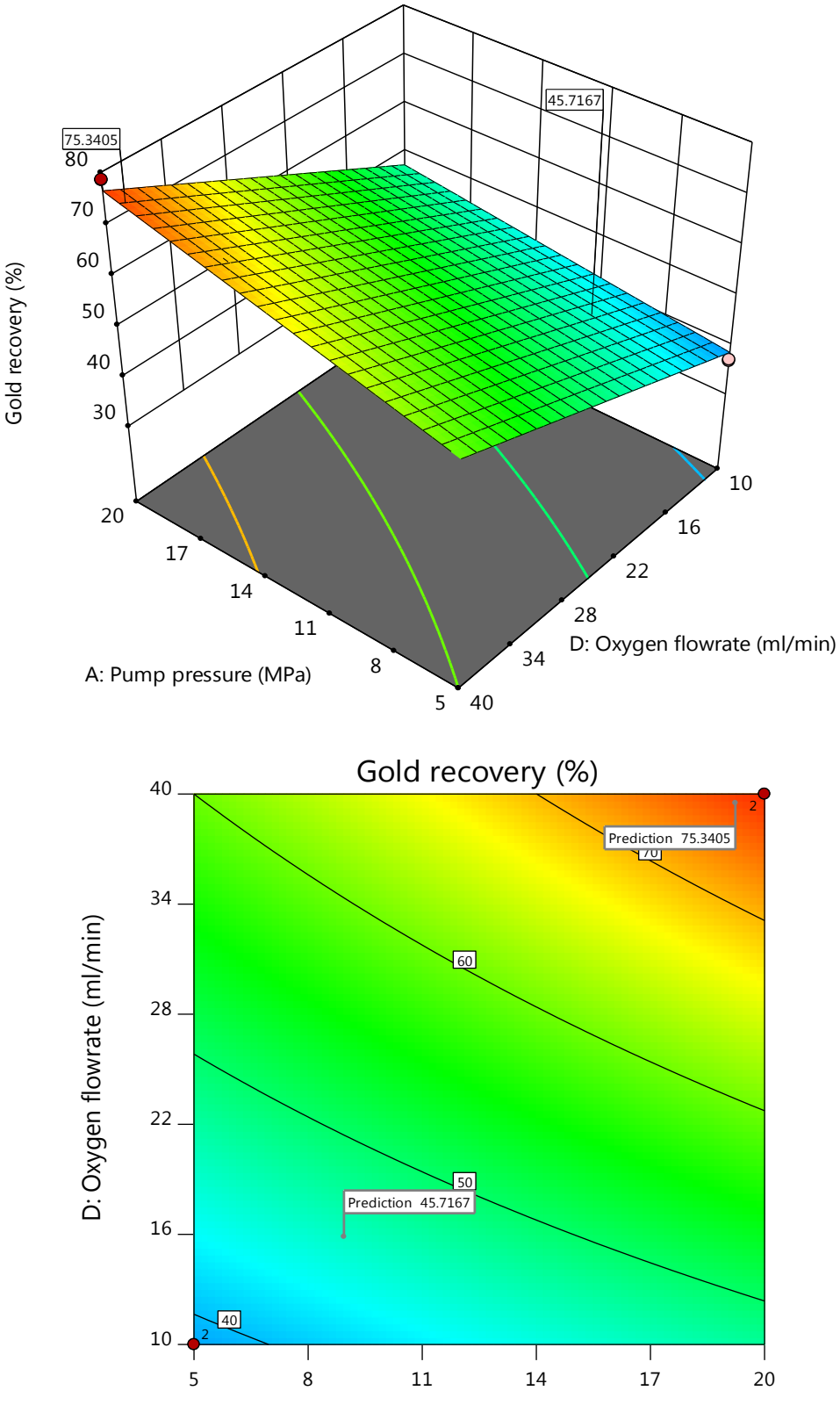


Figure 6.9 : 2D and 3D representation of the interaction effect between oxygen flowrate and pump pressure on gold recovery

It can be seen from **Figure 6.10**, which shows the interaction between the solid percentage and the oxygen flowrate, that the gold recovery increased form 47% to a value more than 74% when the oxygen flowrate is increased from 10 to 40 ml/min and the solid percentage decreased from 46% to 30%. The negative effect of the solid percentage on the gold recovery can be explained by the fact that the number of cavities generated decreases as the slurry density increase (Payri, et al., 2013).

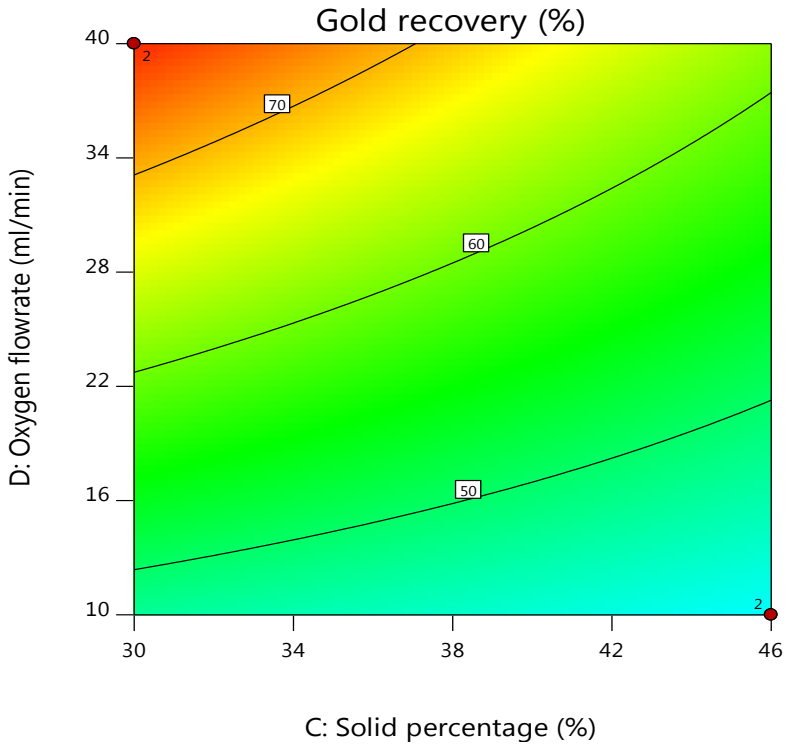


Figure 6.10 : 2D representation of the interaction effect between oxygen flowrate and solid percentage on gold recovery

The same effect observed during the OFAT experiment concerning cyanide concentration can also be seen from **Figure 6.11**. In this figure representing the interaction between cyanide concentration and oxygen flowrate. It was also observed that at maximun pressure of 20 MPa and maximum oxygen flowrate (20ml/min), it was possible to have high gold recoveries (around 70%) even when the cyanide concentration was decreased from 5kg/t to 4.6kg/t. These results show therefore, that for the range interval used in this work, cyanide concentration does not really affect the gold recovery in the Jetleaching process. This is probably due to the high energy released from the cavitation phenomenon during the impact of the two slurry streams which increases the exposure of gold particle to cyanide solution

while increasing the cyanide mass transfer (by reducing the Nernst layer surounding the particles). Therefore, less cyanide is required to leach out gold that was locked in sulphides.

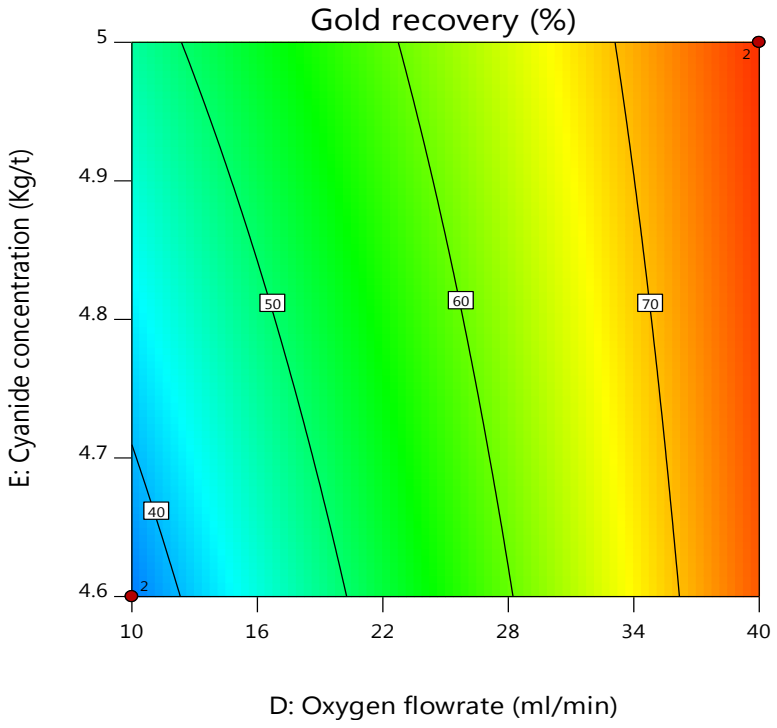


Figure 6.11 : 2D representation of the interaction effect between cyanide concentration and oxygen flowrate on gold recovery

The Residuals vs. Run graph shown in **Figure 6.12** represents a plot of the residuals versus the experimental run order. This plot helps to check for hidden variables that may have influenced the response during the experiment. The trends of this plot indicate a time-related variable lurking in the background. When taken as a whole, **Figure 6.12** essentially shows that residuals bounce randomly around the zero residual line and all values are found within the limits zone (between +3.65807 and -3.65807) as we would hope so. In general, residuals exhibiting normal random noise around the zero residual line suggest that there is no serial correlation and that the model is validated.

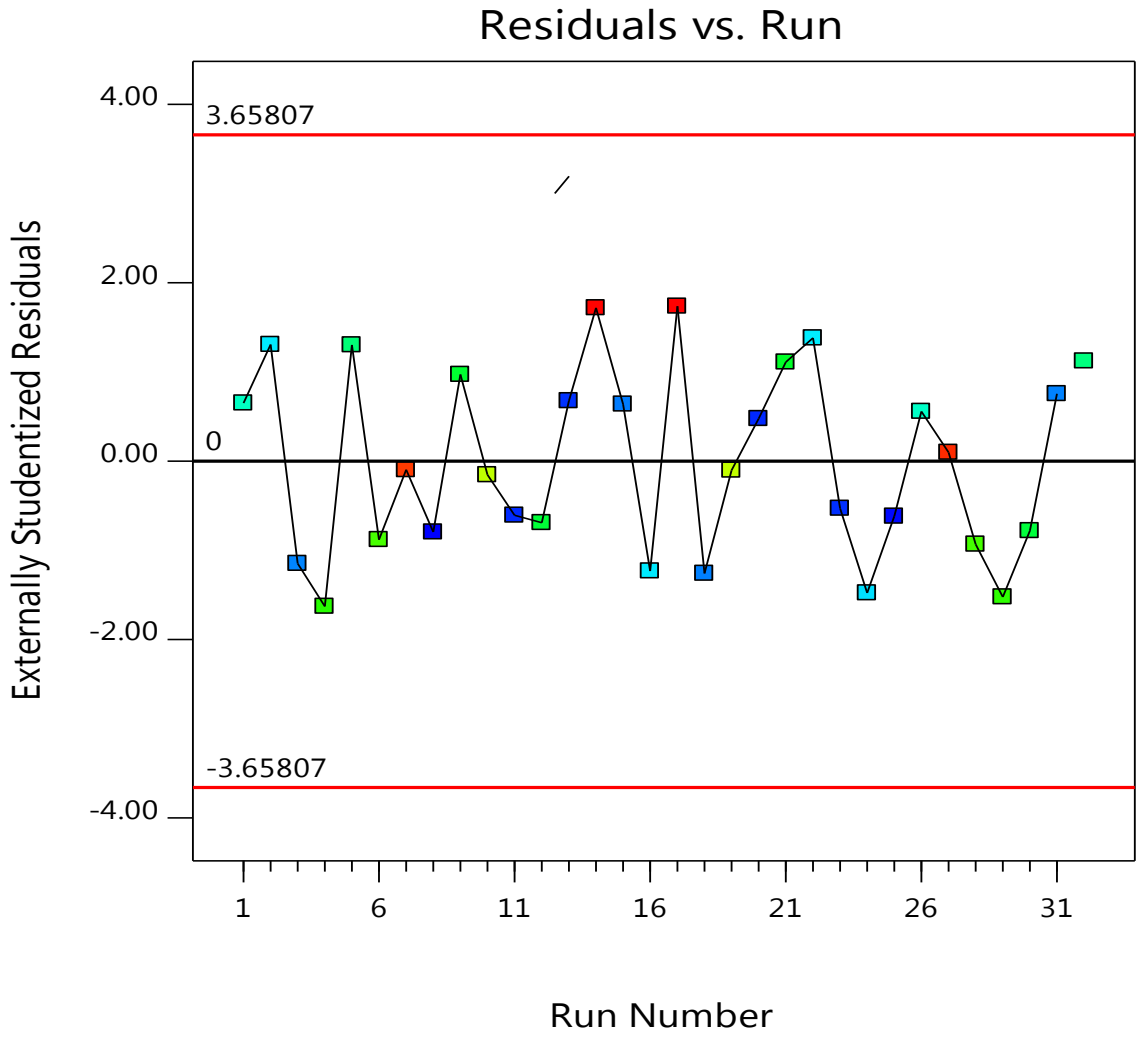


Figure 6.12 : Residuals vs Runs

6.3 Summary and conclusions

This two set of experiments were all done on the Ergo sample (pyrite flotation concentrate). The first set of experiment consisted of a one factor at a time experiment. In these experiments, each factor was varied on its own while keeping the other constant. Five parameters were involved: solids percentage, the space between nozzles, the pump pressure, the cyanide concentration and the oxygen flowrate. The oxygen flowrate, the solid percentage and the pump pressure were found to have a more significant effect on the gold recovery. However, cyanide concentration as well as the spacing between nozzles was found not to have a significant effect on the gold recovery. The best gold recovery of almost 80% was obtained at a solid percentage of 17%, cyanide concentration of 4.8kg/t, pump pressure of 20 MPa, space between nozzle of 0.5 cm and an oxygen flowrate of 40 ml/min. however, practically it is difficult to run a plant at a solid percentage of 17% (high water consumption), therefore a solid percentage of 40% would be practically acceptable.

Furthermore, the five parameters were also assessed in a statistically designed set of experiments (DOE). This set of experiments was designed and analyzed using the software Design-Expert 11. In these experiments and similar to the one factor at a time experiments, three significant factors were found: the pump pressure, the oxygen flowrate and the solids percentage. However, three interactions were also found to be significant: the interaction between the pump pressure and the oxygen flowrate; the interaction between the oxygen flowrate and the solid percentage; and the interaction between the cyanide concentration and the oxygen flowrate.

A maximum gold recovery of almost 80% was obtained at a solid percentage of 30%, an oxygen flowrate of 40 ml/min, a space between nozzles of 0.5 cm, and pump pressure of 20 MPa and a cyanide concentration of 5 kg/t. It was also possible to reach a gold recovery of 76.7% at a cyanide concentration of 4.6 kg/t, space between nozzle of 1.2 Cm, at a maximum pressure and oxygen flowrate. However, in both set of experiments (OFAT and DOE) it was strangely found that for the range used in this work, cyanide concentration does not have a significant effect on the gold recovery (within the limits explored). Therefore, there is potential to further reduce the amount of cyanide required for the gold cyanidation just by using the Jetleach process.

Based on these findings, an optimization test can be performed using only three parameters: the oxygen flowrate, the solid percentage and the cyanide concentration while maintaining the pump pressure at maximum and the space between nozzles at minimum.

This chapter has covered the effect of physical and chemical parameters on the cyanidation process using the Jetleach reactor. The following chapter investigate the impact cavitation phenomenon on the solid particles and how the mechanism of cavitation is done in the Jetleach reactor.

CHAPTER 7 IMPACT OF MICRO-CAVITATION ON THE SOLID PARTICLES AND INVESTIGATION OF THE CAVITATION MECHANISM

7.1 Introduction

Cavitation is defined as a phenomenon in which rapid changes of pressure in a liquid lead to the formation of small vapor bubbles or cavities, in places where the pressure is relatively low. When moving from the low-pressure zone to the high-pressure zone, the cavities previously formed start collapsing. The collapsing phenomenon results in the generation of intense shock waves which have a destructive effect on solid material such as pumps, valves, pipes and tanks, due to the collapsing of bubbles. Since the shock waves generated by the collapsing of bubbles are strong enough to cause significant damage to many apparatuses, this phenomenon (cavitation) is usually considered as an undesirable.

Recent investigations have shown that a controlled use of the cavitation phenomenon can be used to enhance the leaching kinetics of slow reactions (see section **2.6.4**). This was also shown in the previous chapters (chapter 5 and 6), where it was observed that the energy released by cavitation can be used to increase the leaching kinetics and the gold recovery of refractory gold ores. The main hypothesis explaining this improvement is that the cavitation process produces micro-bubbles which, once collapsing, propagate stress at the inter-phase bubble-particle, and increase the local pressure and temperature. The energy released produces intense shock waves which generate cracks and cavities on the surface of particles exposing gold particles to the cyanide solution. This phenomenon is schematically represented as illustrated in **Figure 7.1** below. Therefore, the aim of this study was to investigate the effect of cavitation on the solid particles (especially silicates and pyrites particles), and also to investigate the mechanism of generation of cavitation in the Jetleach reactor.

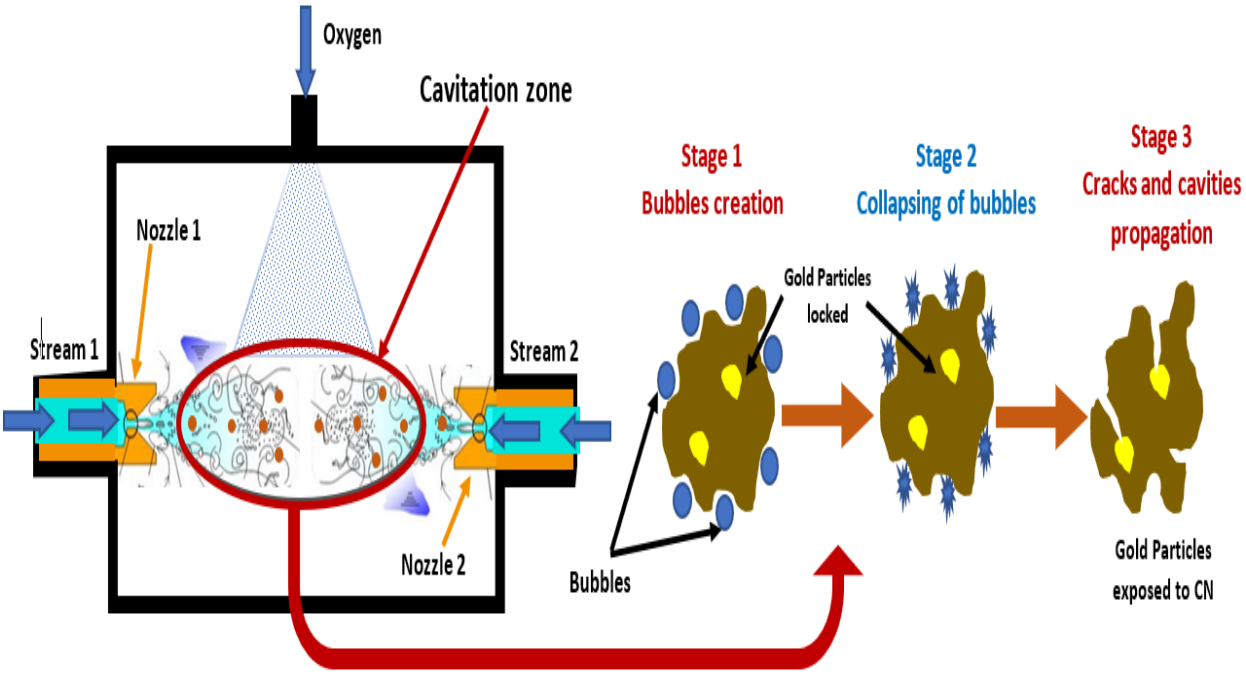


Figure 7.1 : Schematic representation of the cavitation mechanism in the Jetleach

To validate the above hypothesis, two studies were done: the first study consisted on investigating if the cavitation process and impact in the Jetleach resulted in size reduction of solid particles involved in the process. This was done by undertaking a particle size analysis on the solids before and after passing through the Jetleach reactor using the Malvern Mastersizer. On the other hand, the second study consisted of investigating any potential presence of cracks or cavities on the surface of solid particles by using the Scanning Electron Macroscopy of the sample before and after Jetleaching.

To understand the mechanism of cavitation, generation and collapsing of bubbles, a special design was made. The design consists of a transparent tube reactor in which one of the Jetleach nozzles was isolated and water was passing through at a very high velocity to simulate the impact generated in the impactor of the Jetleach reactor. A high-speed camera was placed outside the reactor to capture the cavitation phenomenon that takes place in the reactor. In these set of experiment, the focus was more on capturing how cavitation is generated. This was done by investigating the effect water flowrate has on the generation of cavitation.

7.2 Results and discussions

7.2.1 Particle Size Distribution (PSD)

As it can be seen from **Figure 7.2**, the particle size distribution of the sample A before Jetleaching have a d90 of 46.553μm, a d50 of 11.996 μm and a d10 of 3.266 μm. Results of the PSD analyses of the same sample (A) after Jetleaching revealed that there was comminution happening in the Jetleach reactor; the d90, d50 and d10 shifted from the initial values to 43.243 μm, 10.992 μm and 2.855 μm respectively (see **Figure 7.3**). For confirmation purposes, another PSD analysis was performed on another sample named sample B. Results from **Figure 7.4** (before Jetleaching) and **Figure 7.5** (after Jetleaching) show that once again there is a comminution happening in the Jetleach reactor. The second sample shows that the d90, d50 and d10 were respectively at 82.163 μm, 14.306 μm and 3.207 μm before Jetleaching. After being passed through the Jetleach reactor, the d90 shifted form 82.163 μm to 74.349 μm, while the d50 and d10 remained almost the same. The decrease in term of the particle size can also be one of the factors explaining why the cavitation phenomenon contribute to enhance the leaching kinetics and the gold recovery of these samples. Results obtained from sample A and B show that the impact of cavitation process affected mostly particles of bigger size than that of smaller particles. This is because smaller particles require higher energy to break than larger particles (Bwalya, et al., 2014; Deniz, 2012; Petrakis, et al., 2016). This is also the reason why the d90 of all samples decreased significantly compared to the d50.

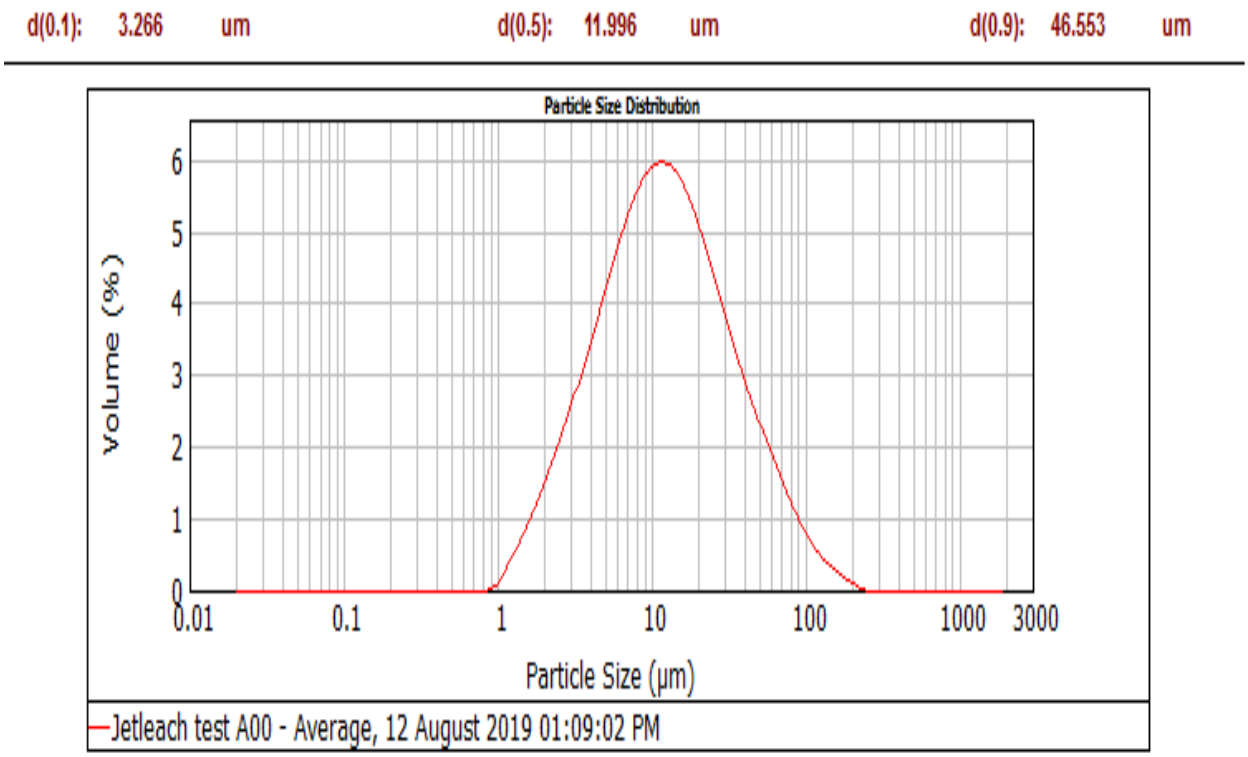


Figure 7.2 : Particle size analysis distribution of Ergo sample A before Jetleaching

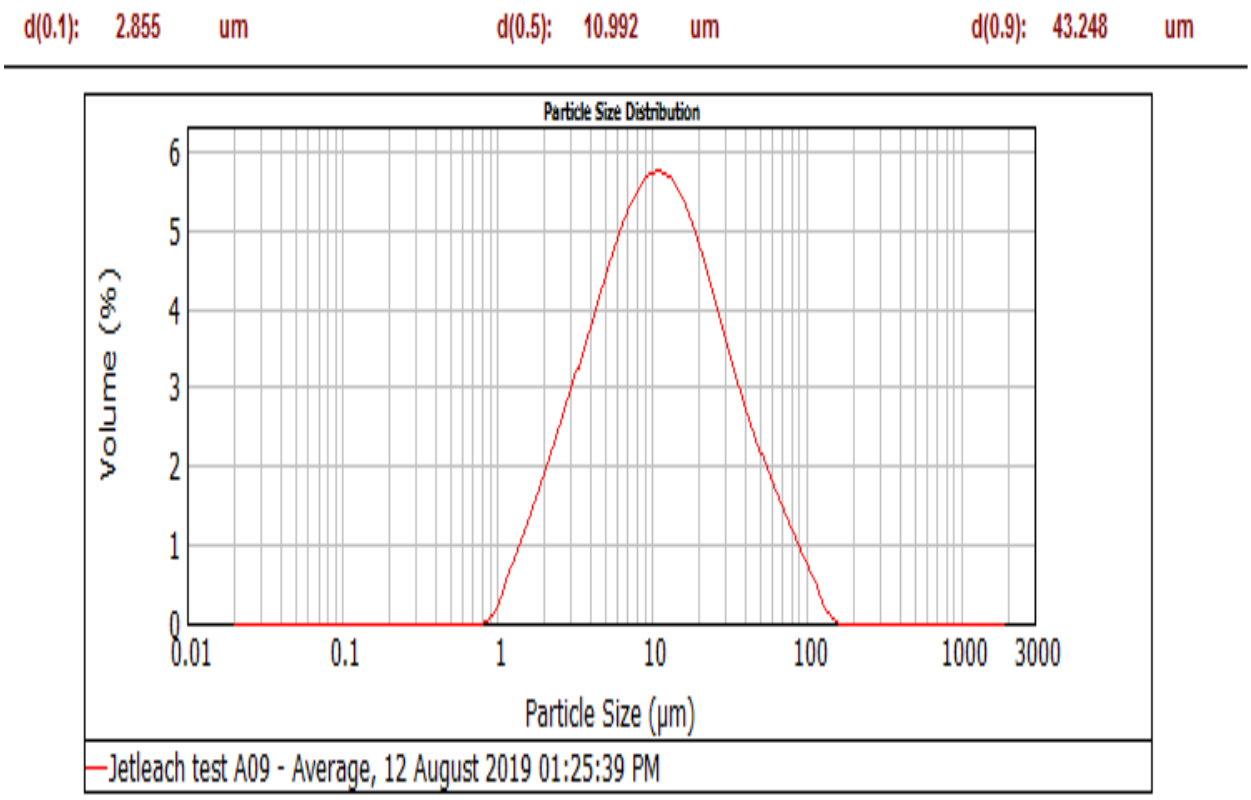


Figure 7.3 : Particle size analysis distribution of Ergo sample A after Jetleaching

d(0.1): 3.207 um d(0.5): 14.306 um d(0.9): 82.163 um

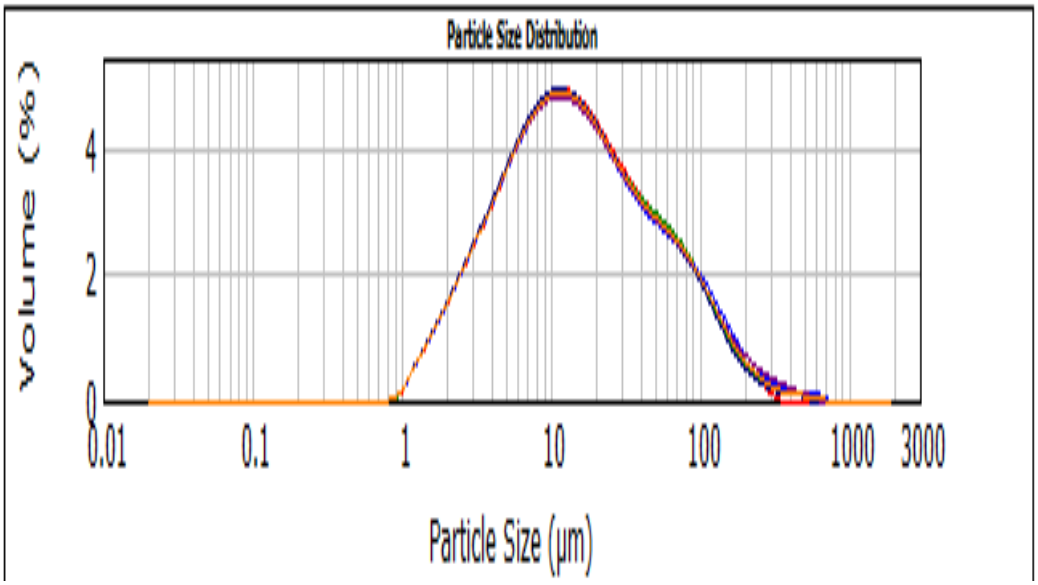


Figure 7.4 : Particle size analysis distribution of Ergo sample B before Jetleaching

d(0.1): 3.325 um d(0.5): 14.310 um d(0.9): 74.349 um

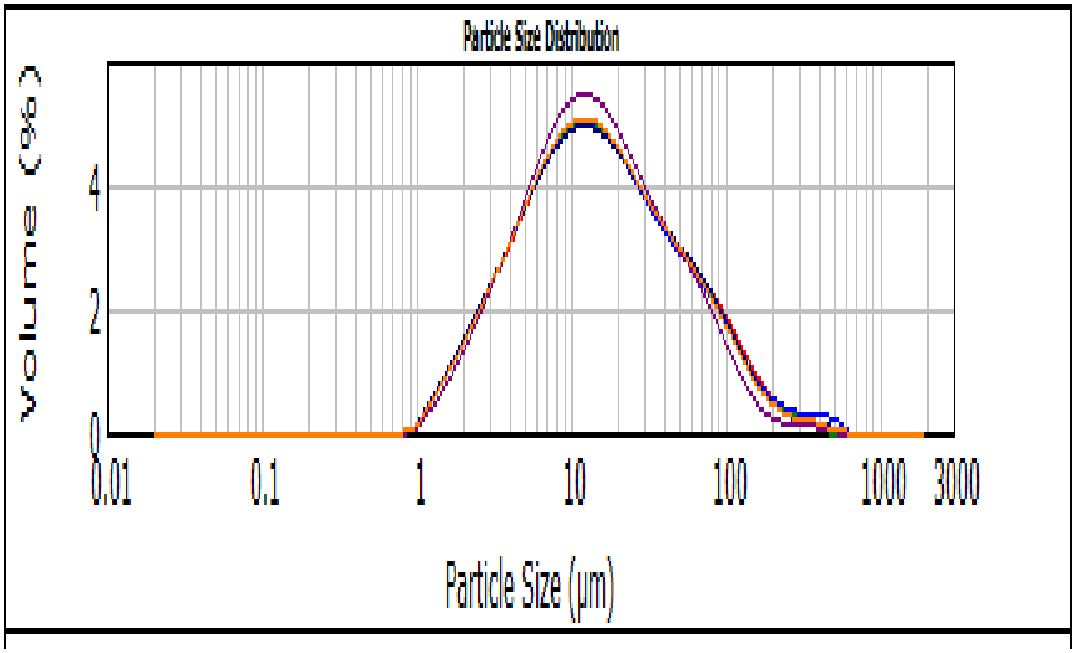


Figure 7.5 : Particle size analysis distribution of Ergo sample B after Jetleaching

7.2.2 Scanning Electron Microscopy (SEM) analysis

These analyses were done to verify the hypothesis that the leaching kinetics in the Jetleach reactor were probably due to cracks propagation and erosion phenomenon resulting in cavities and cracks on the surface of the particles. The SEM analysis were mostly focused on particles of pyrites and silicates since they are the major minerals in association with gold in the Ergo sample. Results from the SEM analysis before Jetleaching shown in **Figure 7.6** revealed no cracks or cavities on the surface of particles. However, results from the SEM analysis after Jetleaching shown in **Figure 7.7** revealed the presence of cavities on the surface of a particle of silicate (magnification of 1.97 KX) probably due to the impact of microbubbles and erosion phenomenon generated during cavitation. When investigating the presence of cracks on the surface, it was difficult to really confirm the presence of cracks at the same magnification as in the previous analysis. However, at a magnification close to 3.53 KX, it was possible to identify and confirm the presence of some cracks and cavities on the surface of some particles of silicate and pyrite (see **Figure 7.8**). The evidence of the presence of cracks and cavities on the surface of particles can also explain why it is possible to leach some gold particles that were locked in pyrite and silicate.

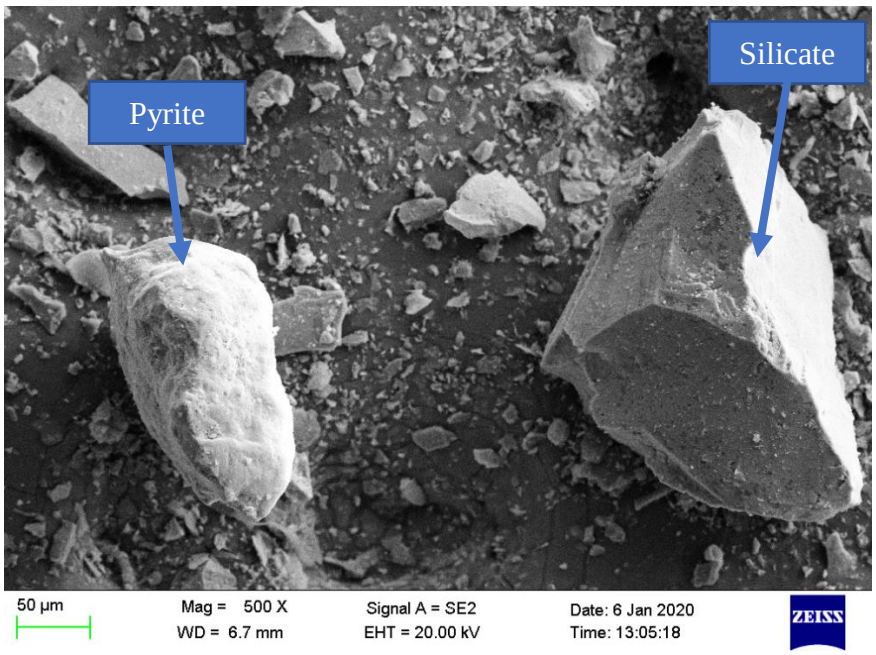


Figure 7.6 : Silicate and pyrite particles before Jetleaching (no presence of cracks or/and cavities on the surface)

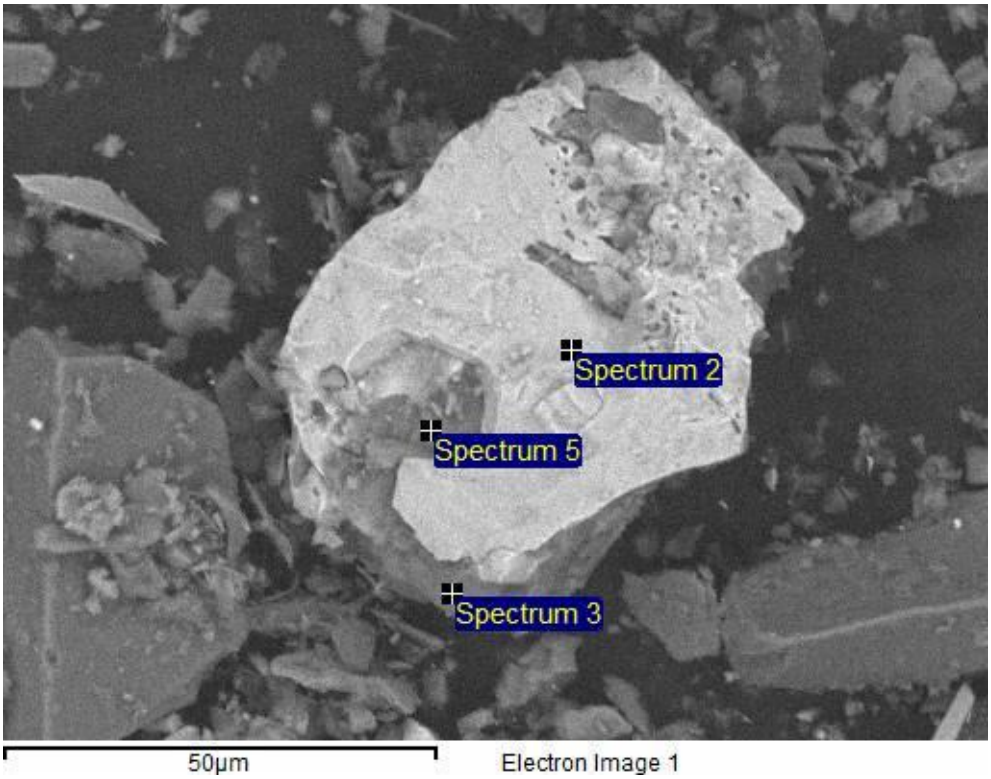


Figure 7.7 : Presence of cavities on the surface of a silicate particle after Jetleaching

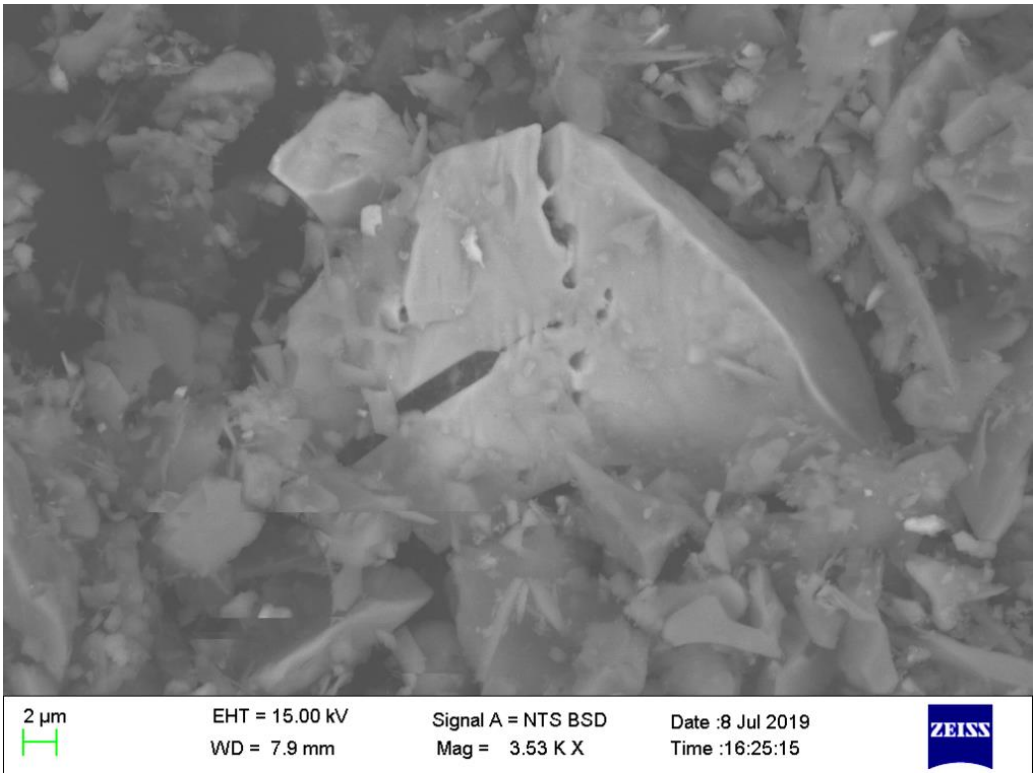


Figure 7.8 : Presence of cracks and cavities on the surface of a silicate particle after Jetleaching

7.2.3 Mechanism of cavitation generation

The generation of cavities was captured using a high-speed camera (Chronos 1.4). It can be seen from **Table 7.1** that no cavitation was generated at a flowrate below 10 l/min. However, the generation of cavitation started at a flowrate around 20 l/min. From 20 l/min and above, the cavitation zone increased as the flowrate increased until it reached a cavitation zone with a length around 36-41 cm at a maximum flowrate of 100 l/min. **Figure 7.9** present the generation of micro-cavitation in the tube reactor. More details about the cavitation mechanism are found in **Table 7.2** showing the different stages of the cavitation process. It can also be seen from the figures in **Table 7.2** that cavities are first produced as very small bubbles right after passing through the nozzle. Then these bubbles grow exponentially as they are moving from the low-pressure zone to the high-pressure zone. Once reaching the high-pressure zone, the cavities start collapsing. During these investigations, the pipe was divided into six zones. The first zone, found just after the nozzle, consists on the formation of bubbles or cavities in the liquid. This zone was characterized by the presence of very small bubbles or macro bubbles in the liquid. The second zone (or growth zone) is characterised by the presence of bubbles of wider diameter compared to the ones found in the first zone. The diameter of these bubbles increases as they move further in the pipe. This second zone is divided into three phases (phase 1 and 2). In the phase 1, there is a mixture of small and wider bubbles at the same time while, in the phase 2, there is a predominance of wider bubbles. In the third phase, only wider bubbles are found. The last zone, or collapsing zone, the bubbles reach a zone of high pressure and start collapsing.

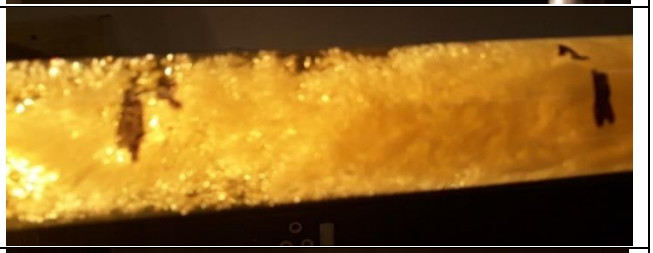
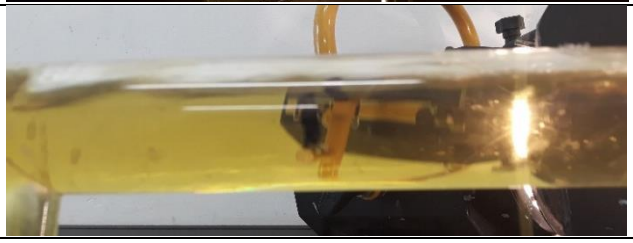
Table 7.1 : Variation of the cavitation depending on the flowrate

Test	Flowrate (l/min)	Cavitation zone (cm)
1	10	No cavitation
2	20	7-11
3	40	17-22
4	60	20-28
5	80	28-33
6	100	36-41



Figure 7.9 : Generation of macro cavitation

Table 7.2 : Images of different cavitation zones

Zone name	Images
Bubbles generation	
Bubbles growth phase 1	
Bubbles growth phase 2	
Bubbles growth phase 3	
Bubbles collapse	
No trace of cavitation	

7.3 Summary and conclusion

It can be seen from the PSD analysis that indeed a size reduction happened on the Ergo sample A and B after passing through the Jetleach reactor. It is important to note that the cavitation phenomenon mostly affected larger particles than the finer ones.

The SEM analysis confirmed the presence of cracks and cavities on the surface of some silicate and pyrite particles. These cracks and cavities allow cyanide solution to reach some locked gold particles that are not accessible when using conventional leaching methods. This can be the reason of the observed faster leaching kinetics as well as higher gold recoveries obtained when using the Jetleach reactor.

The cavitation mechanism was observed using the high-speed camera (Chronos 1.4). The images obtained from the high-speed camera revealed the presence of three zones, the bubble generation zone which is found just after the nozzle. The growth zone coming after the bubble creation zone and finally the collapsing zone characterized by the release of high energy.

This chapter has covered the impact cavitation has on the solid particles and how the mechanism of cavitation is generated in the Jetleach reactor. The next chapter presents the general conclusions and recommendations

CHAPTER 8 GENERAL CONCLUSION AND RECOMMENDATIONS

8.1 Introduction

The cyanidation process of refractory gold ores presents many challenges such as reduced leaching kinetics, difficulties to access gold particles and low gold recovery. These problems are usually connected to the association of gold with other minerals. However, even after a lot of developments and improvements in the cyanidation process of refractory gold ores, it is still difficult to have both high gold recovery and faster kinetics.

The cavitation process has been recently introduced as a promising technology which can transform the cyanidation process. The process uses a reactor named a Jetleach. This reactor has shown impressive results in terms of leaching kinetics and gold recovery when tested on free milling ores. Therefore, the objective of this study was to find out if the Jetleach reactor could also improve the gold recovery and the leaching kinetics of refractory gold ores.

Three refractory gold ore samples were involved in this study; two rougher flotation samples from West Africa (DIO: diorites ore and MVO: meta-volcanic ore) and one sample from South Africa (Ergo flotation concentrate).

To achieve the objectives assigned, the aims of this study were defined as follow:

- Compare the Jetleach to the conventional methods used in the cyanidation process and evaluate the benefits of using this reactor.
- Investigate the effect of physical and chemical parameters on the cavitation process.
- Investigate the effect of cavitation on the solid particles.
- Explain the cavitation mechanism that takes place in the Jetleach reactor.

8.2 Comparison between conventional methods and Jetleaching method

This investigation was divided in three stages, the pre-aeration test, leaching in cyanide solution and evaluation of the potential benefits of using the Jetleach process.

8.2.1 Pre-aeration tests

Preliminary tests consisted on a pre-aeration of the slurry of each ore involved in this study in order to reduce the cyanide consumption by oxidizing iron (II) into iron (III). The pre-

aeration stage was done over a period of 20 hours using 25KPa of pure oxygen gas. Three parameters were followed during the pre-aeration, the pH, Eh and concentration of dissolved oxygen.

Samples with and without pre-aeration were subjected to cyanidation using the same leaching conditions. Results from these experiments revealed that cyanide consumption was reduced for all three types of refractory ores. A decrease of almost 0.15kg/t, 0.5kg/t and 0.6kg/t were observed for the Ergo, DIO and MVO samples, respectively. This confirms the fact that pre-aeration can be used to reduce cyanide consumption of sulphidic ores which have a high pyrite content. Therefore, before cyanidation, all slurry involved in this work was pre-aerated for 20 hours using pure oxygen.

8.2.2 Comparison between conventional methods and Jetleaching method

Three cyanidation methods were involved in this set of experiments. Two methods representing the conventional methods and the Jetleaching method. The two conventional methods consisted of the bottle roll and the normal leaching (leaching in agitated vessel). In order to do an accurate comparison, the same leaching condition were used in all three set of experiments. The pH was kept between 10.5-11.5; the solid percentage was at 40% weight ratio and the cyanide concentration was kept at 5kg/t. However, for the normal leaching and the Jetleach process, the oxygen flowrate and the mixing rate were kept at 30 ml/min and 400 rpm. In the Jetleach process the pump pressure was kept at 15 MPa slurry.

Results from these experiments show that after a leaching period of 24 hours, the Jetleach reactor performance was far above that of the other two leaching methods. On the DIO sample, gold recoveries of 65.27% and 76.42% were obtained with the bottle roll and normal leaching methods, respectively. While 84.18% gold recovery was obtained with the Jetleach process. On the MVO sample, the Jetleach process obtained a gold recovery of 91.28%, whilst the bottle roll and the normal leaching method obtained gold recoveries of 74.36% and 81.7%, respectively.

On the Ergo sample however, since most gold particles were locked in pyrite, silicates and other sulphides; gold recoveries were lower than in the other two samples. Gold recoveries of 56.59% and 59.83% were obtained with the bottle roll and normal leaching tests. Despite all the challenges faced with the Ergo sample, the Jetleach reactor managed to reach a gold recovery of 72.85% (recovery which has never been reached at Ergo plant). The most

important finding was that the performance of the two conventional methods, after a leaching period of 24 hours (for all three samples: DIO, MVO and Ergo), were far below that of the Jetleach performance after only 2 hours of leaching.
This confirms that the use of micro-cavitation generated in the Jetleach reactor can be used to enhance the leaching kinetics of refractory ores while providing high gold recovery.

8.2.3 Potential benefits of using the Jetleach reactor

An analysis based on Ergo plant revealed that the Jetleach reactor can increase the annual revenue by almost R 123.3 million by reducing the amount of gold lost in the residues. Some of the other benefits are: high throughput and high gold recovery; reduced reagent consumption; faster leaching kinetics; smaller leach tanks requirements, reduced number of leach tanks and high energy savings by reducing the leaching time by almost 90%. All these benefits can contribute to the reduction of the overall processing cost of refractory gold ores as well as the capital necessary to start a new leaching section.

8.3 Investigation of the effect of physical and chemical parameters

Five parameters or factors were studies in these sets of experiments: oxygen flowrate, cyanide concentration, pump pressure, space between nozzles and solid percentage. For the studies, two approaches were used: the first one consisted of a one factor at-a-time experiment (OFAT) and the second one consisted on a statistical designed experiment or Design of Experiment (DOE) to evaluate the interaction between factors.

Results obtained from the OAFT experiments revealed that three parameters had a significant effect on the gold recovery whilst two parameters were insignificant. The three significant parameters are: oxygen flowrate, pump pressure and solid percentage. However, the increase in oxygen flowrate and pump pressure had a positive effect on the gold recovery; while, an increase of the solid percentage had a negative effect on the gold recovery. Cyanide concentration, which is one of the most important parameters in the conventional methods, was revealed not to have much of an effect on the gold recovery (applicable to the range used in this study). A maximum gold recovery of 76% was obtained at pH: 10.5-11.5, oxygen flowrate of 40 ml/min, solid percentage of 40%, space between nozzles of 0.5 Cm, cyanide concentration of 5kg/t and a pump pressure of 20 MPa.

The statistical designed experiment consisted of a factorial “green” design involving all five parameters and gold recovery was taken as the measured response. Results obtained from this

set of experiments (DOE) revealed that, as in the OAFT, the cyanide concentration and the space between nozzles were not significant. However, this experiment revealed that beside the pump pressure, oxygen flowrate and solid percentage, three interactions between the five factors also had a significant effect on the gold recovery. These interactions are; interaction between pump pressure and oxygen flowrate, interaction between oxygen flowrate and solid percentage; and the interaction between cyanide concentration and oxygen flowrate. Despite being among the significant parameters, the oxygen flowrate is also the common parameter involved in all three interactions. This simply mean that the oxygen flowrate is the main parameter in the Jetleach process for the parameter intervals chosen in this investigation. The results also indicated that gold recovery was maximized at higher pump pressure, oxygen flowrate and lower solid percentage.

8.4 Impact of Micro-cavitation on the Solid particles and investigation of the cavitation mechanism

To explain the effect of micro-cavitation on the solid particles, two analysis were done: a Particle Size Distribution (PSD analysis) and a Scanning Electron Microscopy (SEM analysis). However, the investigation of the cavitation mechanism was done using a high-speed camera and replacing the slurry with water.

8.4.1 Particle size distribution

The PSD analysis was conducted on the solid samples before and after the Jetleach process. The objective of these tests was to verify if any comminution was happening in the reactor which could explain the increase in gold recovery and the faster leaching kinetics. Results obtained from the Malvern Mastersizer revealed that there was comminution of solid particles happening in the Jetleach reactor. The d90 of the first sample shifted from 46.553μm before Jetleaching to 43.243 μm after passing through the Jetleach. The d90 of the second sample was reduced from 82.163 μm before to 74.349 μm after passing through the Jetleach.

8.4.2 Scanning Electron Microscopy (SEM)

The SEM analysis were conducted on samples before and after Jetleaching. Results obtained from the SEM on samples before passing through the Jetleach did not show any presence of cavities or significant cracks on the surface of particles of silicates and pyrites. However, results obtained on samples after passing through the Jetleach revealed the presence of some cracks and cavities on the surface of particles such as pyrite and silicates. The presence of

cracks and cavities can also explain why higher gold recovery and faster leaching kinetics were obtained with the Jetleach reactor compared to the conventional methods.

8.4.3 Investigation of the mechanism of cavitation

The aim of this investigation was to understand how cavitation is generated in the Jetleach reactor. For this to be possible, a transparent reactor which uses water instead of slurry was designed to simulate the impact phenomenon happening in the Jetleach. Results obtained from a high-speed camera revealed that cavities were generated in the water after passing through the nozzles. One main parameter was investigated in these experiments: the solution flowrate through the nozzle. Results from these experiments revealed that the cavitation zone is directly connected to the flowrate of solution and that a maximum cavitation zone was obtained at a maximum flowrate of 100 litres/min.

8.5 Recommendations

8.5.1 Optimization

This work had identified that the pump pressure, the solid percentage and the oxygen flowrate were the three significant factors. It further showed that three interactions between factors were also significant; interactions between: oxygen flowrate-solid percentage, pump pressure-oxygen flowrate, and cyanide concentration-oxygen flowrate. Since cyanide concentration was shown not to be significant for the range chosen in this study, the optimization stage can be an opportunity to reduce cyanide consumption by extending the range of cyanide levels. Therefore, this work can be extended by optimizing the entire Jetleaching process. The optimization model can involve the oxygen flowrate, cyanide concentration and solid percentage while keeping the pump pressure at its maximum value. In the case of using a more powerful pump, the pressure range can also be expanded to increase the intensity of the cavitation phenomenon.

8.5.2 Cost evaluation (Energy savings)

One of the most critical aspect that must be investigated before the integration of this reactor in the cyanidation process, is the energy consumption. This investigation can be done by doing a comparative evaluation of the energy consumption between the conventional cyanidation processes and the Jetleach process. The most crucial parameters to follow will be the power consumption of the slurry pump and the nozzles resistance and replacement cost.

The results that will be obtained from this investigation must be balanced to the benefits the Jetleach process is able to bring. The best cost evaluation can be done at a pilot scale running in a continuous process.

8.5.3 Deeper study and understanding of the cavitation phenomenon

This work can also be extended in the sense of studying and understanding the effect of cavitation on the Nernst Layer and the detailed kinetics mechanism involved in the leaching of gold ores in cyanide solution. This investigation can be done by using an Infra-Red Camera and a Potentiostat. The IR camera will help to investigate the difference in local temperature at the interphase bubble-particle during cavitation. The Potentiostat will assist in the understanding of the effect of cavitation on the Tafel curve of oxidation of gold in cyanide solution by doing a comparison between the oxidation curve (Tafel curve) of gold with and without the use of cavitation.

References

1. Abbruzzese, C., Ubaldini, S., Veglio, F. & Toro, L., 1994. reparatory bioleaching to the conventional cyanidation of arsenical gold ores. *Minerals Engineering,* 7(1), pp. 49-60.
2. Adams, M., 2013. Impact of recycling cyanide and its reaction products on upstream unit operations. *Minerals Engineering,* Volume 53, pp. 241-255.
3. Adams, M., 2016. Gold Ore Processing (Project Development and Operations). *Elsevier Science,* Volume 15.
4. Adams, M. D. & Wills, B., 2005. Advances in Gold Ore Processing. *Elsevier,* pp. 1-1027.
5. Afenya, P., 1991. reatment of carbonaceousrefractory gold ores. *Minerals Engineering,* 4(7-11), pp. 1043-1055.
6. Aghamirian, M. & Yen, W., 2005. Mechanisms of galvanic interactions between gold and sulfide minerals in cyanide solution. *Minerals Engineering,* 18(4), pp. 393-407.
7. Ahmed, S. & Ahmed, S., 2013. *Cavitation nanobubble enhanced flotation process cavitation nanobubble enhanced flotation process for more efficient coal recovery for more efficient coal recovery.* s.l.:University of Kentucky, Theses and Dissertations-Mining Engineering.
8. Amankwah, R. & Pickles, C., 2009. Microwave roasting of a carbonaceous sulphidic gold concentrate. *Mineral Engineering,* pp. 1095-1102.
9. Amankwah, R., Yen, , W.-T. & Ramsay, J., 2005. A two-stage bacterial pretreatment process for double refractory gold ores. *Minerals Engineering,* Volume 18, pp. 103-108.
10. Angelov, A. & Groudev, S., 2002. *Treatment of gold-bearing solutions by cementations with metallic zinc,* Sofia 1700, Bulgaria: s.n.
11. Archibald, F. R., 1949. Roasting Arsenical Gold Ores and Concentrates. *The Canadian Mining and Metallurgy Bulletin for March,* April.pp. 76-86.
12. Asamoah, R., Amankwah, R. & Addai-Mensah, J., 2014. Cyanidation of Refractory Gold Ores: A Review. *Elsevier,* Volume 3rd UMaT Biennial International Mining and Mineral Conference, pp. 204-212.
13. Aydin , b., Basturkcu, h. & Gul, a., 2015. Influence of pre-aeration on cyanide leaching of a non-refractory sulphide gold and silver ore. *Physicochemical Problems of Mineral Processing,* 51(2), p. 647−660.

14. Baláž , P. & Achimovičová, M., 2006. Mechano-chemical leaching in hydrometallurgy of complex sulphides. *Hydrometallurgy*, Volume 84, pp. 60-68.
15. Baláž, &. G., 2005. Mechanochemical preparation of metal/sulphide nanocomposite particles. *International Journal of Material and Product Technology 23,* pp. 26-41.
16. Baláž, P. & Achimovičová, M., 2006. Mechano-chemical leaching in hydrometallurgy of complex sulphides. *Elsevier,* pp. 60-68.
17. Bas, A. D., Ghali, E. & Choi, Y., 2017. A review on electrochemical dissolution and passivation of gold during cyanidation in presence of sulphides and oxides. *Elsevier/Hydrometallurgy,* Volume 172, pp. 30-44.
18. Bowell, R., 1999. The occurrence of gold at the Getchell mine, Nevada. *Journal of Geochemical Exploration,* Volume 67, pp. 127-143.
19. Breuer, P. L., Jeffrey, M. I. & Hewitt, D. M., 2008. Mechanisms of Sulfide Ion Oxidation during Cyanidation. Part I: The Effect of Lead (II) Ions.. *Minerals Engineering* , pp. Vol 21, pp. 579-586.
20. Bwalya, M., Moys, M., Finnie, G. & Mulenga, F., 2014. Exploring ball size distribution in coal grinding mills. *Elsevier,Powder Technol.,* Volume 257, pp. 68-73.
21. Campbell, J. & Watson, B., 2003. *Gravity Leaching with the Consep Acacia Reactor.* s.l., Results from AngloGold Union .
22. Celep, O. et al., 2014. Improvement of Silver Extraction by Ultra−fine Grinding prior to Cyanide Leaching of the Plant Tailings of a Refractory Silver Ore. *Mineral Processing and Extractive Metallurgy Review.*
23. Chakinala, A. G., Gogate, P. R., Burgess, A. E. & Bremner, D. H., 2008. Treatment of industrial wastewater effluents using hydrodynamic cavitation and the advanced Fenton process. *Ultasonics Sonochemistry 15,* pp. 49-54.
24. Corrans, I. & Angove, J., 1991. Ultrafine milling for the recovery of refractory gold. *Minerals Engineering,* Volume 4, pp. 763-776.
25. Danckwerts, P., 1964. The absorption of gases in liquids. *Pure and Applied Chemistry/ Walter de Gruyter/ Department of Chemical Engineering, University of Cambridge, U.K.,* pp. 625-642.
26. Davidson, R. & Sole, M., 2007. The major role played by calcium in gold plant circuits. *Journal of the Southern African Institute of Mining and Metallurgy* , 107(7), pp. 463-468.
27. de Andrade , . L. . L. & Hodouin, D., 2005. A Lumped Kinetic Model for Gold Ore Cyanidation. *Hydrometallurgy*, pp. Vol 79, pp. 121-137..

28. Deniz, V., 2012. The effects of ball filling and ball diameter on kinetic breakage parameters of barite powder. *Elsevier, Adv. Powder Technol.,* Volume 23, pp. 640-646.
29. Deschênes, G. et al., 2000. Effect if Lead Nitrate on Cyanidation of Gold Ores: Progress on the Study of the Mechanisms. *Minerals Engineering,* pp. Vol 13, No 12, pp. 1263-1279..
30. Deschênes, G., Lacasse, S. & Fulton, M., 2003. Improvement of Cyanidation Practice at Goldcorp Red Lake Mine. *Minerals Engineering,* Volume 16, pp. 503-509.
31. Deschênes, G. & Wallingford , G., 1995. Effect of Oxygen and Lead Nitrate on the Cyanidation of a Sulphide Bearing Gold Ore. *Minerals Engineering,* pp. Vol 8, pp. 923-931..
32. Dular, M. & Petkovšek, M., 2015. On the Mechanisms of Cavitation Erosion – Coupling High Speed Videos to Damage Patterns. *Elsevier, Experimental Thermal and Fluid Science,* Volume 68, pp. 359-370.
33. Dunne, R. et al., 2012. Assessment of options for economic processing of preg-robbing gold ores. *World Gold,* Volume 121, pp. 217-223.
34. Ellis, S., 2003. *Ultra Fine Grinding - A Practical Alternative to Oxidative Treatment ofRefractory Gold Ores,* s.l.: Kalgoorlie Consolidated Gold Mines Kalgoorlie, WA..
35. Ellis, S. & Senanayake, G., 2004. The Effects of Dissolved Oxygen and Cyanide Dosage on Gold Extraction from a Pyrrhotite-Rich Ore.. *Hydrometallurgy,* pp. Vol 72, pp. 39-50..
36. Fast & Associates, LLC, n.d. *Gold Mining Process Development.* [Online] Available at: https://www.denvermineral.com/gold-mining-process-development/ [Accessed 28 September 2019].
37. Flatman , S. et al., 2008. *The Leachox Refractory Gold Process – The Testing, Design, Installation and Commissioning of a Large-Scale Plant* , VASGOLD Gold Mine, Kazakhstan:: s.n.
38. Flatman, S., Battersby, R., Imhof, R. & Ibrayev, S., 2010. The Leachox refractory gold process–the setting, design, installation and commissioning of a large scale plant at the VASGOLD gold mine, Kazakhstan. *Precious Metals,* Volume 10.
39. Flatman, S. & Vorster, . B., 2001. Cyanide control in the metallurgical process of gold extraction in AngloGold (S.A.). *The South African Institute of Mining and Metallurgy,* pp. 359-366.

40. Flatman, S. & Vorster, B., 2001. Cyanide control in the metallurgicalprocess of gold extraction in AngloGold (S.A.). *The Journal of The South African Institute of Mining and Metallurgy*, pp. 359-366.
41. Fleming, C., 2004. Gold Extraction Technology Developments and their Implication to Profitability and Sustainability.. *Elsevier.*
42. Fosu, S., Pring, A., Skinner, W. & Zanin, M., 2015. Characterisation of coarse composite sphalerite particles with respect to flotation. *Minerals Engineering,* Volume 71.
43. Frondel, C., 1938. Stability of colloidal gold under hydrothermal conditions. *Economic Geology,* Volume 33 (1), pp. 1-20.
44. GMRS report, 1997. *An impact on gold,* s.l.: General Metallurgical Research and Services (By Roy Bennetts).
45. Gonzalez-Anaya, J., Nava-Alonso, F. & Pecina-Trevino, E., 2011. Gold recovery optimization of a refractory concentrate by ultrafine grinding - A laboratory study. *Minerals and Metallurgical Processing,* 28(2), pp. 95-101.
46. Gupta, C. & Mukherjee, T., 2000. *Hydrometallurgy in Extraction Processes,* Boston: CRC Press.
47. Haque, K., 2007. Gold Leaching from Refractory Ores-Literature Survey. *Mineral Processing and Extractive Metallurgy Review,* 2(3), pp. 235-253.
48. Harbort, G., Hourn, M. & Murphy, A., 2014. IsaMill ultrafine grinding for a sulphide leach process. *Elsevier.*
49. Hausen, D., 2000. Characterizing the textural features of gold ores for optimizing gold extraction. *JOM,* Volume 52, pp. 14-16.
50. Hlabangana, N. et al., 2018. Optimisation of the Leaching Parameters of a Gold Ore in Sodium Cyanide Solution. *International Journal of Research 6(11-10):2348-697,* Volume 6, pp. 685-697.
51. Hollow, J., Hill, E., Lin, H. & Walsh, D., 2005. *Modeling the influence of slurry temperature on gold leach and adsorption kinetics at the Fort Knox mine,* Fairbanks, Alaska: SME Pre print 05-67. Littleton, CO: SME. .
52. Holmes, R. & Minnitt, R., 2018. The costs of sampling errors and bias to the mining industry. *Journal of the Southern African Institute of Mining and Metallurgy,* 118(12), pp. 787-798.
53. Hourn, M. & Halbe, D., 1999. *The NENATECH Process: Results on Frieda River Copper Gold Concentrate.* s.l., The Randol Gold Conference, pp. 1-102.

54. Jara, J. O. & Bustos, A. A., 1992. Effect of oxygen on gold cyanidation: laboratory results. *Hydrometallurgy*, 30(1-3), pp. 195-210.
55. Kianinia, Y. et al., 2018. Predicting Cyanide Consumption in Gold Leaching: A Kinetic and Thermodynamic Modeling Approach. *Minerals* , Volume 110, pp. 1-13.
56. Kondos, P. D., Deschenes, G. & Morrison, R. M., 1995. Process Optimization Studies in Gold Cyanidation. Hydrometallurgy, Vol 39,. *Hydrometallurgy*, pp. pp. 235-250..
57. Kumar, R. et al., 2016. Remediation of cyanide-contaminated environments through microbes and plants:a review of current knowledge and future perspectives. *The Korean Society of Mineral and Energy Resources Engineers/ Geosystem Engineering.*
58. La Brooy, S., Linge, H. & Walker, G., 1994. Review ofGold Extraction from Ores. *Minerals Engineering*, 7(10), p. 12131241.
59. Ladola, Y., Chowdhury, S., Roy, S. & Pandit, A., 2014. Application of cavitation in uranium leaching. *Desalination and Water Treatment* , pp. 407-414.
60. LI, D., 2009. Developments in the pretreatment of refractory gold minerals. *The Southern African Institute of Mining and Metallurgy*,.
61. Liddell, K. & Adams, M., 2012. Kell hydrometallurgical process for extractionof platinum group metals and base metalsfrom flotation concentrates. *The Journal of The Southern African Institute of Mining and Metallurgy*, Volume 112, pp. 31-36.
62. Liipo, J., 2003. Characterization of the mode of occurrence of gold in Jokisivu pilot feed and products. *Minerals Engineering*, Volume 16, pp. 1317-1321.
63. Liu, G. & Yen, W., 1995. Effects of sulphide minerals and dissolved oxygen on the gold and silver dissolution in cyanide solution. *Minerals Engineering*, Volume 8, pp. 111-123.
64. Loftus, B., Lorenzen, L. & Petersen, K., 1997. The development of a jet reactor for the leaching of valuable metals. *The Journal of The South African Institute of Mining and Metallurgy* .
65. Loftus, B., Lorenzen, L. & Petersen, K., 1997. The development of a jet reactor for the leaching of valuable metals. *The Journal of The South African Institute of Mining and Metallurgy*, Volume A ISSN 0038–223X/3.00 +0.00. , pp. 285-288.
66. Longley, R., McCallum, A. & Katsikaros, N., 2003. Intensive Cyanidation, Onsite Application of the InLine Leach Reactor to Gravity Gold Concentrates. *Minerals Engineering*, pp. Vol 16, pp. 411-419.

67. Lorenzen, L. & Kleingeld, A., 2000. New Generation Leaching Reactors forEffective Mass Transfer in Mineral Processing Operations.. *Minerals Engineering*, pp. Vol 13, pp. 1107-1115.
68. Madhu, G. M., Ashly Thomas, Deepak, S. & Preetham, H. S. R., 2015. Escalation of degradation of malachite green and Methyl violet using hydrodynamic cavitations using different orifice geometry. *INTERNATIONAL JOURNAL OF ENVIRONMENTAL SCIENCES Volume 5,* pp. 880-890.
69. Marsden & House, 2006. *The Chemistry Of Gold Extraction.* Littleton, Colorado, USA 80127: the Society for Mining, Metallurgy, and Exploration, Inc..
70. Marsden, J. O. & House, C. I., 2009. *The Chemistry of Gold Extraction "Second Edition".* Colorado, USA: Society for Mining, Metallurgy, and Exploration, Inc.
71. Miller, P. & Brown, A., 2005. Bacterial oxidation of refractory gold concentrates. In: *advances in gold ore processing.* Perth, Australia: Elsevier (Mineral Processing), pp. 371-402.
72. Mineral, E., 2005. *Collaboration with Gravity Man Yields.* [Online] Available at: http://www.min-eng.com/gravityconcentration/85.html. [Accessed 2 October 2019].
73. Mohammadabad, F. K., Hejazi, S., khaki, J. V. & Babakhani , A., 2016. Mechanochemical leaching of chalcopyrite concentrate by sulfuric acid. *International Journal of Minerals, Metallurgy, and Materials,* Volume 23, pp. 380-388.
74. Nancharaiah, Y., Mohan, S. V. & Lens, P., 2016. Biological and Bioelectrochemical Recovery of Critical and Scarce Metals (Review). *Elsevier (Trends in Biotechnology),* 34(2), pp. 137-155.
75. Nicol, M., 1980. The anodic behaviour of gold. II. Oxidation in alkaline solutions. *Gold Bull,* Volume 13, pp. 105-111.
76. Nicol, M., Schalch, E., Balestra, P. & Hegedus, H., 1979. A modern study of the kinetics and mechanism of the cementation of gold. *Journal of the South African Institute of Mining and Metallurgy,* pp. 191-198.
77. Ofori-Sarpong, G., Adjei, D. & Amankwah, R., 2017. Fungal-Transformation of Surrogate Sulphides andCarbonaceous Matter in Refractory Gold Ores: Revisited. *Ghana Mining Journal,* 17(2), pp. 56-65.
78. Olyaei, Y. et al., 2014. The Optimization of cyanidation for Hamze-Qarnein gold ore. *14th International Mineral Processing Symposium.*

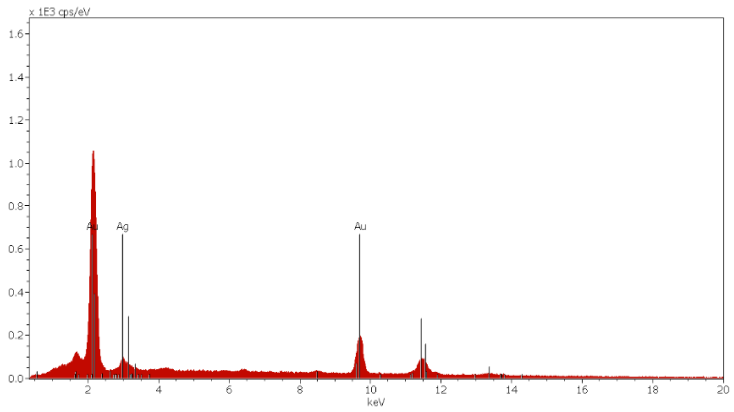
79. Parga, J., Valenzuela, J. & Francisco, C., 2007. Pressure Cyanide Leaching for Precious Metals Recovery. *Aqueous Processing.*
80. Parga, J. R., Valenzuela, J. L. & Díaz, J. A., 2012. New Technology for Recovery of Gold and Silver by Pressure Cyanidation Leaching and Electrocoagulation. *Jornal of Noble Metal*, pp. 72-94.
81. Payri, R., Salvador, F., Gimeno, J. & Venegas, O., 2013. Study of cavitation phenomenon using different fuels in a transparent nozzle by hydraulic characterization and visualization. *Experimental Thermal and Fluid Science 44,* pp. 235-244.
82. Petrakis, E., Stamboliadis, E. & Komnitsas, K., 2016. Evaluation of the relationship between energy input and particle size distribution in comminution with the use of piecewise regression analysis. *Elsevier, Particulate Science and Technology,* 35(4), pp. 479-489.
83. Royer, J.-J.et al., 2017. Thermodynamics of ultra-sonic cavitation bubbles in flotation ore processes. *Journal of Physics Conference Series,* Volume 879.
84. Rusanen, L., Aromaa, J. & Forsen, O., 2013. Pressure oxidation of pyrite-arsenopyrite refractory gold concentrate. *Physicochemical Problems of Mineral Processing,* 49(1), pp. 101-109.
85. Saunders, J., 1990. Colloidal transport of gold and silica in epithermal precious-metal systems: Evidence from the Sleeper deposit, Nevada. *Geology*, Volume 18, pp. 757-760.
86. Senanayake , G. et al., 2018. Predicting Cyanide Consumption in Gold Leaching: A Kinetic and Thermodynamic Modeling Approach. *Minerals*, Volume 8, pp. 110-123.
87. Senanayake, G., 2008. A Review of Effects of Silver, Lead, Sulfide and Carbonaceous Matter on Gold Cyanidation and Mechanistic Interpretation. Hydrometallurgy, Vol 90, pp. 46-73.. *Hydrometallurgy, Vol 90,* pp. pp. 46-73..
88. Stange, W., 1999. The Process Design of Gold Leaching and Carbon-in-Pulp Circuits.. *The Journal of the South Africa Institute of Mining and Metallurgy.*
89. Streltsov, S. V. et al., 2018. Old puzzle of incommensurate crystal structureof calaverite AuTe2and predicted stability ofnovel AuTe2 compound. *PNAS Latest Articles,* pp. 1-6.
90. Tanco, M., Viles, E., Ilzarbe, L. & Alvarez, M. J., 2008. *"Dissecting DoE Software.* s.l., Six Sigma Forum Magazine.

91. Tsaih , M., Tseng, L. & Chen, R., 2004. *Effects of removing small fragments with ultrafiltration treatment and ultrasonic conditions on the degradation kinetics of chitosan.* s.l.: Polym. Degrad. Stab. p.25..
92. Tsaih, M., Tseng, L. & Chen, R., 2004. The effect of removing small fragments with ultrafiltration tretment and ultrasonic conditions on the degradation kinetics of chitosan. *Polymer Degradation and Stability,* Volume 86, pp. 25-32.
93. Ubaldini, S., Veglio, F., Fornari, P. & Abbruzzese, C., 2000. Process Flow-Sheet for Gold and Antimony Recovery from Stibnite. *Hydrometallurgy*, 57(3), pp. 187-199.
94. Wadsworth , M., Zhu, X., Thompson, J. & Pereira, C., 2000. Gold dissolution and activation in cyanide solution: kinetics and mechanism. *Elsevier, Hydrometallurgy,* Volume 57, pp. 1-11.
95. Wadsworth, M., Zhu, X., Thompson, J. & Pereira, C., 2000. Gold dissolution and activation in cyanide solution: Kinetics and mechanism. *Hydrometallurgy,* 57(1), pp. 1-11.
96. Wang, G.-h.et al., 2016. Two-Step Oxidation of Refractory Gold Concentrates with DifferentMicrobial Communities. *J. Microbiol. Biotechnol,* 26(11), pp. 1871-1880.
97. Watson, B. & Steward, G., 2002. *Gravity Leaching-The ACACIA Reactor.*. [Online] Available at: http://www.knelsongravitysolutions.com/sites/knelsongravity/files/reports/report36s.pdf.
98. Yannopoulos, J., 1991. *Extractive Metallurgy of Gold.* New York: VAN NOSTRAND REINHOLD .
99. Zhou, Z. A. et al., 2009. On the role of cavitation in particle collection in flotation. *Mineral Engineering*, pp. 419-433.
100. Zhu, P. et al., 2012. Kinetics of leaching refractory gold ores by ultrasonic-assisted electro-chlorination. *International Journal of Minerals, Metallurgy and Materials,* 19(6), p. 4.

APENDIX A

QEMSCAN ANALYSIS

A.1 Liberated Gold

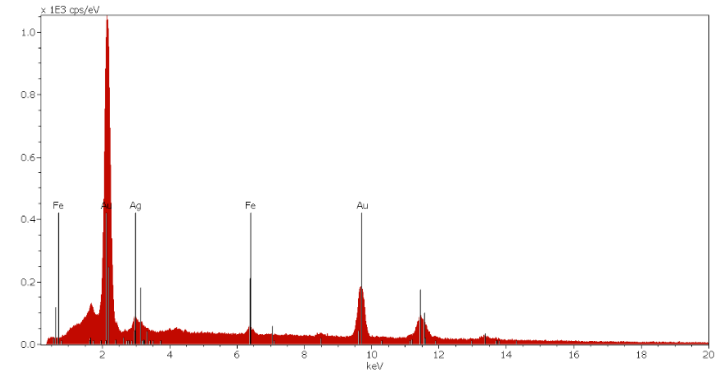


EDS spectra

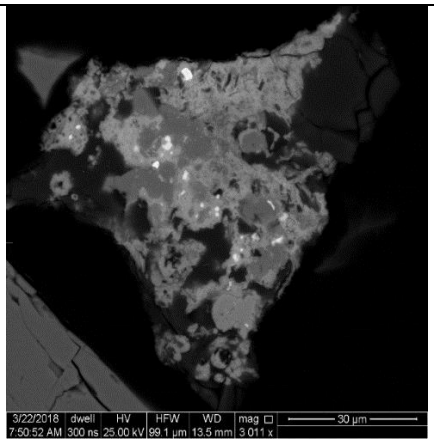


BSE Image

A.2 Gold Locked in particle consisting of pyrrhotite, brannerite, quartz and arsenopyrite

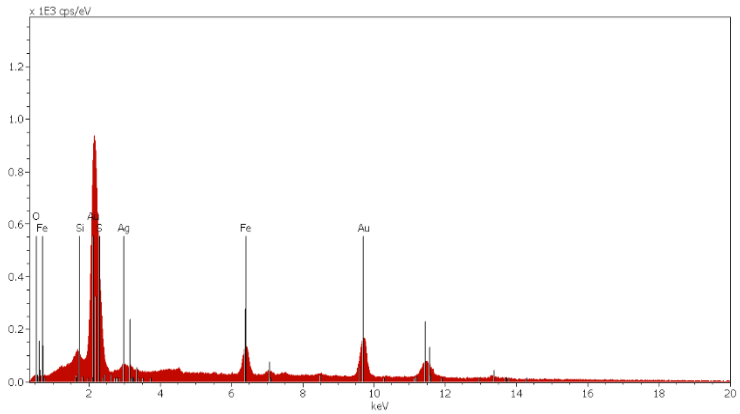


EDS spectra

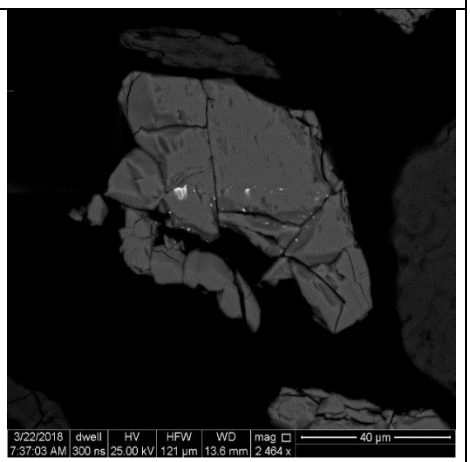


BSE Image

A.3 Gold locked in pyrite

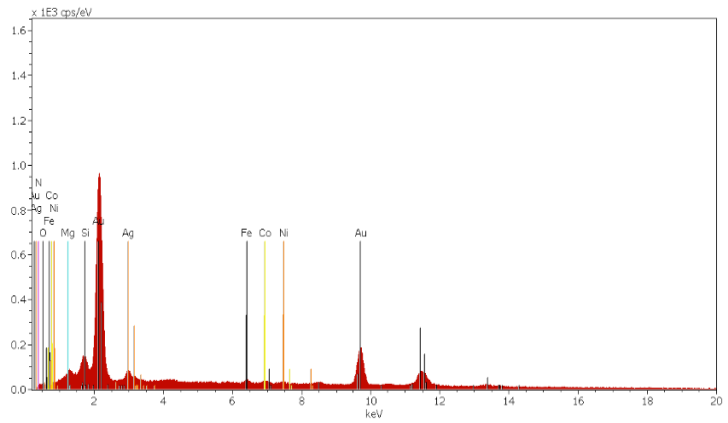


EDS spectra

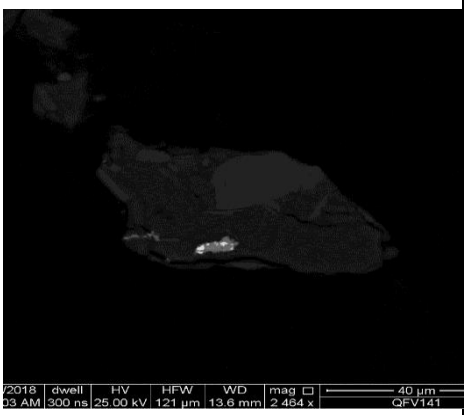


BSE Image

A.4 Liberated Gold

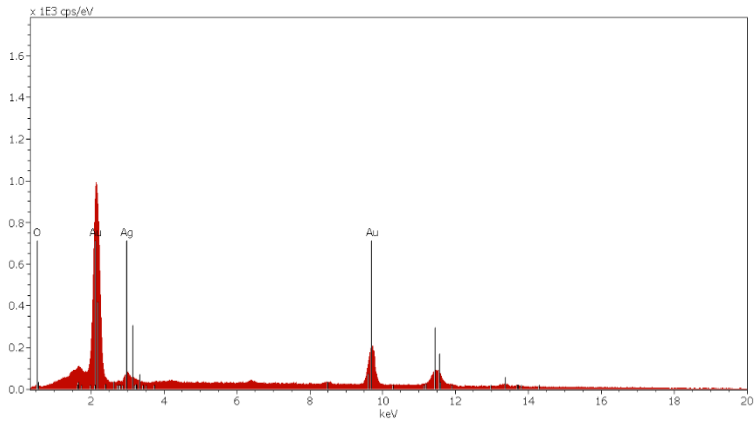


EDS spectra

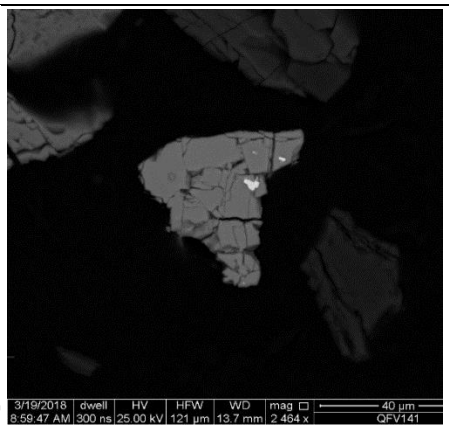


BSE Image

A.5 Gold Locked in arsenopyrite

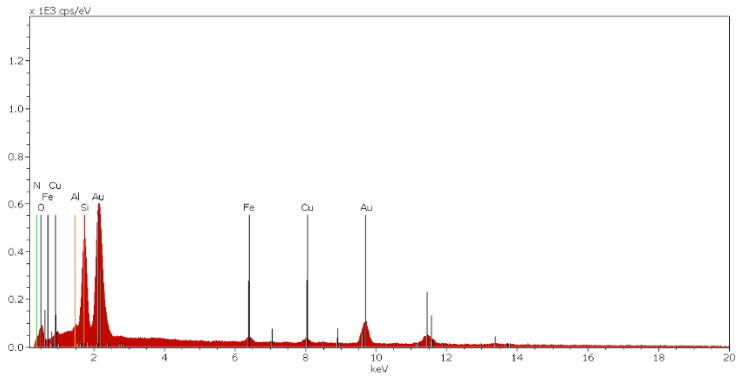


EDS spectra

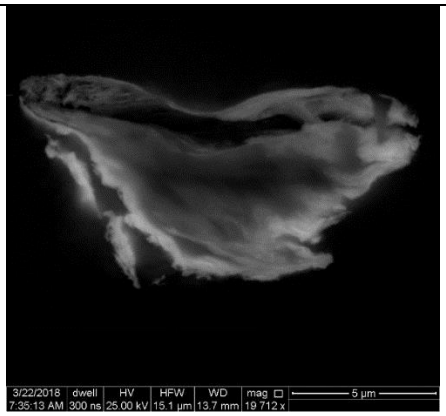


BSE Image

A.6 Gold rim around pyrite



EDS spectra



BSE Image

APENDIX B

LEACHING REPEAT EXPERIEMENTS

Table B: Leaching repeat experiments

Contact time (min)	DIO			MVO			ERGO		
	Bot roll	Conv	Jetleach	Bot roll	Conv	Jetleach	Bot roll	Conv	Jetleach
0	0	0	0	0	0	0	0	0	0
15	16,54	20,45	71,21	33,25	32,04	71,66	25,87	26,21	54,12
30	33,52	34,56	78,07	45,07	48,65	74,23	27,76	31,24	56,05
45	43,12	51,35	80,99	56,68	64,11	77,12	34,89	35,12	62,98
60	52,97	65,23	82,03	62,87	72,6	78,08	36,23	37,67	69,76
75	53,36	69,67	83,28	64	74,21	80	39,41	41,67	70,93
90	53,87	71,03	83,50	67,25	75	81,54	41,98	45,34	71,64
105	55,12	73,14	83,53	68,36	75,97	82,01	44,35	49,03	71,87
120	57,01	73,52	83,74	71,04	77,1	82,93	51,32	53,64	71,92
240	60,08	73,83	83,81	71,28	77,45	86,45	53,12	58,07	72,16
480	64,36	75,04	83,93	72,3	78	87,65	55,03	58,77	72,32
960	65,02	75,25	84,21	73,93	79	88,5	55,97	59,15	72,67
1440	65,19	75,91	84,42	74,36	81,7	91,28	56,64	59,43	72,89